# OPTIMAL PLANNING AND CONTROLLING OF MICROGRID CLUSTER FOR PERFORMANCE ENHANCEMENT

A THESIS SUBMITTED

IN PARTIAL FULFILLMENT OF THE REQUIREMENTS

FOR THE DEGREE OF

MASTER OF SCIENCE

IN

POWER SYSTEM AND ENERGY ENGINEERING

BY

ABENEZER BEKELE

DEPARTMENT OF ELECTRICAL AND COMPUTER ENGINEERING

HAWASSA UNIVERSITY INSTITUTE OF TECHNOLOGY

ADVISOR: DR. BASEEM KHAN (PhD)

HAWASSA (ETHIOPIA)

MAY, 2024

# OPTIMAL PLANNING AND CONTROLLING OF MICROGRID CLUSTER FOR PERFORMANCE ENHANCEMENT

BY

ABENEZER BEKELE

A THESIS SUBMITTED TO THE
DEPARTMENT OF ELECTRICAL AND COMPUTER ENGINEERING,
INSTITUTTE OF TECHNOLOGY, SCHOOL OF
GRADUATE STUDIES
HAWASSA UNIVERSITY
HAWASSA, ETHIOPIA

IN PARTIAL FULLFILLMENT OF THE
REQUIREMENT FOR THE
DEGREE OF

MASTER OF SCIENCE IN POWER SYSTEM AND ENERGY ENGINEERING

MAY, 2024

**ADVISORS' APPROVAL SHEET**

**SCHOOL OF GRADUATE STUDIES**

**HAWASSA UNIVERSITY ADVISORS' APPROVAL SHEET**

This is to certify that the thesis entitled "**Optimal Planning and Controlling of Microgrid Cluster for Performance Enhancement**" submitted in partial fulfillment of the requirements for the degree of Masters of Science in Electrical Engineering with specialization in "**POWER SYSTEM AND ENERGY ENGINEERING**". The Graduate Program of the Department of Electrical and Computer Engineering, and carried out by **Abenezer Bekele** ID. No. GppoSyR/0001/15, under my supervision. Therefore, I recommend that the student has fulfilled the requirements and hence hereby can submit the thesis to the department.

| | | |
|---|---|---|
| Dr. Baseem Khan | _____ | _____ |
| Advisor | Signature | Date |
| Mr. Tesfaye Hailu | _____ | _____ |
| Co-Advisor | Signature | Date |

**EXAMINER'S APPROVAL SHEET**

**SCHOOL OF GRADUATE STUDIES**

**HAWASSA UNIVERSITY EXAMINERS' APPROVAL SHEET**

We, the undersigned, members of the Board of Examiners of the final open defense by **Abenezer Bekele** have read and evaluated his thesis entitled "**Optimal Planning and Controlling of Microgrid Cluster for Performance Enhancement**", and examined the candidate. This is, therefore, to certify that the thesis has been accepted in partial fulfillment of the requirements for the degree.

| | Signature | Date |
|---|---|---|
| Dr. Solomon Mamo<br>Name of Internal Examiner | _____ | _____ |
| Dr. Milkias Berhanu<br>Name of External Examiner | _____ | _____ |
| Mr.Erste Telila<br>Name of the Chair Person | _____ | _____ |
| Dr. Baseem Khan<br>Name of Principal Advisor | _____ | _____ |
| Mr. Tesfaye Hailu<br>Name of the Co-Advisor | _____ | _____ |
| Mr. Dejene Hurissa<br>Dean of Faculty | _____ | _____ |
| SGS Approval | _____ | _____ |

**Stamp of SGS Date: _____**

## DECLARATION

I hereby declare that this MSc thesis is my original work and has not been presented for a degree in any other university, and all sources of material used for this thesis have been duly acknowledged.

| Abenezer Bekele | _____ | _____ |
|---|---|---|
| Name | Signature | Date |

This MSc Thesis has been submitted for examination with my approval as thesis advisor.

| Dr.Baseem Khan | _____ | _____ |
|---|---|---|
| Advisor | Signature | Date |

| Mr. Tesfaye Hailu | _____ | _____ |
|---|---|---|
| Co-Advisor | Signature | Date |

**Abstract**

Access to electricity is a key indicator of a country's development level. However, in Ethiopia, 45.8% of the total population lacks access to electricity, with rural areas facing even higher rates at around 57.2%. In the Southern Nations Nationalities and People's (SNNP) region, the situation is particularly dire, with 62.1% of the population lacking electricity access, the highest among all regions. Consequently, many villages in this region rely on traditional energy sources, leading to environmental pollution, health issues, deforestation, and hindrance to development. To address this challenge, Ethiopia aims to provide electricity access to all by 2030, with microgrid development playing a crucial role. This study utilizes Multi-Tier Framework (MTF) based categorization of village households to develop microgrids, considering factors such as households' income levels and willingness to pay electricity bills. Three villages—Toba, Koza, and Womba—from the SNNP region are selected for optimal microgrid planning and control. Sensitivity analysis is conducted, considering variables such as Global Horizontal Irradiance (GHI) variation, Photovoltaic module and battery prices, allowed battery usage levels, and various capacity shortage levels. The impact of these variables on Net Present Cost (NPC), initial capital cost, and Cost of Energy (COE) is analyzed using HOMER Pro software. In Toba microgrid, for instance, a 10% capacity shortage leads to a 23.82% reduction in COE, illustrating the significance of such considerations. The study also investigates the impact of microgrid clustering by interconnecting three individual microgrids and conducting techno-economic analysis. Despite additional interconnection costs, the benefits in terms of technology, economics, and reliability outweigh standalone microgrid operation. A Master-Slave architecture-based Quasi-Dynamic Simulation Language (QDSL) control model of the microgrid cluster is developed using DIgSILENT PowerFactory2022 software, enabling Quasi-Dynamic Simulation. The results demonstrate improved power utilization, reduced PV curtailment losses, and decreased load shedding compared to operating microgrids individually. Finally, a feasibility study of grid extension for Toba microgrid, located 130 km from the nearby Sawla substation, is performed to assess its viability.

***Keywords:*** *Optimal planning, Microgrid cluster, Multi-Tier Framework, Quasi Dynamic Simulation*

**Acknowledgments**

I express my heartfelt gratitude to the Lord almighty for His guidance and unwavering support throughout every phase of my life, enabling the completion of this work.

I extend my sincere appreciation to individuals from various organizations including Ethiopian Electric Utility, Ethiopian Electric Power, SNNPR Mine and Energy Agency, and Arba-minch municipality for their invaluable contribution in providing essential data and information.

I am deeply thankful to my advisor, Dr. Baseem Khan, for his mentorship, insightful guidance, and encouraging feedback throughout this endeavor. Additionally, I am grateful to Tesfaye Hailu, my co-advisor, for his diligent follow-ups and unwavering support.

## List of Abbreviations

| | |
|---|---|
| ADMM | Alternating Direction Multiplier Method |
| ALO | Ant Lion Optimization |
| BESS | Battery Energy Storage System |
| BFO | Bacterial Foraging Optimization |
| CB | Capacitor Banks |
| CMG | Coupled microgrid |
| COE | Cost of Energy |
| CSO | Cuckoo Search Optimization |
| DES | Distributed Energy Sources |
| DG | Diesel Generator |
| DOD | Depth of Discharge |
| DR | Demand Response |
| DSM | Demand Side Management |
| e4D | Energy for Development |
| EEU | Ethiopian Electric Utility |
| ENS | Energy Not Supplied |
| ESS | Energy Storage System |
| EV | Electric Vehicles |
| GA | Genetic Algorithm |
| GHG | Green House Gas |
| GHI | Global Horizontal Irradiance |
| GW | Giga-watt |
| GWCSO | Grey Wolf with Cuckoo Search Optimization |
| GWO | Gray Wolf Optimization |
| HESS | Hybrid Energy Storage System |
| HH | Households |
| HOMER | Hybrid Optimization Model for Electric Renewable |
| IEA | International Energy Agency |
| IRENA | International Renewable Energy Agency |

| | |
|---|---|
| LCC | Life Cycle Cost |
| LCOE | Levelised Cost of Energy |
| LFP | Lithium-ion iron phosphate |
| MATLAB | Matrix Laboratory |
| MGC | Microgrid Cluster |
| MGs | Microgrids |
| MILP | Mixed-Integer Linear Programming |
| MPPT | Maximum Power Pont Tracking |
| MTF | Multi-Tier Framework |
| NEP2.0 | National Electrification Program 2.0 |
| NPC | Net Present Cost |
| O&M | Operations and Maintenance |
| PCDP DRP | Power Capacity-based Dynamic Pricing Demand Response Programs |
| PSIM | Power Electronics Simulator |
| PSO | Particle Swarm Optimization |
| PV | photovoltaic |
| QDSL | Quasi-Dynamic Simulation Language |
| RES | Renewable Energy Sources |
| RPF | Reverse Power Flow |
| SC | Super Capacitor |
| SNNP | Southern Nation Nationality People |
| SOC | State of Charge |
| WG | Wind generation |
| WSO | War Strategy Optimization |

## Table of Contents

## List of Figures

## List of Tables

# Chapter 1

# Introduction

## 1.1. Background

Access to electricity plays a crucial role in determining the development status of a country. In 2021, it was reported that 45.8 percent of Ethiopia's total population lacked access to electricity, a figure that escalated to approximately 57.2 percent in rural areas [1]. Various initiatives aim to address this issue, with the Ethiopian National Electrification Program (NEP2.0) undergoing updates to achieve complete electrification by 2030. As part of this endeavor, standalone microgrid development is slated to electrify around 35 percent, equivalent to approximately six million customers [2].

Ethiopia boasts abundant renewable energy sources such as wind, geothermal, solar, and hydroelectric power. Studies indicate that the country has the potential to generate over 60 gigawatts (GW) of electric power from these mixed sources [3]. Despite this diversity, the country predominantly relies on hydropower, which contributes 90 percent of the total power generation. However, challenges persist in hydropower generation, including environmental concerns stemming from landscape alterations due to reservoirs and the impact of drought on hydropower output. Additionally, the dispersed rural population complicates centralized hydropower electrification, rendering it more costly and challenging [4].

In lieu of a centralized hydropower system, the development of microgrids utilizing photovoltaic (PV), micro-hydro, wind, and diesel generators emerges as a viable solution to electrify remote communities, particularly in rural areas. The Ethiopian government has expressed interest in diversifying the power generation mix to incorporate additional renewable sources like wind, solar, and geothermal energy. Plans are underway to install a total of 10.4 gigawatts of power by 2022, with the goal of increasing solar, wind, and geothermal energy contributions to nearly 45 percent by 2040, as outlined in the updated electrification plan of the Ethiopian Electric Power (EEP) [3] [5].

The Ethiopian Electric Utility (EEU) assumes primary responsibility for implementing the grid initiative, coordinating efforts between public and private sectors for standalone scale-up projects [2]. Priority is given to developing mini-grids in remote rural areas, as stipulated in

NEP2.0. As shown in Table 1-1, an analysis of energy access across different regions of Ethiopia reveals that despite its sizable population, 62.1 percent of the Southern Nations, Nationalities, and Peoples' Region (SNNP) lack access to electricity, the highest among all regions. Consequently, this study focuses on three villages—Toba, Koza, and Womba—within this region, with an emphasis on optimizing microgrid and microgrid cluster development.

Table 1-1: Energy access percentage at various regions of Ethiopia

| Region | Population | Grid Access (%) | Off-grid Access (%) | No Access (%) |
|---|---|---|---|---|
| Tigray | 5,056,000 | 50.9 | 36.9 | 12.3 |
| Amhara | 20,401,000 | 28.6 | 22.5 | 48.7 |
| Oromia | 33,692,000 | 26.7 | 36.3 | 36.7 |
| SNNP | 18,276,000 | 30.1 | 7.8 | 62.1 |
| Addis Ababa | 3,373,000 | 99.9 | 0 | 0.1 |

### 1.2. Problem Statement

In the villages of Toba, Koza, and Womba, with a combined population of approximately 15,244 individuals across 3,048 households, traditional energy sources such as wood and animal dung are predominantly utilized. Lighting primarily relies on 'kuraz,' a traditional kerosene-based lamp, which emits smoke, hindering reading activities and causing respiratory issues. These conventional energy practices contribute significantly to environmental pollution, health concerns, deforestation, and overall deterioration in the quality of life, impeding socio-economic development.

Furthermore, despite the agricultural potential of Toba, Koza, and Womba villages, inadequate access to stored water for irrigation purposes, coupled with reliance solely on seasonal rainfall, limits agricultural productivity. This disparity between agricultural effort and output discourages farmers.

Moreover, students in these villages face challenges in their education due to the dual responsibilities of fetching water from distant sources and other household chores, leaving them with limited study time during daylight hours. However, using kerosene lamps for extended periods is financially burdensome for most households, and the discomfort associated

with traditional lighting sources affects reading conditions. Consequently, students struggle to concentrate on their studies, leading to a decline in the educated population.

The geographical remoteness of these villages from the nearby Sawla substation, located 130 kilometers away from Toba village, suggests that accessing electricity from the grid is a distant prospect, making it a long-term solution.

## 1.3. Objective

### 1.3.1. General Objective

The general objective of this study is optimal planning and controlling of microgrid cluster for performance enhancement.

### 1.3.2. Specific Objective

To achieve the general objective, the following specific objectives should be pursued.

- Multi Tire Framework (MTF) based categorization of study case villages' households.
- Optimal planning and sensitivity analysis of microgrids using HOMER Pro software.
- Developing MGs and an MG-cluster, and conducting a comparison between them.
- Developing Quasi-Dynamic Simulation Language (QDSL) control model to perform quasi-dynamic simulation analysis of MG and MG-cluster using DIgSILENT PowerFactory2022 software.
- Feasibility study of Grid extension of Toba MG.

# Chapter 2

# Literature Review

## 2.1. Introduction

The escalating demand for electricity, coupled with the environmental consequences of generation emissions, the imminent risk of fossil energy depletion, and the challenges associated with grid expansion to supply remotely located villages due to economic and technical constraints, underscore the imperative of utilizing Renewable Energy Source (RES) based microgrids (MGs) as the optimal approach to electrify both rural and urban areas. Beyond merely providing illumination, access to electricity plays a pivotal role in fostering the sustainable development of a nation. This section reviews the latest literature pertaining to MGs and MG clusters.

## 2.2. Microgrid

MG is defined as a small active distribution system with RES [6]. MGs contain components such as wind generation (WG), photovoltaic (PV) power, flexible loads and Energy Storage System (ESS) capable of performing a buffer role between electric demand and distributed generation. In [7] it is described as an aggregation of distributed sources, energy storage systems and loads. MGs also have a potential to provide electric power to areas after disturbance, which occur due to natural disruptive events, hence increasing the reliability and resilience of the system [8].

MGs could operate in standalone or grid connected mode. If any condition that could have interrupted power throughout such as fault occur in the main grid, then the MG disconnects from the grid and starts operating in an autonomous way by supplying local loads. After fault clearance the isolated MG will reconnect and start operating in grid connected mode. During autonomous operation critical loads should be supplied first and the other loads would be supplied based on the availability of resources [8]. Critical loads are loads which could not be interrupted no matter what.

Severe weather conditions affect the power system and the frequency of the system could deviate from the standard. During such conditions the extent of impact could vary depending on several factors but for most cases it is difficult for the power system to recover from such natural disasters and MGs are the emerging potential source of resiliency.

A paper presented in [9] proposed a way of enhancing resilience against extreme weather conditions and categorized resiliency as infrastructure resiliency and operational resiliency. Under infrastructural resilience two ways are considered I) hardening: which is concerned in reinforcing power system components against severe distractions II) planning: aimed at increasing redundancy, automation, and flexibility of the network by installing new components. Under operational resiliency preventive and corrective measures are proposed. The objective of the study is combining operation and planning of microgrid placement for enhancing the resiliency of the distribution network.

### 2.3. Benefits and Drawbacks of Integrating Renewable Energy Sources

Even though increasing the penetration of RES into existing systems has many advantages, it could cause stability problems in the existing grid system. This is due to mainly the intermittent (solar radiation, wind speed) nature of renewable resources causing imbalance between demand and supply resulting in reliability, voltage fluctuations and stability problems in grid systems. In addition to stability problems, high penetration of RES could also result in power losses caused by excess supply rather than demand [10]. However the impact of properly planned and developed MGs is more positive. It is presented in [11] that MGs have a potential to increase stability and decrease the Levelised Cost of Energy (LCOE) of the system but faces many challenges due to the intermittent nature of RES used.

The solution for aforementioned challenges caused by penetrating RES into the system is using ESS and it is proven that for MGs it is better to use single shared ESS than multiple individual ESS from cost point of view [10], [11].

For rural areas where distribution network expansion is either uneconomical or infeasible, renewable energy based MGs are promising solutions to provide electric service. Autonomous MGs with RES guarantee system security and reliability accompanied with cost effective solutions.

To get feasible solutions from environmental issues and economic consideration it is necessary to pay attention to the technology and cost of batteries, being one of the main components in standalone MGs [12]. Battery Energy Storage System (BESS) appropriate sizing is required otherwise too large capacity is a waste of money and too small cannot fulfill the required

demand. Besides sizing, the charging/discharging strategy should consider the intermittent nature of RES and should avoid charging of battery during limited resource periods [8], [13]. The work in [14] describes the impact of considering the size, cycle of lifetime and technology of BSS simultaneously in MGs during both standalone and grid tied mode of operation. The impact of Depth of Discharge (DOD) on the service lifetime of the battery is also clearly presented and the authors developed a model which quantifies the equivalent complete cycles of the battery till its lifetime. The proposed method shows how it is different to consider complete cycle (full discharge of a fully charged battery) from partial cycle. Another arrangement of storage systems considering the MG components such as PV, Diesel Generator (DG) and Hybrid Energy Storage System (HESS) which is a combination of battery and Super Capacitor (SC) is described in [15]. In the study, service lifetime of the battery is enhanced by using SCs.

### 2.4. Optimization in Micro-grids

Optimization is a method of getting optimal solutions while subjected to different constraints. In MG planning it is a process of getting optimal size of MG components, their optimal location, type of technology used etc. subjected to one or more constraints like investment cost, life cycle of BESS, reliability, extent of Green House Gas (GHG) emission, electricity price, etc. Having different objectives and constraints, researchers use different optimization techniques which best suit the situation.

Optimal sizing of MG components makes the system more reliable and more economical. Oversized systems result in excess energy and high running cost whereas undersized systems cannot fulfill the demand. To get the most out of it, RES based MGs should be optimally sized and energy should be managed [16]. Impact of optimal sizing is clearly presented in [8] by considering island operation mode of MG containing only PV source. In the system if the supply is less than the demand, the bus bar voltage will be reduced and on the contrary if the supply exceeds the demand then Reverse Power Flow (RPF), loss of voltage control, increased impact of short circuit etc. occur. So in order to reduce this unbalancing problem an optimal sizing of components is required and to regulate the energy from intermittent sources it is better to incorporate BESS into the system so that it would provide during supply deficit.

In [10] minimization of electricity cost during day time is the main objective and to achieve this economic dispatch of MGs containing a shared ESS is considered and for optimization

Mixed-Integer Linear Programming (MILP) approach is developed. The algorithm manages the power outputs of PV generators, a shared ESS, main grid and controllable loads in order to satisfy the supply-demand balance and reduce energy costs. To show the performance of the approach three cases were considered i.e. (I) without using MILP optimization (II) using MILP optimization (III) using both MILP optimization and demand response strategy. The results obtained show a significant cost reduction in case II and even more reduction in case III showing how profitable it is to use MILP optimization and demand response strategy in shared ESS of MG. The proposed approach is evaluated and verified in green and smart building park, Benguerir, Morocco.

The microgrid components considered in [8] are PV, BESS and loads. Optimization of their capacity, the selection of charging strategy and the possible optimal locations while fulfilling the requirements of minimum investment cost, supplying maximum energy demand and minimal RPF microgrid configuration are done using Genetic Algorithm (GA). In the study the requirement of using ESS managing technique and proper MG configuration to satisfy energy demand and optimize costs in autonomous MG which serve as backup power during extended disruption are described.

For cost optimization of MG the initial State of Charge (SOC), the load profile and operating costs of ESS, RESs are considered in [17]. By using the optimization technique it is possible to benefit from efficient use of available resources besides achieving an optimal operation cost.

### 2.5. Impact of Demand Side Management and Economic Concern in MG Optimization

Demand Side Management (DSM) is a method which shapes customers electric power consumption behavior to change through minimizing peak load and price. It should be considered at the planning stage of the system. Flexible loads such as electric charging, washing machines and disinfection cabinets can be served during off-peak/low tariff periods of the day. A paper presented in [6] analyzes economic scheduling of renewable sources within MG's and this is done by demand management strategy considering peak-valley tariff mechanism. The optimization method used is based on price-based demand response. In the study an improved War Strategy Optimization (WSO) algorithm is suggested while considering three cases 1) without battery 2) with battery and 3) with battery and demand response. In addition the demand response optimization also takes place using Particle Swarm

Optimization (PSO) and WSO for the case with battery and demand response and the result is compared with four other optimization techniques and it is found out improved WSO has better performance in resolving the scheduling model. Besides optimal scheduling WSO reduces the overall cost and power supply pressure during peak hours.

A realistic power-scheduling approach using meteorological data and annual electrical load demand is developed in [18]. In addition to that, the feasibility and productivity of the system is illustrated by analyzing the techno-economic performance. In the study residential MG is considered where the primary concern is to achieve reliability and maximizing economic benefits. In order to size the components optimally and find out the best configuration in terms of costs; techno-economic analysis of three cases using MILP optimization technique are considered. For case-1 the proposed MG configuration contains PVs and BESS; for case-2 PVs, BESS and DG; for case-3 PVs, BESS and DG in collaboration with grid systems are used to supply the demand. According to the analysis it is found out that case-2 is preferred, being not dependent on grid power and having a small Life Cycle Cost (LCC). The LCC value of case-2 decreases as it is compared with the other cases and shows the effectiveness of using PVs, a BESS, and a DG.

An improved Bacterial Foraging Optimization (BFO) technique for optimal dispatching of MG considering economy is used in [19]. By using the proposed optimization technique the economic benefit is improved, environmental emission and operational cost are reduced. In [20] techno-economic benefits, energy dispatching and optimal capacity of autonomous MG is presented. For the study PV, WT, BESS and DG are considered and for optimization Hybrid Optimization Model for Electric Renewable (HOMER) software is used. In the study load side management is also considered by involving impact of Demand Response (DR) on the optimization of the system. In this case elastic loads i.e. shift-able and curtailable loads are basically considered which gives the flexibility for MG operators to flatten the load profile and this enhances the reliability of MG. In order to determine the optimal configuration of hybrid energy sources eight different configurations of MG energy sources are managed based on Cost of Energy (COE) and annual Net Present Cost (NPC) while considering seasonally varying commercial and residential loads with different renewable fractions. Based on this PV+BESS configuration is found the most economical compared with the rest simulated feasible combinations. It is also addressed that the renewable penetration fraction is inversely

varying with COE and NPC i.e. as the fraction of renewable sources decreases, NPCs and COEs increases.

During the planning phase much consideration should be given for accurate sizing of microgrid components, assessing the required network upgrade and flexible components which have impact in cost optimization so as to reduce costs. To achieve this goal there are various optimization techniques that can be used with different constraints.

Optimization considering capacity sizing and optimal upgrade of generation resources is proposed in [21]. Having been considered in the planning phase the flexibility of different distributed assets can reduce the investment cost by varying the operation scenario. In this paper PVs and BESSs are used as generation sources, Electric Vehicles (EVs) are considered as flexible assets and storage, generation capacity and network upgrade are considered for problem formulation using a mixed integer piecewise linear problem.

Optimal sizing of standalone MG considering the impact of variability of load, renewable sources, various battery types, battery life cycle energy and their impact on cost, for Indian condition, are analyzed in [7]. In the study multi objective optimization method and a tradeoff between cost effectiveness and possibilities of energy sustainability through choice of different batteries is presented. The considered microgrid contains WT, PV and BESS and for optimal sizing of components GA is used considering the impacts of environmental issues, energy and lifecycle cost.

In [15] the proposed PV model is suited for areas having no historical operational data and its impact on microgrid sizing process, the involvement of critical loads, the Energy Not Supplied (ENS) must be zero with a cost of economy and a sensitivity analysis based on energy storage system is clearly presented. According to [22] environmental impact is considered and the size of microgrid components are optimized. Analyzing the benefit between using only grid systems or MGs having PV, WT, BESS and DG to supply the load is compared and the latter is found to be more economical. A paper in [16] illustrates the environmental and techno-economic impact on islanded MGs considering different renewable penetration levels, minimizing total number of components and varying priority to supply the demand. The system contains PV, BESS, bio-gasifier, WT, DG and loads.

Hybrid Grey Wolf with Cuckoo Search Optimization (GWCSO) method in order to optimally size components of the microgrid with minimum costs is applied in [16]. The simulation result

of GWCSO is compared with results from GA, Gray Wolf Optimization (GWO), Cuckoo Search Optimization (CSO), PSO and Ant Lion Optimization (ALO) and it is found out that the proposed optimization is more robust than the other optimizations, has lowest deviation and its annual cost, LCOE, optimal number of components are superior. In the study the characteristic of BESS being dependent on a real time economic model is used to optimize economy in real time for dispatching of island MG. In order to determine the current time suitable energy dispatch of ESS, operational profit in the future time and acquisition cost in the past time of ESS are considered in the proposed model and Alternating Direction Multiplier Method (ADMM) is used in order to get the optimal solution.

Emission-free nature and low operational costs make renewable energy sources best for maintaining carbon neutral operation of electric power grid and effective capacity sizing have impact on reliability and adequate generation supply with a reasonable operation cost.

Optimization based on demand response programs has the benefit of enhancing the reliability and stability of the power grid [23]. This is done by rescheduling total capacity /part of flexible loads to be supplied by intermittent renewable sources to the time where there is excess power supply. In the study cost-benefit advantages based on different demand response strategy and energy storage dependency of MG containing variable energy sources to meet load demand while attaining pre-determined reliability index are investigated. For the suggested autonomous microgrid, a cost effective optimal planning method is realized by using Power Capacity-based Dynamic Pricing Demand Response Programs (PCDP DRP). In this Bi-optimization planning is a mechanism of attaining both optimal capacity sizing and operational planning in the same study i.e. the optimal capacity of WT, PV and BESS in one hand and the most effective operative schedule to attain best operating strategy in other hand both to achieve minimum total annual costs and maximum component installed capacity while minimizing the loss of power probability. To decide the best techno-economic planning method four simulation scenarios are used and solved using the MILP optimization solver in MATLAB.

Optimal size of photovoltaic, diesel and battery for island MG by considering economic and reliability are analyzed in [24]. In order to perform detailed reliability it costs more and as a result a tradeoff is required between economy and reliability. Planning of MG considering reliability takes time and according to the results it is required to install larger sized RES in order to get better reliability criterion. For the study an autonomous MG containing BESS, PVs

and DG are considered and optimal sizing is performed using MILP algorithm while considering reliability.

Optimal sizing of storage systems has a high impact on the economy of microgrid systems. ESS needs to be properly sized to reduce the effect of increased investment cost due to oversizing or below required reliability level by under-sizing it. Therefore the necessary attention should be given for optimization of ESS. According to [13] the major things to consider in optimization of ESS for MGs are:

a) Energy storage configuration methods i.e. the energy storage (ES) is either single or composite configuration.
b) The principles and technique of ES configuration under standalone and grid-tied operation of MGs.
c) Optimization analysis technique used.
d) Quantitative analysis to show the impact on customers from income and system economy point of view.

Harmonized planning of BESS and PVs with deployment of demand side resources are also presented in the study.

In MG planning, a low carbon economy is becoming a major factor. A paper presented in [25] utilized double-layer optimization techniques to get optimal capacity of MG components and their optimal locations subjected to minimizing carbon emission cost. For optimal sizing carbon subsidy fee policy to encourage the use of clean energy generation (photovoltaic, wind power) and carbon tax system for carbon generating sources (diesel generator) in MG to combat climate change are used. The used optimization method considering carbon emission penalty and carbon subsidy resulted in reducing the carbon emission of MGs to great extent and increasing the development of renewable sources.

### 2.6. Microgrid Cluster

A microgrid is a small scale electrical grid containing distributed generation and loads. It can operate in standalone mode or grid connected mode. Standalone MGs operate in an autonomous control of the MG while isolated from the grid and majorly contain RES along

with BESS or/and diesel/gas driven generators. Due to the intermittent nature (solar radiation, wind speed) of RES the MGs are exposed to phenomena like overloading and over generation. Overloading implies a condition by which the generated power is not enough to supply the load. One way of mitigating such problems is load shedding. On the other hand, over generation is excess power generation than the demand. For this condition curtailing non dispatch-able renewable sources could be a solution. Both overloading and over generation conditions affect the frequency and voltage of MG.

Curtailment of renewable energy sources and load shedding are the usual way to prevent short time over generation and overloading in standalone MGs. But both curtailing and load shedding are not economical solutions. So another option is to use an energy storage system which can solve the problem but with large installation and operational cost. Therefore there is a need to find an optimal solution for this problem.

Thus such problems can be overcome by interconnecting nearby MGs to exchange power between them. This type of configuration obtained by interconnecting two or more neighboring MGs is termed as Coupled microgrid (CMG) or Microgrid Cluster (MGC).

Individual MGs have the responsibility to fulfil their local load demand and whenever there is excess generation that can be provided to the interconnected MG in need. By sharing power within the cluster both curtailment of renewable sources and load shedding of MGs would be reduced and the reliability of the system as a whole can be enhanced.

In [26] the MGs of a cluster are interconnected through 3-phase ac link and back-to-back converter. The suggested Power exchange and control strategy efficacy are confirmed over the simulation analysis using PSIM.

The interconnection of commercial MG with that of residential MG to form a MGC is presented in [11]. In the mentioned MGs there is a weekly variation of load pattern i.e. residential peak load occurs during weekends of the residential MG while commercial peak load occurs during weekdays of commercial MGs. Therefore by considering this different power requirement of residential and commercial loads, extra power of commercial MG can be used to supply residential peak load during the weekends thereby increasing the reliability of the cluster.

As it is in any power system, in order to maintain voltage and frequency of the cluster within the standard the balance between supply and demand should be achieved.

Figure 2-1(a) shows a standalone microgrid containing PV, micro-Hydro, battery and different types of loads and Figure 2-1(b) shows a MG cluster.

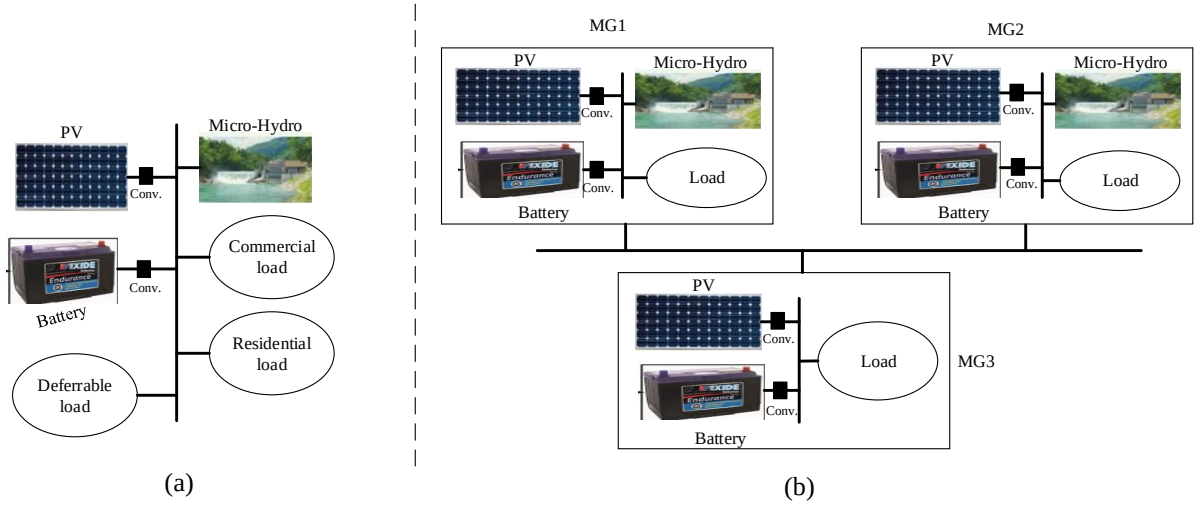


*Figure 2-1: (a) standalone MG (b) three individual MGs interconnected to form MG cluster*

## 2.7. Research Gaps

While previous studies on MGs have primarily focused on limited factors such as capacity shortage, economy, or the economic impact of MG clustering, a comprehensive examination of various factors is lacking. This study addresses this gap by adopting a broader approach to MG analysis. Specifically, it explores optimal sizing and sensitivity analysis of microgrids considering variations in GHI, the price of PV systems, the cost of batteries, and battery lifetime concerning the minimum allowable SOC using HOMER Pro software. Furthermore, the study investigates different levels of capacity shortage and their impacts on both economy and reliability. It also delves into the development of MGs relying solely on renewable sources, as well as the interconnection of standalone MGs to form MG clusters. Additionally, the study assesses the impact of operating MGs individually versus in clustered form and involves the modeling of controllers for both MGs and MG clusters to perform quasi-dynamic simulations using DIgSILENT software. Finally, the study examines the feasibility of grid extension to an MG. By addressing these aspects, this research contributes to filling the existing gaps in the literature on MG analysis and optimization.

# Chapter 3

# Methodology

## 3.1. Procedure of the Study

The planned procedure to attain the objectives of this study, as illustrated in Figure 3-1, is outlined below. The workflow commences with a comprehensive literature review of the latest papers related to the study, followed by site selection and data collection. Data collection entails gathering the electrical load data of the case study villages, employing MTF-based categorization of households, and acquiring natural resource data such as GHI of the villages, along with the costs of various system components. Utilizing the collected information, an optimization analysis of the system is conducted, taking into account both economic and reliability factors. Subsequently, sensitivity analysis is performed to evaluate the impact of sensitivity variables on optimization using HOMER Pro software. Upon determining the optimal values, individual MGs and MG cluster are developed. Quasi-dynamic simulation analysis is carried out using QDSL controlling models for both individual MGs and MG cluster, employing DIgSILENT PowerFactory2022 software. Comparisons between standalone MGs and MG cluster are then conducted from multiple perspectives. Finally, a feasibility study of grid extension is analyzed to assess its feasibility.

## 3.2. Selection of Case Study Area

Achieving the sustainability of MG development projects presents challenges, as it involves navigating the complexities of balancing high-level reliability requirements with the imperative of reducing implementation periods, optimizing efficiency, and ensuring affordability. To address such issues, a method known as the Multi-Tier Framework (MTF) has been developed, aiming to facilitate the attainment of universal electricity access in both urban and rural areas [27].

The NEP2.0 emphasizes the potential of the MTF to significantly advance the national electrification objective. Figure 3-2 illustrates the household energy consumption based on the MTF across different regions of Ethiopia, revealing that a majority of consumers fall within Tier 0 to Tier 3 categories [27]. The Tier system, a component of the MTF, categorizes households based on their level of access to electricity, with lower Tier numbers indicating

lesser access per household, and Tier 0 signifying households with minimal or no electricity access.

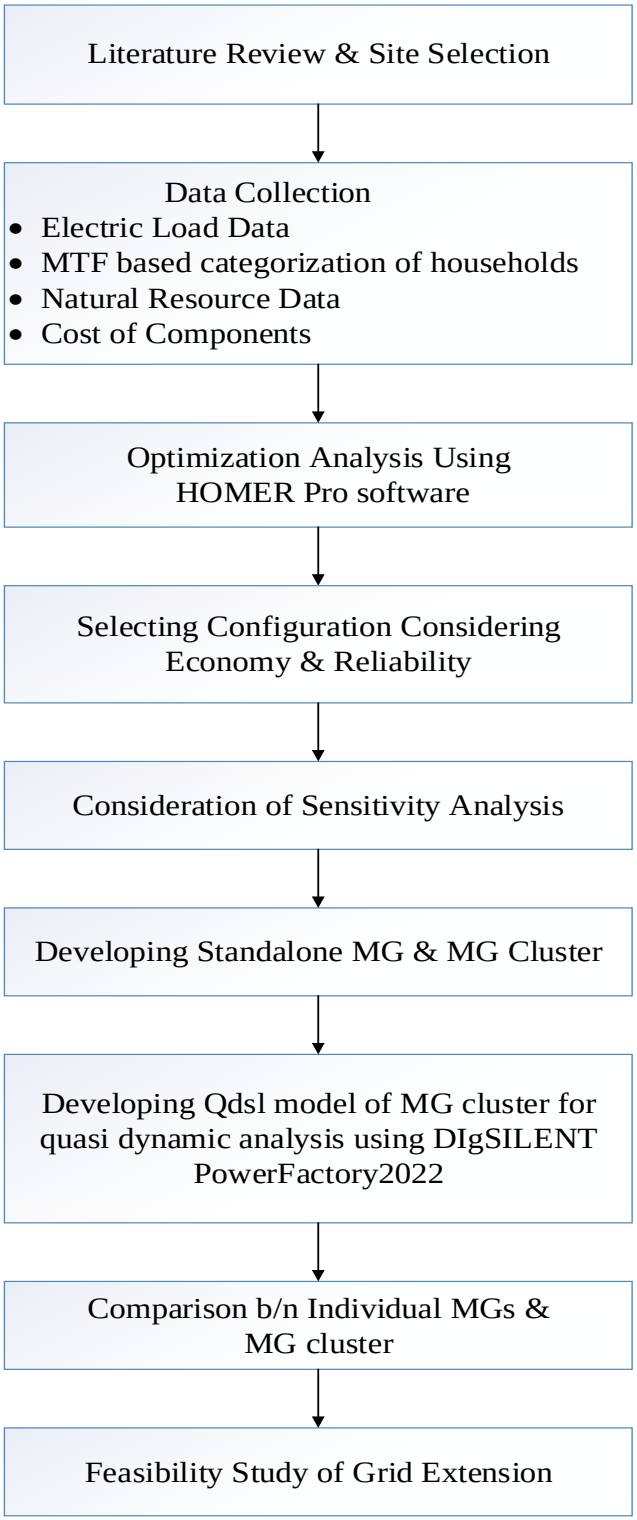


*Figure 3-1: Procedure of the Study*

The figure indicates that sixty-two percent of households in the SNNP region fall into Tier 0, representing the highest percentage of Tier 0 households among all regions.

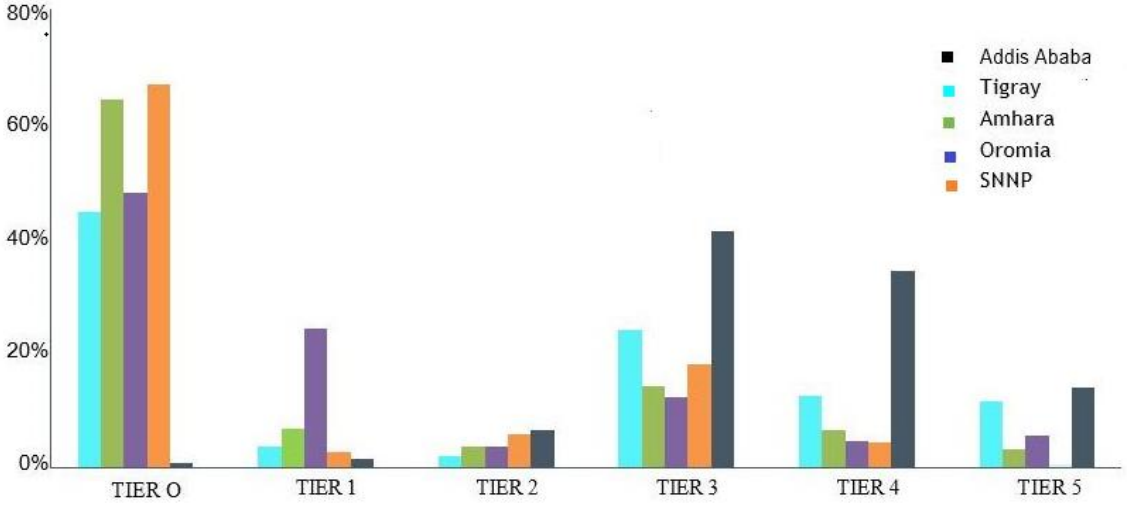


*Figure 3-2: MTF based household consumption by regions in Ethiopia [27]*

Taking into account access to different sources of electricity, in the SNNP region, the percentages of grid-access, off-grid access, and no-access to electricity are 30.1, 7.8, and 62.1 percent, respectively, as illustrated in Figure 3-3. This places the region at the bottom in terms of electricity access compared to other regions. Consequently, the SNNP region has been chosen as the focus for achieving national universal electricity access in this study. Specifically, three villages—Toba, Koza, and Womba—have been selected from this region for the optimization of MG and microgrid cluster development.

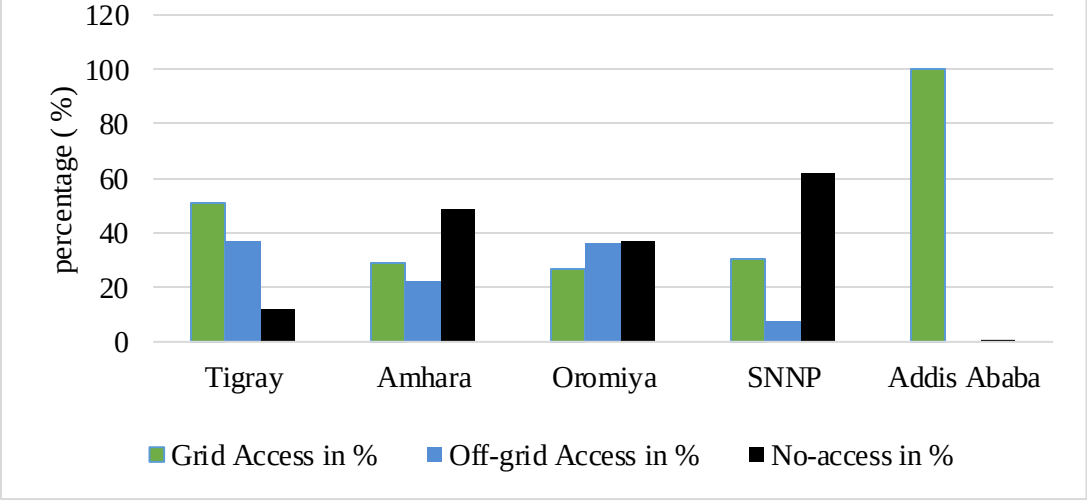


*Figure 3-3: Access to various sources of electricity in regions of Ethiopia*

### 3.3. Categorization of Household Electricity Access Based on MTF

MTF, or the Multi-Tier Framework, serves as a method for classifying households based on various criteria related to electricity access. This electrification approach entails a comprehensive assessment of energy access to deliver tailored energy services that cater to different household levels, taking into account consumption patterns, economic status, and willingness to pay for services [27]. Unlike the conventional approach of assuming average electricity usage across a village, MTF hierarchically categorizes households from Tier 1 to Tier 5.

In this study, an MTF-based energy access matrix is employed, wherein demands are categorized according to service type and energy consumption levels to derive optimal solutions. The MTF-based energy access matrix, depicted in Table 3-1, illustrates the categorization of Tiers based on attributes such as electric power capacity, availability, supported appliances, reliability, and affordability.

Leveraging the proposed framework of MTF-based categorization offers several advantages, including the consideration of household income to denote affordability, the incorporation of outage frequency per week to signify reliability, and the delineation of energy access services for each Tier, among others.

Table 3-1: MTF based energy access matrix.

| Attributes | | Tier 1 | | Tier 2 | | Tier 3 | | Tier 4 | | Tier 5 | |
|---|---|---|---|---|---|---|---|---|---|---|---|
| Power Capacity | Peak power | ≥ 3 W | | ≥ 50 W | | ≥ 200 W | | ≥ 800 W | | ≥ 2 KW | |
| | Daily | ≥12 Wh | | ≥200 Wh | | ≥ 1 KWh | | ≥ 3.4 KWh | | ≥ 8.2 KWh | |
| Availability | Daily hours | ≥4 hrs. | | ≥ 4 hrs. | | ≥ 8 hrs. | | ≥ 16 hrs. | | ≥ 23 hrs. | |
| | Hrs. per night | ≥ 1 hr. | | ≥ 2 hrs. | | ≥3 hrs. | | ≥ 4 hrs. | | ≥4 hrs. | |
| Supported Appliances | Per Household | Very low-power appliances (3-49 W) | | Low-power appliances (<200 W) | | Medium-power appliances (<800 W) | | High-power appliances (<2000 W) | | Very high-power appliances (2KW or more) | |
| | | Equi. W (quant.) | Daily energy | Equi. W (quant.) | Daily energy | Equi. Watt (quant.) | Daily energy | Equi. Watt (quant.) | Daily energy | Equ. Watt (quant) | Daily energy |
| | Lighting | 6W (3) | 36Wh | 10W(5) | 80Wh | 10W(5) | 80Wh | 10W(5) | 80Wh | 10W(5) | 80Wh |
| | Phone charging | 6W (2) | 24Wh | 9W (3) | 72Wh | 9W (3) | 72Wh | 9W (3) | 72Wh | 9W (3) | 72Wh |
| | Radio | 3W (1) | 12Wh | 6W (2) | 48Wh | 6W (2) | 48Wh | 6W (2) | 48Wh | 6W (2) | 48Wh |
| | TV | | | 12W (1) | 96Wh | 12W(1) | 96Wh | 12W (1) | 96Wh | 12W (1) | 96Wh |
| | Fan | | | 15W (1) | 90Wh | 30W (2) | 240Wh | 30W (2) | 240Wh | 30W (2) | 240Wh |
| | Fridge | | | | | 75W (1) | 600Wh | 100W (1) | 800Wh | 200W(1) | 1600 Wh |
| | Rice cooker | | | | | 250W (1) | 250Wh | 350W (1) | 350Wh | 400W (1) | 400Wh |
| | Iron | | | | | | | 1.1KW (1) | 330Wh | 1.1KW (1) | 330Wh |
| | Washing machine | | | | | | | 0.5KW(1) | 500Wh | 0.5KW (1) | 500Wh |
| | Air conditioner | | | | | | | | | 1.5kW (1) | 4.5 KWh |
| Reliability | | ≥ 14 disruptions per week | | | | <14 disruptions per week | | <14 disruptions per week, total duration < 2hrs | | < 3 disruptions per week, total duration < 2hrs | |
| Affordability | | Low income | | Medium income | | High income | | | | | |

### 3.4. Microgrid Development (Case Study: *Toba Village)*

#### 3.4.1. Site Description

The proposed villages for this study, namely Toba, Koza, and Womba, are situated in the SNNP region, specifically within the Gofa zone. Table 3-2 provides details regarding the population count, number of households, latitude and longitude coordinates, classification of village households based on income levels as low, middle, or high, and the presence of available rivers for micro-hydro installations.

In these villages, electricity access is nonexistent, and their considerable distance from the nearby substation suggests that obtaining electricity from the grid is likely a long-term aspiration.

Table 3-2: Selected villages information.

| Site | population | Household | Latitude | Longitude | Income | | | River |
|---|---|---|---|---|---|---|---|---|
| | | | | | Low (%) | Middle (%) | High (%) | |
| Toba | 4882 | 976 | $6^0$ 28' N | $36^0$ 40'E | 58 | 26 | 16 | Toba |
| Koza | 6210 | 1242 | $6^0$ 28' 59''N | $36^0$ 43'E | 60 | 25 | 15 | - |
| Womba | 4152 | 830 | $6^0$ 33'N | $36^0$ 47'E | 60 | 20 | 20 | Ergino |

Toba village is positioned at 6°28' N latitude and 36°40' E longitude. It is home to a population of 4,882 individuals residing in 976 households. The households in this village are classified into low, middle, and high-income groups, constituting 58%, 26%, and 16% of the total households, respectively. Additionally, Toba village benefits from the presence of the Toba River, which holds potential for micro-hydro power generation.

#### 3.4.2. Solar Energy Assessment of Toba Village

In Toba village, Figure 3-4 illustrates the monthly average solar Global Horizontal Irradiance (GHI) data. The annual average GHI in Toba village is recorded at 5.67 kWh/m²/day. The highest average GHI of 6.24 kWh/m²/day is observed in March, while the lowest average GHI of 4.89 kWh/m²/day occurs in July.

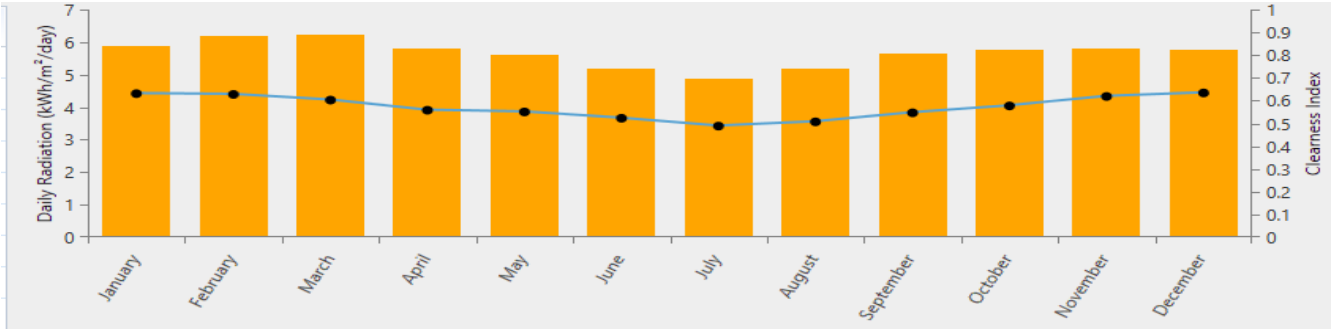


*Figure 3-4: Monthly average GHI in Toba village.*

### 3.4.3. Electrical Loads of Toba Microgrid

Based on the Multi-Tier Framework, households in Toba village are categorized into Tier 1 to Tier 3. Table 3-3 presents the Toba microgrid residential load profile, segmented into Tier 1, Tier 2, and Tier 3 categories. Each tier level is associated with specific types of loads, their quantities, operating hours per day, power ratings, and daily energy consumption. Similarly, commercial loads are delineated in Table 3-4.

Table 3-3: Toba MG residential load profile categorized as Tier1, Tier2 and Tier3.

Tier 1 Toba residential load profile

| Load Type | Availability (Hrs.) | Rating P (W) | Quantity | Power (W) | Energy (Wh/day) | L.F | Energy (Wh/day) |
|---|---|---|---|---|---|---|---|
| Lighting | 5 | 3 | 3 | 9 | 45 | 0.9 | 40.5 |
| Phone charge | 4.5 | 3 | 2 | 6 | 27 | 0.9 | 24.3 |
| Total-1household | | | | | 72 | | 64.80 |

Tier 2 Toba residential load profile

| Load Type | Availability (Hrs.) | Rating P (W) | Quantity | Power (W) | Energy (Wh/day) | L.F. | Energy [Wh/day] |
|---|---|---|---|---|---|---|---|
| Lighting | 8 | 3 | 3 | 9 | 72 | 0.9 | 64.8 |
| Phone charge | 8 | 3 | 2 | 6 | 48 | 0.9 | 43.2 |
| Radio | 8 | 3 | 2 | 6 | 48 | 0.6 | 28.80 |
| Fan | 8 | 15 | 1 | 15 | 120 | 0.75 | 90.00 |
| TV | 8 | 12 | 1 | 12 | 96 | 0.7 | 67.2 |
| Total (1hh) | | | | | 384 | | 294 |

Tier 3 Toba residential load profile

| Load Type | Availability (Hrs.) | Rating P (W) | Quantity | Power (W) | Energy (Wh/day) | L.F. | Energy (Wh/day) |
|---|---|---|---|---|---|---|---|
| Lighting | 8 | 3 | 5 | 15 | 120 | 0.9 | 108 |
| Phone charge | 8 | 3 | 2 | 6 | 48 | 0.9 | 43.20 |
| Radio | 8 | 3 | 2 | 6 | 48 | 0.6 | 28.80 |
| Fan | 4 | 30 | 1 | 30 | 120 | 0.75 | 90 |
| TV | 8 | 12 | 1 | 12 | 96 | 0.7 | 67.2 |
| Fridge | 12 | 75 | 1 | 75 | 900 | 0.4 | 360 |
| Rice cooker | 1 | 200 | 1 | 200 | 200 | 0.4 | 80 |
| Total (1household) | | | | | 1532 | | 777.2 |

Table 3-4: Toba MG Commercial load profile.

| Load Type | Watt | LF | Hrs. | Demand (kW) | Qty. | Demand (Kw) | Energy (kWh) |
|---|---|---|---|---|---|---|---|
| Fridge Cafe | 500 | 0.8 | 12 | 0.4 | 4 | 1.6 | 19.2 |
| Hotel | 300 | 0.7 | 12 | 0.21 | 4 | 0.84 | 10.08 |
| Barber | 125 | 0.6 | 9 | 0.075 | 4 | 0.3 | 2.7 |
| Tailors | 250 | 0.8 | 10 | 0.2 | 4 | 0.8 | 8 |
| Tea house | 400 | 0.6 | 12 | 0.24 | 3 | 0.72 | 8.64 |
| Flour mill | 12500 | 0.85 | 10 | 10.625 | 4 | 42.5 | 425 |
| Wood Works | 3500 | 0.7 | 10 | 2.45 | 2 | 4.9 | 49 |
| Iron Works | 5000 | 0.7 | 10 | 3.5 | 1 | 3.5 | 35 |
| Financial Inst. | 120 | 0.9 | 9 | 0.108 | 2 | 0.216 | 1.944 |
| Fridge Clinic | 100 | 0.6 | 12 | 0.06 | 1 | 0.06 | 0.72 |
| Clinic | 5000 | 0.6 | 9 | 3 | 1 | 3 | 27 |
| Vet clinic | 3000 | 0.4 | 9 | 1.2 | 1 | 1.2 | 10.8 |
| School (1-8) | 1000 | 0.9 | 6 | 0.9 | 3 | 2.7 | 16.2 |
| School(9-12) | 4000 | 0.9 | 6 | 3.6 | 1 | 3.6 | 21.6 |
| Govt. Office | 100 | 0.8 | 8 | 0.08 | 4 | 0.32 | 2.56 |
| Church | 670 | 0.9 | 3 | 0.603 | 3 | 1.809 | 5.427 |
| Total | | | | | | 68.065 | 643.871 |

By aggregating the Tier 1, Tier 2, and Tier 3 loads of the village, accounting for their respective operating periods per day, the total residential load profile of the village can be derived. Similarly, incorporating the commercial loads with their corresponding operating periods per day yields the total commercial load profile of the village.

Figure 3-5 shows the total residential and commercial load profile of Toba MG within 24 hour.

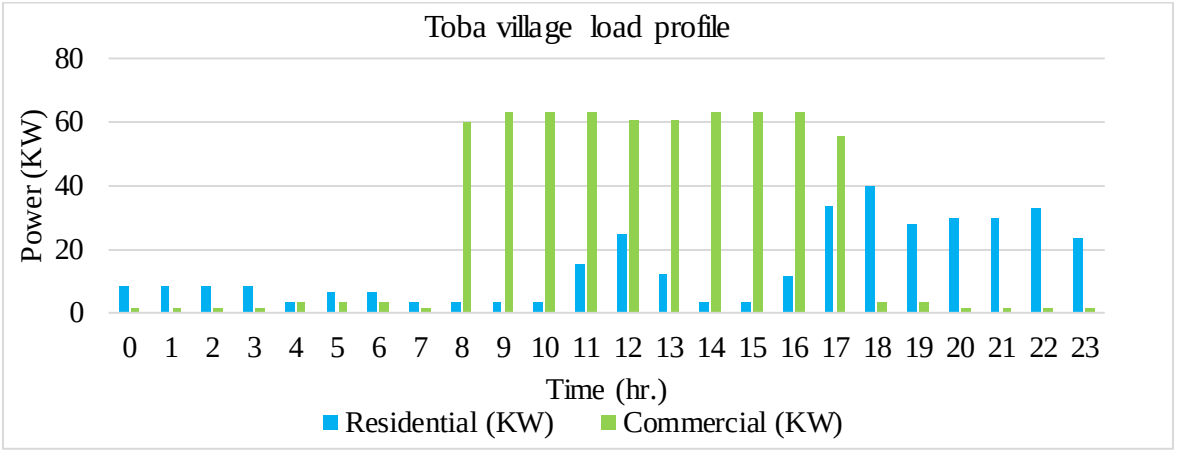


*Figure 3-5: Residential and Commercial load profile of Toba MG.*

In this study, instead of employing uniform load data for each day and throughout the day, random variability inputs are utilized on the load profile. This approach introduces randomness to the load data, enhancing its realism. The random variability inputs encompass both day-to-day and time-step variability. Day-to-day variability entails random changes to the load profile on a daily basis, maintaining the same shape while scaling the load upward or downward. Time-step variability alters the shape of the load profile without impacting its overall magnitude.

### 3.4.4. Toba MG Deferrable Load

In Toba village, deferrable load for irrigation purposes, represented by pumps, is taken into account. Figure 3-6 depicts the deferrable load demand of the village, highlighting a noticeable decrease in water pump demand during the rainy seasons, from May to October.

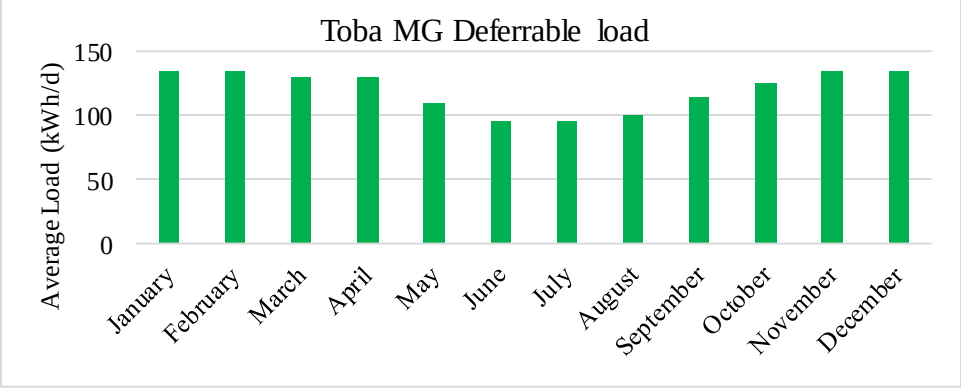


*Figure 3-6: Toba MG pump load demand.*

The storage capacity and peak load of the deferrable load of Toba village is shown in Table 3-5.

Table 3-5: input data for deferrable load consideration.

| Description | Units | value |
|---|---|---|
| Storage capacity | KWh | 230 |
| Peak Load | KW | 75 |

The capacity of the storage tank, measured in terms of kilowatt-hours (kWh) of energy required to fill it, is referred to as storage capacity. Meanwhile, the peak load denotes the rated power of the pump [28, p. 19].

### 3.4.5. Micro-Hydro Power of Toba MG

In Toba village, there is a Toba River suitable for micro-hydro power generation, from which output power can be obtained using the following formula:

$$P_{hyd} = \eta_{hyd} * \rho_{water} * g * h_{net} * Q_{turbine}$$

*Where* $P_{hyd}$ = output power of hydro turbine (W)

$\eta_{hyd}$ = hydro turbine efficiency (%)

$\rho_{water}$ = density of water (1000 kg/$m^3$)

$g$ = acceleration due to gravity (9.81 m/$s^2$)

$h_{net}$ = effective head (m)

$Q_{turbine}$ = hydro turbine flow rate ($m^3$/s)

Substituting the values, Toba Micro hydro power output will be

$$P = 0.8 * 1000\frac{Kg}{m^3} * 9.81\frac{m}{s^2} * 60m * 0.11\frac{m^3}{s}$$

$$P = 51796.8\ W = 51.796KW$$

Table 3-6 presents some of the micro-hydro input data necessary for the optimal analysis of the Toba microgrid.

Table 3-6: input data of Toba Micro-hydro power.

| Description | Units | Value |
|---|---|---|
| River name | | Toba |
| Available Head | m | 60 |
| Design flow rate | L/s | 110 |
| Efficiency | % | 80 |
| Capital cost | $ | 129,500 |
| Replacement cost | $ | 64,750 |
| O&M cost | $/year | 2,694 |
| Lifetime | Years | 40 |
| Capacity $P = \rho g h Q \eta$ | KW | 51.797 |

Capital Cost refers to the initial investment required for the micro-hydro system. Based on [29] and [30], a capital cost of $2500 per kilowatt (kW) is considered in this study.

Operations and Maintenance (O&M) Cost represents the annual expenditure associated with the operation and maintenance of the micro-hydro system. As per [30], the average O&M cost for micro-hydro power is $52 per kW per year. Consequently, the corresponding O&M cost for the Toba micro-hydro system amounts to $2694 per year.

Lifetime denotes the anticipated operational duration of the hydro system. In accordance with [30], the expected lifetime of the Toba micro-hydro system is 40 years.

Available Head signifies the vertical distance between the intake and the turbine.

Design Flow Rate refers to the flow rate at which the hydro turbine is designed to operate, representing its maximum efficiency.

Efficiency measures the effectiveness of the hydro system in converting the energy from water into electricity [28, p. 290].

### 3.4.6. Toba MG Photovoltaic system

Table 3-7 outlines some of the PV system input data necessary for the optimal analysis of the Toba microgrid.

Table 3-7: input data of Toba MG PV system.

| Descriptions | Units | Values |
|---|---|---|
| Name | | Generic flat plate PV |
| Capital cost | $/KW | 900 |
| Replacement cost | $/KW | 900 |
| O&M cost | $/years | 18 |
| Derating factor | % | 85 |
| Lifetime | years | 25 |
| Temperature coefficient | $\%/^0C$ | -0.5 |
| Operating temperature | $^0C$ | 47 |
| Efficiency | % | 13 |

### 3.4.7. Toba MG Converter

Table 3-8 presents some of the converter input data necessary for the optimal analysis of the Toba microgrid.

Table 3-8: input data of Toba MG converter.

| Description | Units | value |
|---|---|---|
| Capital cost | $/KW | 300 |
| Replacement cost | $/KW | 300 |
| O&M cost | $/years | 6 |
| efficiency | % | 95 |
| lifetime | years | 15 |

### 3.1.1. Toba MG Battery

Table 3-9 offers some of the battery input data required for the optimal analysis of the Toba microgrid.

Table 3-9: input data of Toba MG Battery.

| Description | Units | Value |
|---|---|---|
| Name | | Li-ion Battery |
| Capital cost | $/unit | 300 |
| Replacement cost | $/unit | 300 |
| O&M cost | $/year | 6 |
| Round trip efficiency | % | 90 |
| String size | | 8 |
| Nominal voltage | V | 6 |
| String voltage | V | 48 |

In Toba microgrid, alongside the costs associated with various microgrid components mentioned earlier, distribution network costs are also factored in. These include a capital cost of $94,000 and an O&M cost of $4,700/yr.

### 3.2. Development of Microgrid Cluster

A Microgrid cluster involves the interconnection of neighboring independently operating MGs for mutual benefit. In this study, to analyze the MG cluster, a hypothetical system is constructed comprising the combined load profiles of Toba, Koza, and Womba MGs (including both primary and deferrable loads), the average GHI of the three villages, Micro-Hydro power with a capacity equivalent to the sum of Toba and Ergino micro-hydro, distribution network costs encompassing the combined three villages, and the expenses associated with interconnecting the villages. Table 3-10 outlines the three individual MGs utilized to develop the MG cluster, while Table 3-11 presents the residential, commercial, and deferrable load consumptions of the respective MGs.

Table 3-10: The three villages' data for MG cluster development.

| Site | Population | House hold | Latitude | Longitude | Income | | | River | hydro Power(KW) |
|---|---|---|---|---|---|---|---|---|---|
| | | | | | Low (%) | Middle (%) | High (%) | | |
| Toba | 4,882 | 976 | $6^0$28' N | $36^0$40'E | 58 | 26 | 16 | Toba | 51.8 |
| Koza | 6,210 | 1,242 | $6^0$28'59"N | $36^0$43'E | 60 | 25 | 15 | | |
| Womba | 4,152 | 830 | $6^0$ 33'N | $36^0$ 47'E | 60 | 20 | 20 | Ergino | 23.5 |

Table 3-11: Residential, commercial and agricultural consumptions of MG

| | Residential | | Commercial | | Deferrable (pump) | | Total | |
|---|---|---|---|---|---|---|---|---|
| | Energy (kWh/d) | Peak Power (kW) | Energy (kWh/d) | Peak Power (kW) | Average load (kWh/day) | Peak Power (kW) | Energy (kWh/d) | Peak P (kW) |
| Toba | 350.19 | 55.72 | 647.39 | 93.79 | 120.00 | 75.00 | 1117.58 | 88.99 |
| Koza | 426.09 | 67.6 | 169.22 | 25.01 | 100.00 | 45.00 | 695.31 | 52.29 |
| Womba | 318.85 | 51.11 | 144.61 | 21.36 | 107.50 | 55.00 | 570.96 | 44.92 |

In the development of the MG cluster, the interconnection system cost is factored in by considering the distances between the villages, as presented in Table 3-12.

Table 3-12: Distance between villages.

| Village #1 | Village #2 | Distance between (in Km) |
|---|---|---|
| Toba | Koza | 8.5 |
| Koza | Womba | 9.1 |
| Toba | Womba | 19.5 |

Figure 3-7 displays the geographical locations of Toba, Koza, and Womba villages.


*Figure 3-7: Geographical locations of Toba, Koza and Womba villages.*

### 3.2.1. Load profile of Microgrid Cluster

Figure 3-8 illustrates the total primary load profile of the MG cluster, encompassing all residential and commercial loads of the three MGs.

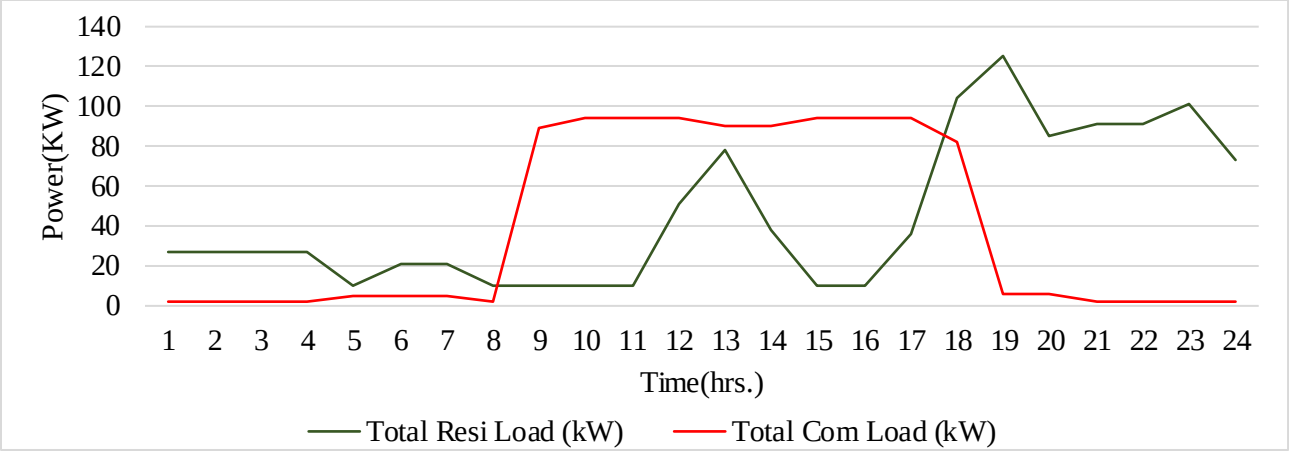


*Figure 3-8: Total Residential and Commercial loads of three MGs.*

### 3.2.2. Distribution Network and Interconnection Cost of Microgrid Cluster

In the optimal planning of MGs, it is crucial to include distribution network costs to ensure a more realistic techno-economic analysis. Additionally, for MG cluster development, the costs associated with interconnection systems between individual MGs should also be taken into consideration. Table 3-13 presents the distribution network costs, while Table 3-14 outlines the costs of the interconnection systems.

Table 3-13: Distribution network cost of individual microgrids

| | Capital Cost ($) | O&M ($/yr.) |
|---|---|---|
| Toba | 94000 | 4700 |
| Koza | 127000 | 6350 |
| Womba | 82000 | 4100 |

Table 3-14: Interconnection cost of microgrids.

| | Voltage (KV) | Distance (Km) | Unit Cost ($/Km) | Cost ($) | Transformer 50KVA ($) |
|---|---|---|---|---|---|
| Toba to Koza | 15 | 8.5 | 15,000 | 127,500 | 2x10,000 |
| Koza to Womba | 15 | 9.1 | 15,000 | 136,500 | 10,000 |
| Microgrid Cluster | | | | 264,000 | 30,000 |

### 3.3. Development of MG Control System for Quasi-Dynamic Simulation

The aim of this section is to develop an MG control system model to perform a quasi-dynamic simulation analysis. But what is quasi-dynamic analysis?

#### 3.3.1. Quasi Dynamic Analysis

Load flow analysis considers the flow of load within a system under a single set of operating conditions. However, it is often necessary to assess the system's performance under the most adverse operating conditions, which can be achieved by conducting multiple load flow analyses encompassing a range of system operating conditions. This is facilitated by quasi-dynamic analysis, which entails conducting load flow analyses in a series of time intervals. To conduct quasi-dynamic analysis, a time-dependent model of the system is required, as various components such as load, PV, SOC, etc., vary with time. Quasi-dynamic analysis typically spans from medium to long-term time scales, ranging from minutes/hours to months/years. By performing quasi-dynamic analysis, the system's operating conditions at different times of the day/month/year can be examined. If a more detailed analysis is warranted, dynamic analysis can be pursued by narrowing the analysis time and incorporating additional detailed modeling. However, dynamic analysis is beyond the scope of this study. Instead, the study focuses on the development of the QDSL control model, which operates within a medium to long-term time range.

Now, let's proceed with the development of the QDSL control model using DigSILENT PowerFactory2022 software. The modeling procedure commences by creating a one-line diagram of the MG.

#### 3.3.2. One Line Diagram of Toba Microgrid

The one-line diagram of Toba MG is depicted in Figure 3-9, clearly illustrating that bus-1 is connected to PV, BESS, residential load, commercial load, deferrable load, and two lines. One line extends to the Hydro-bus, which is linked to Micro-Hydro, while the other line connects bus-1 to bus-2. Bus-2, in turn, is connected to residential load, commercial load, and a line connecting it to bus-3. Finally, bus-3 is linked to residential and commercial loads.

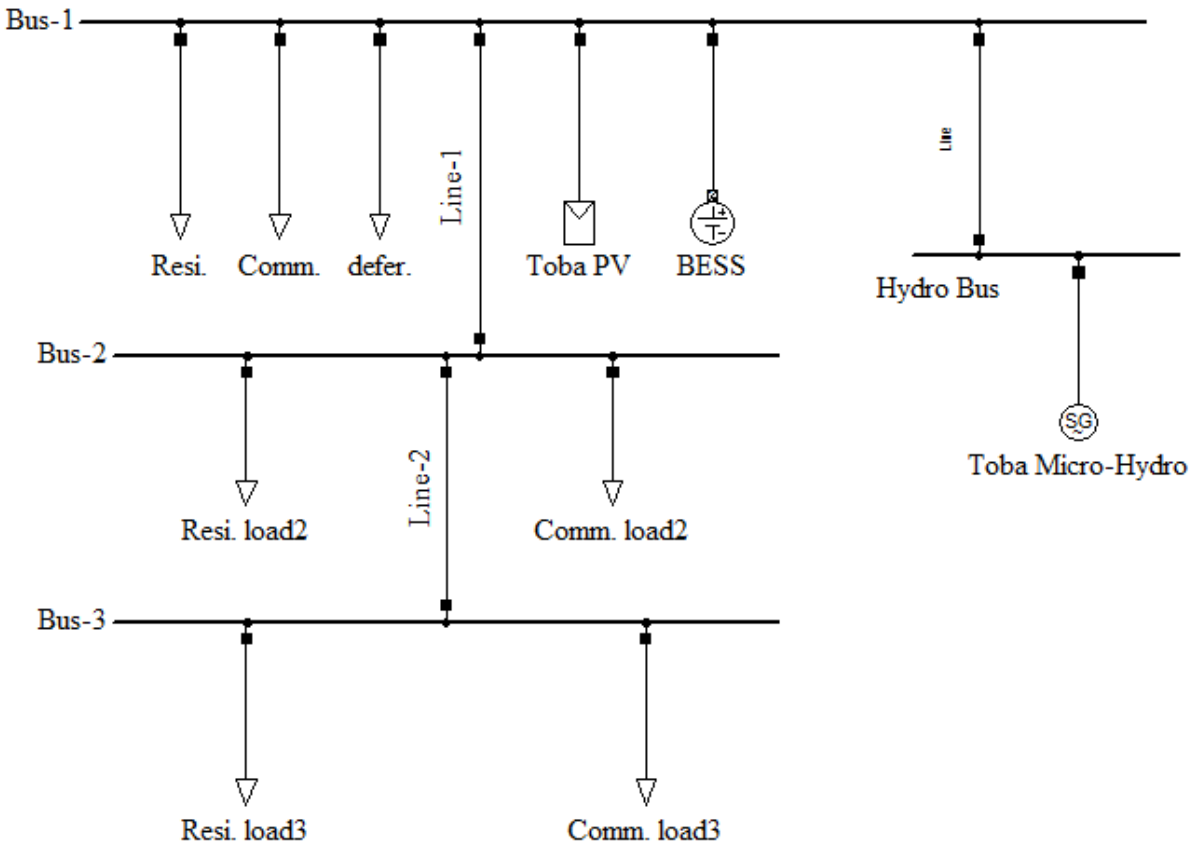


*Figure 3-9: one line diagram of Toba MG.*

### 3.3.3. Architecture of Toba MG

In Toba MG, the energy suppliers include PV and micro-hydro, while the energy storage system consists of batteries, and various loads consume the supplied energy. However, to maintain stable operation of the MG, coordination and control of these components are essential. This responsibility falls on the MG controller, which is tasked with controlling the operation of all components within the MG.

The interaction between the MG controller and the different components of the MG is depicted in the architecture of Toba MG, as shown in Figure 3-10. Various components of the MG, such as micro-hydro, battery, PV, and different load categories such as essential, flexible, and deferrable loads, communicate with the MG controller. The dotted lines in the system architecture represent the data exchange between different components of the microgrid and the MG controller.

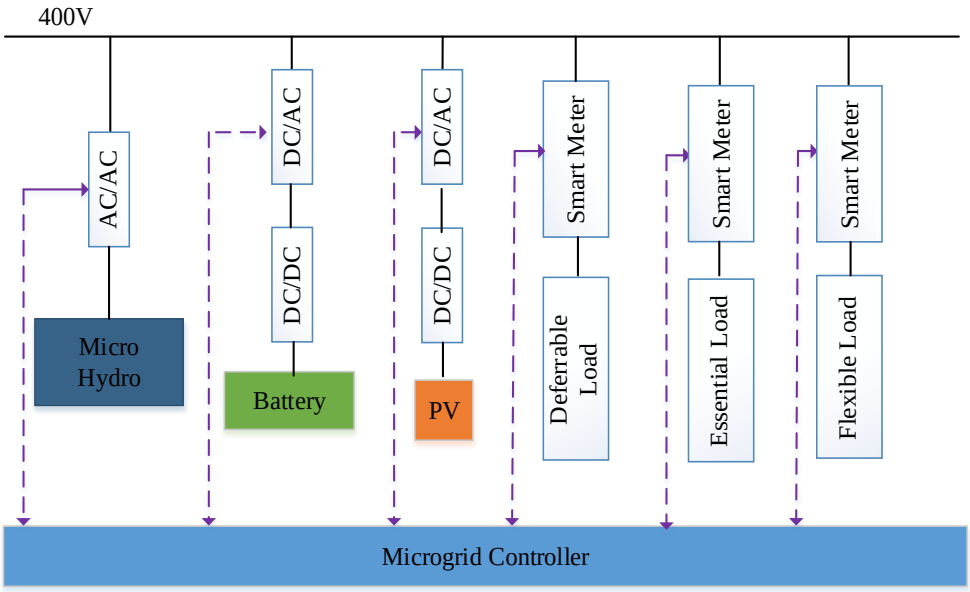


*Figure 3-10: Architecture of Toba MG*

Indeed, it is a two-way communication process. Measurement data and the status of the components are provided to the controller, which then oversees the status of all components, processes the information, and generates controlling signals in response. These signals are then transmitted to each component accordingly, ensuring that the MG operates in a stable manner.

The electrical loads are categorized into three types: essential load, flexible load, and deferrable load, based on their criticality, ability to be shifted, and potential for postponement, respectively.

Essential loads are critical and must be continuously powered to maintain essential services. They are non-negotiable in terms of power availability and must be sustained regardless of other operational considerations. Examples include health centers with critical medical equipment.

Flexible loads are electrical loads that can be adjusted or shifted in response to changes in energy availability. These loads offer flexibility in controlling energy consumption and reducing peak demand, thereby helping to balance supply and demand. In this study, commercial and residential loads excluding critical loads are considered as flexible loads.

Deferrable loads are electrical loads that can be postponed or deferred to a later time without significant impact on operational requirements. These loads can be intentionally shifted to

periods of lower energy demand or higher renewable energy generation to optimize resource utilization and reduce costs. In this study, the irrigation pump is considered as a deferrable load.

### 3.3.4. Microgrid Controller Interface

In the architecture of the MG, the general communication route between MG components and the MG controller is presented. Now, let's take a closer look at the specific parameters the controller uses as input from the MG components and the controlling reference signals the controller sends to each component. The MG controller interface is depicted in Figure 3-11 and explained as follows:

The SOC of the battery, power measurements of the micro-hydro, PV, essential load, flexible load, and deferrable load are provided to the MG controller as input. With these input values and considering predefined constraint conditions, the controller performs a series of computations and generates controlling reference signals based on the MG's operational objective. These output controlling signals are then sent to the respective components of the MG to perform the intended tasks. These output controlling signals include:

The signal "$Ctrl\_PV$ (Mode)" indicates the operation mode of the PV system, such as MPPT or PV curtailment.

During periods when the supplied power is insufficient to meet the primary (residential and commercial) demand, the MG controller initiates load shedding to maintain power balance. Load shedding follows a priority order determined by the controller. Initially, shedding begins with loads categorized as 1st priority, and the shedding percentage may increase depending on the amount of power deficit. It may escalate to the point where all 1$^{st}$ priority loads are disconnected. If demand is still not met, shedding of 2$^{nd}$ priority loads begins, proceeding based on the required power. Both 1st and 2nd priority loads fall under the category of flexible loads and are categorized based on their relative importance level. Loads under 2$^{nd}$ priority are considered "more important" than those under 1$^{st}$ priority. The control signals "Ctrl_1$^{st}$pload" and "Crtl_2$^{nd}$pload" are used to control shedding of 1$^{st}$ priority and 2$^{nd}$ priority loads, respectively.

The control signal "$Ctrl\_Pdfload$" manages the start, stop, or sets the available power for deferrable loads.

The signal "$Pbat\_ref$" regulates the charging/discharging power of the battery.

If the PV system is not required to operate at MPPT mode due to power balance issues, its output follows the reference power signal "$Ppv\_ref$", indicating PV curtailment.

For a micro-hydro generator, the controller sends a reference signal "$Phydro\_ref$" for the output of the micro-hydro to follow. In this study, since constant power output is assumed for the micro-hydro, the reference signal is set to the rated hydro power.

In this manner, the MG controller communicates with the MG components to achieve the operational objectives of the MG.

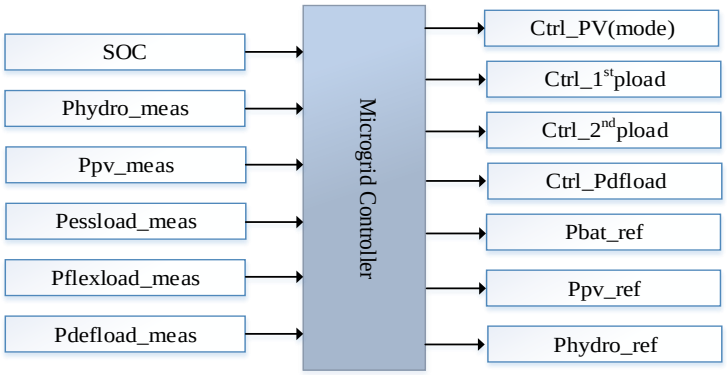


*Figure 3-11: Microgrid Controller Interface*

Having observed the controller interface, let us proceed to explore how the QDSL controller model is organized to achieve stable operation of the MG.

## 3.4. QDSL Modeling Approach

### 3.4.1. Objects of QDSL model

In PowerFactory2022 it is possible to create user defined quasi dynamic model and it includes two objects:

I. $TypQdsl$: library type object and

II. $ElmQdsl$: Network element object

I. $TypQdsl$ :In the QDSL type object the following constituents of the object are need to be develop such as: variables table, connected network elements, results table, initialization script, inputs/outputs for load flow equations, load flow equations script, load flow control script, quasi-dynamic simulation equations and quasi-dynamic simulation control equations.

II. $ElmQdsl$ : In the QDSL element object, part of the components which were defined in a specifically selected $TypQdsl$ are displayed and provided with actual parameters of the respective element. From the selected $TypQdsl$: parameter of variables, connected network elements and load flow network elements inputs/outputs are displayed in the element object.

The load flow equations script of Toba MG controller is presented in the APPENDIX.

### 3.4.2. QDSL Model Integration within DIgSILENT Project

The integration of QDSL model within DIgSILENT project is shown in Figure 3-12 and it is clearly displayed that the power equipment element represents the MG network elements together with their respective parameters and they exchange data with $ElmQdsl$ object. The $ElmQdsl$ takes measurements from the power equipment element and provides a reference value to the MG elements. Both $ElmQdsl$ and power equipment element are confined inside the network data model of DIgSILENT project. Inside the project library there is $TypQdsl$ object and it is referred by $ElmQdsl$ object.

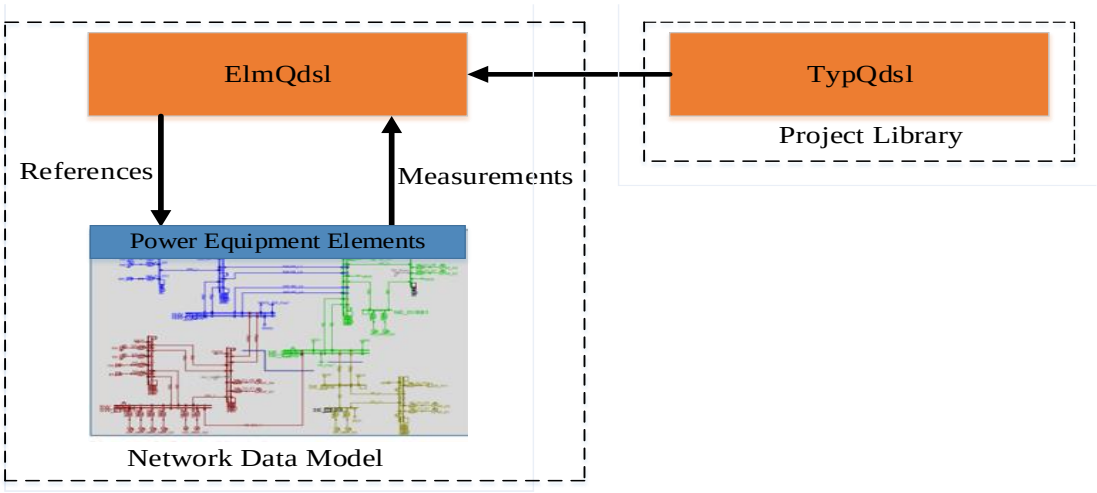


*Figure 3-12: QDSL model Integration within the DIgSILENT project*

### 3.4.3. Quasi-Dynamic Model Algorithm Flow

Having the *Qdsl* model developed and seen how it is integrated within DIgSILENT project let proceed to the control algorithm flow of the model. Since the model contain time dependent state variable like SOC, the control algorithm flow starting from current time to the next time step is shown in Figure 3-13 and a short description of the functionality of each blocks of simulation procedure is presented as follows:

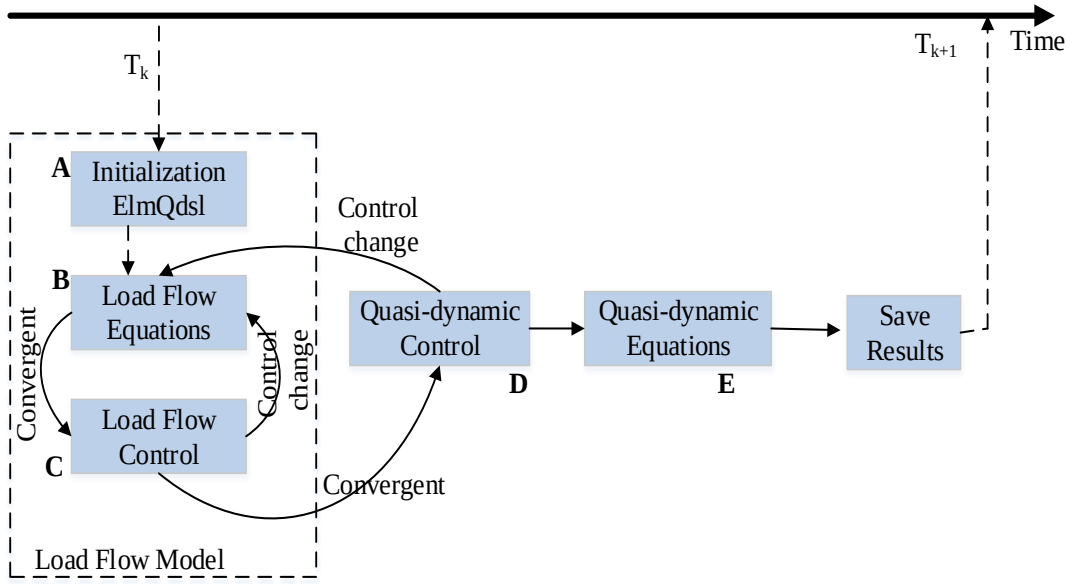


*Figure 3-13: Simulation Procedure of QDSL model*

A. Initialization block: this block contains the initialization script with the aim of initializing the model state variable, parameters and result variables. The initialization could be using constant value or equations containing network elements parameters. During load flow calculation this block is executed once before load flow iteration starts. Once the initialization is run then load flow proceeds. In the load flow section there are two parts: the load flow equation and load flow control.

B. Load Flow Equations block: contain load flow equations script which is the load flow equation of the model at fixed state i.e. while it is running the state of the model does not change. Taking battery as example, during this period the battery injection power making the load flow stable is determined while neither the state of charge nor the charging mode of the battery is changed. If the load flow converges then proceed to load flow control.

C. Load Flow Control block: contain load flow control script and unlike load flow equation here the state of the model can be changed to get satisfactory operating point. So if a control change is required then return to load flow equation and the load flow is performed with the changed control condition else proceed to quasi-dynamic control.

D. Quasi-Dynamic Simulation Control block: contains quasi-dynamic simulation control script which checks the convergence of quasi dynamic simulation solution at a time step of $T_k$. It is in this script that a simulation event is generated and one more iteration of load flow loop will run. So if a control change is required then it goes to load flow equation else proceed to quasi dynamic equation.

E. Quasi-Dynamic Simulation Equations block: contains quasi-dynamic simulation equations script which is the differential equations of all state variables in the model and it runs only once per simulation time step.

At this stage the results are saved and be ready for the next time step $T_{k+1}$ and the procedure continues.

### 3.5. Operating Conditions of Microgrid

In this section, the overall control strategy of the MG is presented, considering Toba MG. The MG components have different operating conditions at different times of the day. Let's consider the operating conditions of MG components under various circumstances and then illustrate the MG controller's overall management strategy during such situations.

A. Battery Operation Conditions

The MG controller performs the power balance of the MG using the following equation

$$P_{hydro} + P_{PV} = P_{load} + Pdfload - P_{bat}$$

Where: $P_{hydro}$= output power of micro-hydro

$P_{PV}$=Pv output power

$P_{load}$=primary load (residential + commercisl load)

$Pdfload$=deferrable load

$P_{bat}$=battery charging/discharging power (charging is negativ)

The microhydro and PV supply power, while loads consume the supplied power, and the battery operates as a supply during discharging and as a load during the charging period. But

when does the battery charge/discharge? To determine when the battery charges/discharges, $P_{meas}$ (power measurement at a given time without considering the battery and deferrable load) is used.

$$P_{meas} = P_{PV} + P_{\text{hydro}} - P_{\text{load}}$$

A positive $P_{meas}$ implies that the supply power exceeds the primary (residential + commercial) load, and depending on the SOC condition, the battery may charge. Conversely, a negative $P_{meas}$ implies that the supply power is less than the primary load, and again depending on the SOC, the battery may discharge. Therefore, regardless of the sign of $P_{meas}$, the state of charge of the battery is crucial in determining whether the battery charges or discharges.

In addition to SOC, the amount of power available for charging or required to be discharged is another factor that determines the battery's charging or discharging. Hence, to ascertain whether the battery is in a charging or discharging mode of operation, it must be considered from two perspectives.

I. Power perspective
II. Energy perspective.

Operation mode of battery from Power perspective

Charge P =
1. Battery charging
2. Battery inactive
3. Battery discharging

1. Battery charging: is an operation state by which the battery charging power is within $P_{min}^{char.} \leq P_{bat} \leq P_{max}^{char.}$ .
2. Battery inactive: is an operation state where the battery receive/supply zero power and it occurs when $P_{bat} < P_{min}^{char.}$ or $P_{bat} < P_{min}^{discha.}$.
3. Battery discharging: is an operation state by which the battery discharging power is within $P_{min}^{discha.} \leq P_{bat} \leq P_{max}^{discha.}$

Operation mode of battery from Energy perspective

$$chargeE = \begin{cases} 1.\ SOC \leq SOC_{min} \\ 2.\ SOC_{min} \leq SOC \leq SOC_{max} \\ 3.\ SOC \geq SOC_{max} \end{cases}$$

Where: $SOC_{max}$ and $SOC_{min}$ are the maximum and minimum state of charge of battery respectively.

Considering both power and energy perspectives, Figure 3-14 illustrates the various operational conditions of the battery. The terminologies used in the figure are explained as follows:

The left vertical axis represents AC power, while the right vertical axis represents battery charging/discharging power. On the AC power axis, different set points are indicated where $P_{meas}$ (the pink line in the figure) is compared, and based on this comparison, the charging/inactive/discharging state is determined.

$P_{startstore}$ and $P_{startfeed}$ are values set in $ElmQdsl$ and indicate the minimum $P_{meas}$ required for charging and discharging to start, respectively. When $P_{meas} \geq P_{startstore}$, the battery begins charging, and when $P_{meas} \leq -P_{startfeed}$, the battery begins discharging. The battery remains inactive when $P_{meas}$ falls within these threshold values.

In this study, to clearly illustrate the relationship between surplus/deficit power and the charging/discharging of the battery, $P_{startstore}$ and $P_{startfeed}$ values are set to zero.

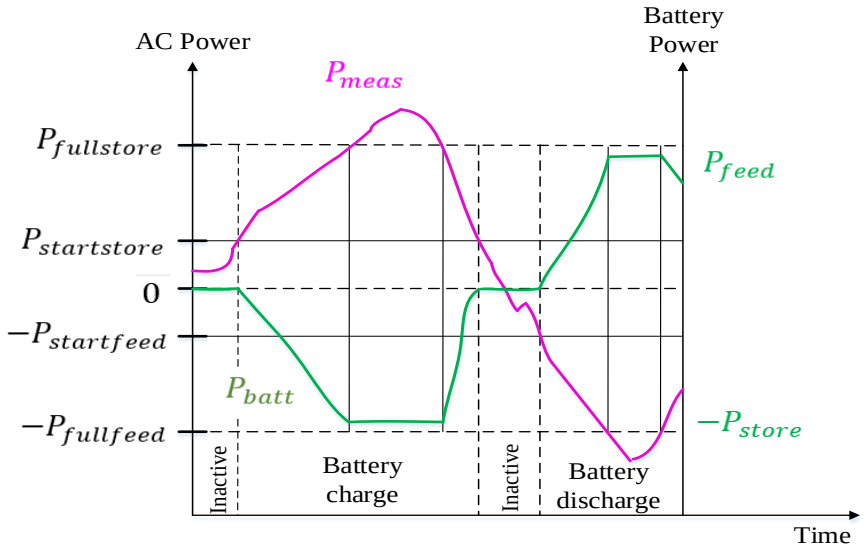


*Figure 3-14: Different battery operation conditions.*

$P_{fullstore}$ and $P_{fullfeed}$ are values set in $ElmQdsl$, indicating the threshold values of $P_{meas}$ at which the battery starts charging or discharging with its rated power. When $P_{meas} \geq P_{fullstore}$, the battery charges with its rated charging power. Conversely, when $P_{meas} \leq -P_{fullfeed}$, the battery discharges with its rated discharging power.

$P_{store}$ and $P_{feed}$ : are values set in $ElmQdsl$ and indicate the rated charging and rated discharging power of battery respectively.

In the figure, the green line represents the battery charging/discharging power. It's clearly indicated that the battery remains in an inactive state, neither charging nor discharging, when $P_{meas}$ is within the range of $P_{startstore}$ and $P_{startfeed}$. However, when $P_{meas} \geq P_{startstore}$, the battery begins charging with power less than $P_{store,}$ and when $P_{meas} \geq P_{fullstore}$, it starts charging with $P_{store}$. Similarly, when $P_{meas} \leq -P_{startfeed}$, the battery starts discharging with power less than $P_{feed}$, and when $P_{meas} \leq -P_{fullfeed}$, it begins discharging with $P_{feed}$.

The charging/discharging power of the battery remains constant at $P_{store}$ or $P_{feed,}$ respectively, when $P_{meas} \geq P_{fullstore}$ or $P_{meas} \leq -P_{fullfeed}$.However, determining the charging or discharging power of the battery when $P_{meas}$ is within the range of $P_{startstore}$ and $P_{fullstore}$ or $P_{startfeed}$ and $P_{fullfeed}$ involves using a reduction factor.

These reduction factors are calculated as follows:

- Discharging reduction factor $= 1 - \frac{P_{meas} + P_{fullfeed}}{P_{fullfeed} - P_{startfeed}}$

The battery discharging power when $P_{meas}$ is within the range of $P_{startfeed}$ and $P_{fullfeed}$ is obtained by applying a reduction factor.

$$P_{batt} = P_{feed} * \left(1 - \frac{P_{meas} + P_{fullfeed}}{P_{fullfeed} - P_{startfeed}}\right)$$

Similarly,

- Charging reduction factor $= 1 - \frac{P_{fullstore} - P_{meas}}{P_{fullstore} - P_{startstore}}$

Similarly, the battery charging power when $P_{meas}$ is within the range of $P_{startstore}$ and $P_{fullstore}$ is obtained by applying a reduction factor.

$$P_{batt} = -P_{store} * \left(1 - \frac{P_{fullstore} - P_{meas}}{P_{fullstore} - P_{startstore}}\right)$$

The negative sign indicates the battery charging state.

B. Photovoltaic Operation Conditions

In this study, two operation modes are considered for the PV system: MPPT and PV curtailment.

The PV operates with MPPT throughout the available hours of irradiance during the day, unless all primary and deferrable loads are supplied, the $SOC \geq SOC_{max}$ or the battery is charging with rated power and there is still excess power available. Under these conditions, the PV undergoes PV curtailment.

C. Micro-Hydro Operation Conditions

In this study the micro-hydro is assumed operating with rated power all the time.

D. Load Operating Conditions

In this study, the loads are categorized into essential, flexible and deferrable loads. Flexible loads are further divided into 1st priority and 2nd priority loads, with priority given to load shedding. The shedding starts with 1st priority loads and progresses until complete disconnection, based on requirements. If further shedding is needed, 2nd priority load shedding commences.

Deferrable loads are supplied power if there is surplus after fulfilling the primary load requirements and if the battery is either charging at the rated power or has already reached $SOC \geq SOC_{max}$.The essential and flexible loads are categorized from combined residential and commercial load.

E. Overall MG Controller Managing Strategy

After discussing the different operating conditions of MG components, let's proceed to the overall MG control strategy, depicted in the flowchart of Figure 3-15.

The control strategy begins with the initialization of PV, micro-hydro, BESS and loads, defining the behavior of the battery from both power and energy perspectives, stating various constraint conditions of MG components and defining load prioritization.

Once the initialization is completed, at every time step, the controller updates measurements of MG components such as $P_{hydro}$, $P_{PV}$, $P_{flexload}$, $P_{essload}$ and $P_{dfload}$. It then checks the energy state of the battery, which could be in any one of the following states.

I. If $chargeE = 3$, i.e. $SOC \geq SOC_{max}$, the battery stops charging, and the deferrable load is switched on. If the available deferrable load power exceeds the maximum limit $\left(P_{max}^{dfload}\right)$, then it is fixed to $P_{max}^{dfload}$, and the extra power is managed by controlling the output of the PV through PV curtailment. Then, in the next predefined time step, the controller goes back to the initial point, updates the measurements of MG components, checks for the SOC of the battery etc. If the SOC doesn't belong to the $chargeE = 3$ state, then the controller checks the $chargeE = 2$ state. In such a way, the control strategy procedure continues.

II. else $chargeE = 2$, i.e. $SOCmin \leq SOC \leq SOCmax$, in this state, the battery could be either in $chargeP = 1$ or $chargeP = 3$ operating condition.

A) If $chargeP = 1$, i.e. the battery is in charging mode. During this period, if the charging power exceeds rated charging power, also called maximum charging power $\left(P_{max}^{charge}\right)$, then the battery is set to charge with $P_{max}^{charge}$, and the extra power energies the deferrable load. In this state, the PV operates in MPPT. During this operational state, if the deferrable load exceeds $P_{max}^{dfload}$, then the deferrable load is set to $P_{max}^{dfload}$, and the extra power is removed through PV curtailment. Then, in the next predefined time step, the controller goes back to the initial point, updates the measurements of MG components, checks for the SOC of the battery, etc. In such a way, the control strategy proceeds. However, if the $chargeE = 2$ condition is satisfied but $chargeP = 1$, then the controller proceeds to $chargeP = 3$.

B) else $chargeP = 3$, i.e. the battery is in discharging mode. During this period if the discharging power exceeds rated discharging power, also called maximum discharging power($P_{max}^{discha.}$), then the battery is set to $P_{max}^{discha.}$ and the extra power requirement is maintained by shedding 1st priority load. During this condition PV operates in MPPT mode. If the power requirement is not satisfied with 1st priority load shedding, then 2nd priority load shedding is initiated. If these proceed and the whole flexible load shedding is not enough then it is the worst extreme state which causes critical load shedding. But with micro-hydro power, which can supply during night time as well, the occurrence of critical conditions is very rare. Then, in the next predefined time step, the controller goes back to the initial point, updates the measurements of MG components, checks for the SOC of the battery, etc.

III. else $chargeE = 1$, i.e. $SOC \leq SOC_{min}$. in this state, the battery stops discharging. During this period, if the supplied power is insufficient to meet the primary load, 1st priority load shedding is initiated. If shedding 1st priority loads is not enough, then then 2nd priority load shedding proceeds, and afterwards, the same procedure as presented in part IIB above is carried out.

### 3.7.1. Operating modes of MG

Different operating modes for the power management strategy of MG is presented in Table 3-15.

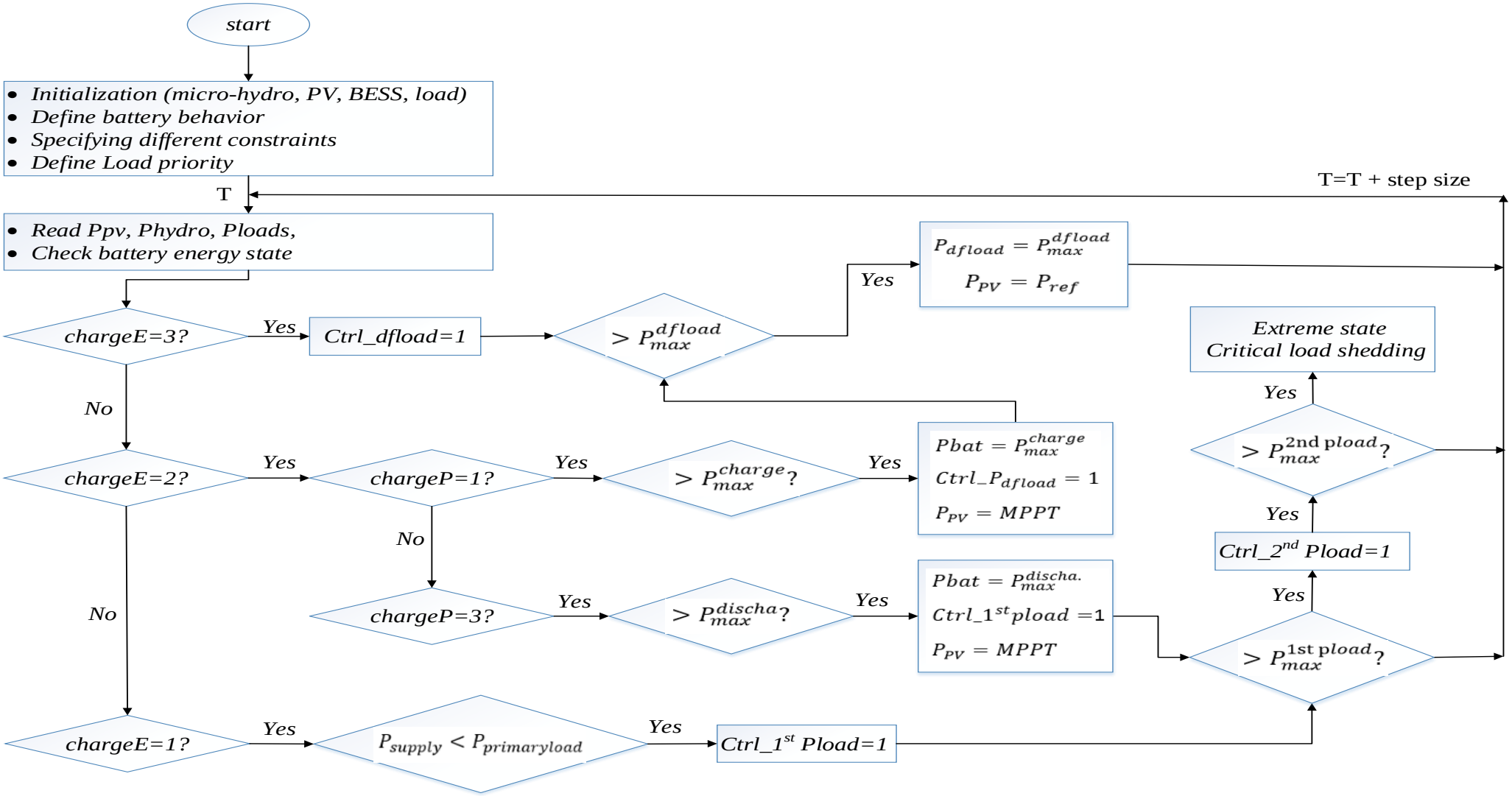


*Figure 3-15: Flowchart of MG control strategy.*

Table 3-15: Different operating mode and power management strategies of MG

| Operation mode | Description | energy state of battery | PV operation mode | Deferrable load | Flexible load |
|---|---|---|---|---|---|
| 1 | $SOC < SOC_{min}$, start 1st priority load shedding | $chargeE = 1$ | MPPT | Off | 1st priority load shedding<br>2nd priority load operating |
| 2 | Transfer from mode 1, 1st priority load is completely shed= 0, start 2nd priority load shedding | $chargeE = 1$ | MPPT | Off | 1st priority load stop<br>2nd priority load shedding |
| 3 | Transfer from mode 2, 2nd priority load is completely shed=0, extreme state, critical load shedding | $chargeE = 1$ | MPPT | Off | 1st priority load stop<br>2nd priority load stop<br>Critical load shedding |
| 4 | $SOC_{min} \leq SOC \leq SOC_{max}$, battery discharging within power limit | $chargeE = 2$ | MPPT | Off | 1st priority load operating<br>2nd priority load operating |
| 5 | $SOC_{min} \leq SOC \leq SOC_{max}$, battery discharging over power limit, start 1st priority load shedding | $chargeE = 2$ | MPPT | Off | 1st priority load shedding<br>2nd priority load operating |
| 6 | Transfer from mode 5, 1st priority load is 0, start 2nd priority load shedding | $chargeE = 2$ | MPPT | Off | 1st priority load stop<br>2nd priority load shedding |
| 7 | Transfer from mode 6, 2nd priority load is 0, extreme state, critical load shedding | $chargeE = 2$ | MPPT | Off | 1st priority load stop<br>2nd priority load stop<br>Critical load shedding |
| 8 | $SOC_{min} \leq SOC \leq SOC_{max}$, battery charging within power limit | $chargeE = 2$ | MPPT | Off | 1st priority load operating<br>2nd priority load operating |
| 9 | $SOC_{min} \leq SOC \leq SOC_{max}$, battery charging over power limit, switch on deferrable load | $chargeE = 2$ | MPPT | On | 1st priority load operating<br>2nd priority load operating |
| 10 | Transfer from mode 9, deferrable load over $P_{max}^{defer}$ start PV curtailment | $chargeE = 2$ | $P_{PV\_ref}$ | On | 1st priority load operating<br>2nd priority load operating |
| 11 | $SOC > SOC_{max}$, start deferrable load | $chargeE = 3$ | MPPT | On | 1st priority load operating<br>2nd priority load operating |
| 12 | Transfer from mode 11, deferrable load over $P_{max}^{defer}$ start PV curtailment | $chargeE = 3$ | $P_{PV\_ref}$ | On | 1st priority load operating<br>2nd priority load operating |

### 3.8. Control Strategy of Microgrid Cluster

In the previous section the control strategy of individual MG is discussed and in this section the control strategy of interconnected MGs forming an MG cluster is presented. For MG cluster there are different controlling approaches such as decentralized architecture [31], [32], centralized architecture [33], distributed architecture [34], [35] etc. and each of the controlling architecture has advantages and disadvantages. However, it is not the intention of this study to compare between different controlling strategies of MG cluster and instead one of the hierarchical control architectures the so called master-slave is used [36]–[40].

#### 3.8.1. One Line Diagram of MG Cluster

The one line diagram of the MG cluster is shown in Figure 3-16. In the figure three MGs Toba, Koza and Womba are interconnected through their respective transformers to develop MG cluster and the components of each MGs are also indicated.

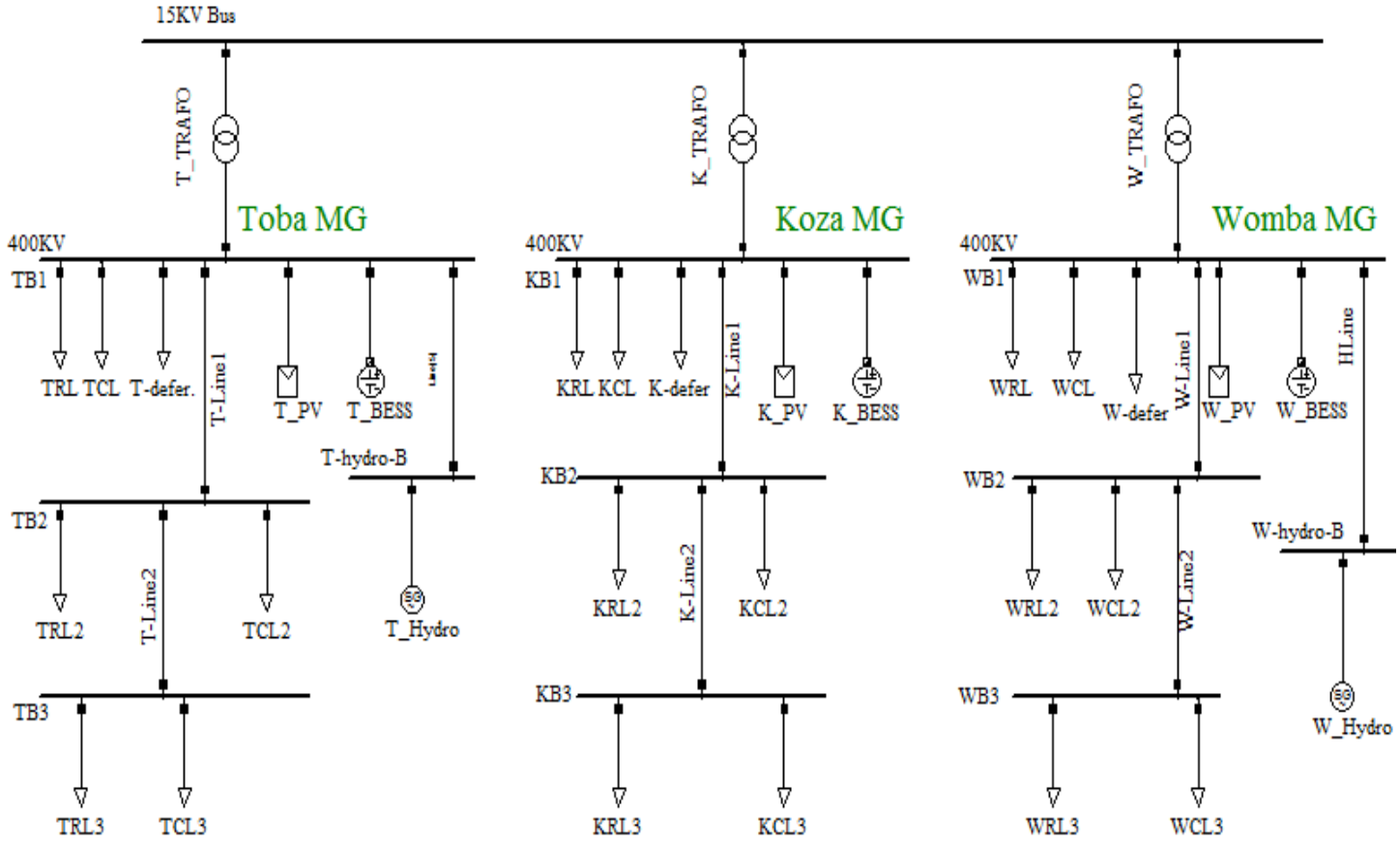


*Figure 3-16: One line diagram of MG cluster*

### 3.8.2. Architecture of MG cluster

The components mentioned in one line diagram of MG cluster need to be controlled for stable operation of MG cluster and to achieve that the proposed architecture of MG cluster containing MG components, controllers, the interconnection between MGs to form MG cluster and planned master-slave control strategy are clearly shown in Figure 3-17.

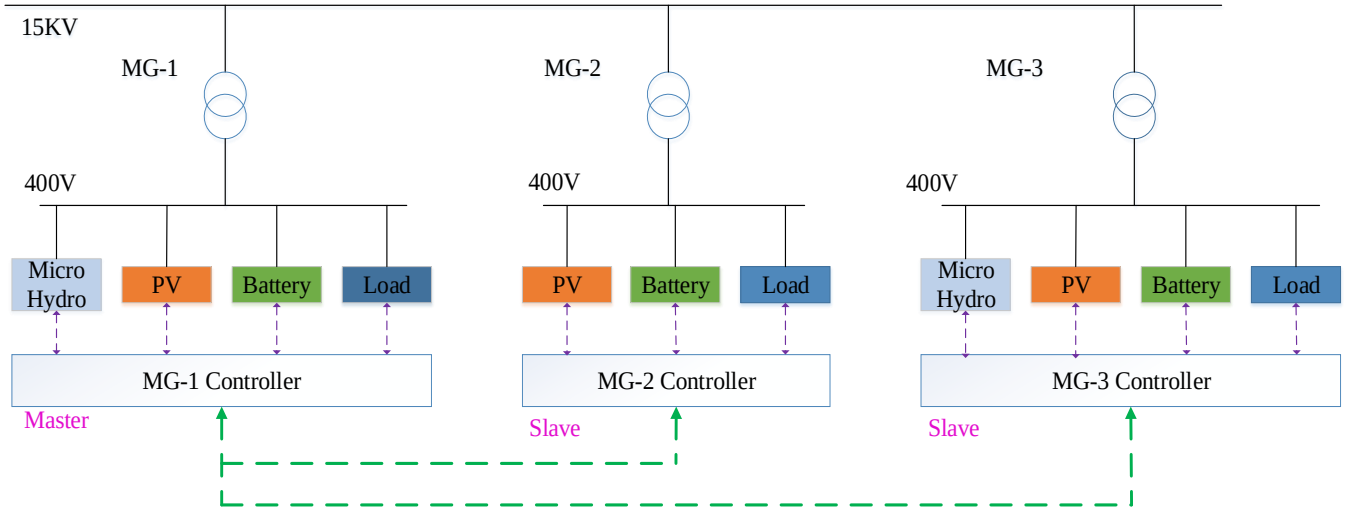


*Figure 3-17: Architecture of MG cluster*

MG-1, MG-2 and MG-3 represent Toba, Koza and Womba MGs respectively and each of them has their own controller for stable operation of the respective MG. Besides maintaining stable operation of MG-1, the master controller oversees and manages the MG cluster. In the architecture, the controller of MG-1 is the master whereas MG-2 and MG-3 are slaves. The master controller manages the operation of all MGs and sends controlling signals to the slave controllers whenever necessary.

### 3.8.3. Data Exchange within MG Cluster

To manage the overall operation of the MG cluster, there must be an appropriate data exchange between the master-slave controllers. Communicating signals between master-slave controllers and MG controller interface are shown in Figure 3-18. The master controller oversees each MG operation status and sends controlling signals like load shedding, power transfer etc. so as to share the burden of individual MG power deficit and for better operation of the overall system.

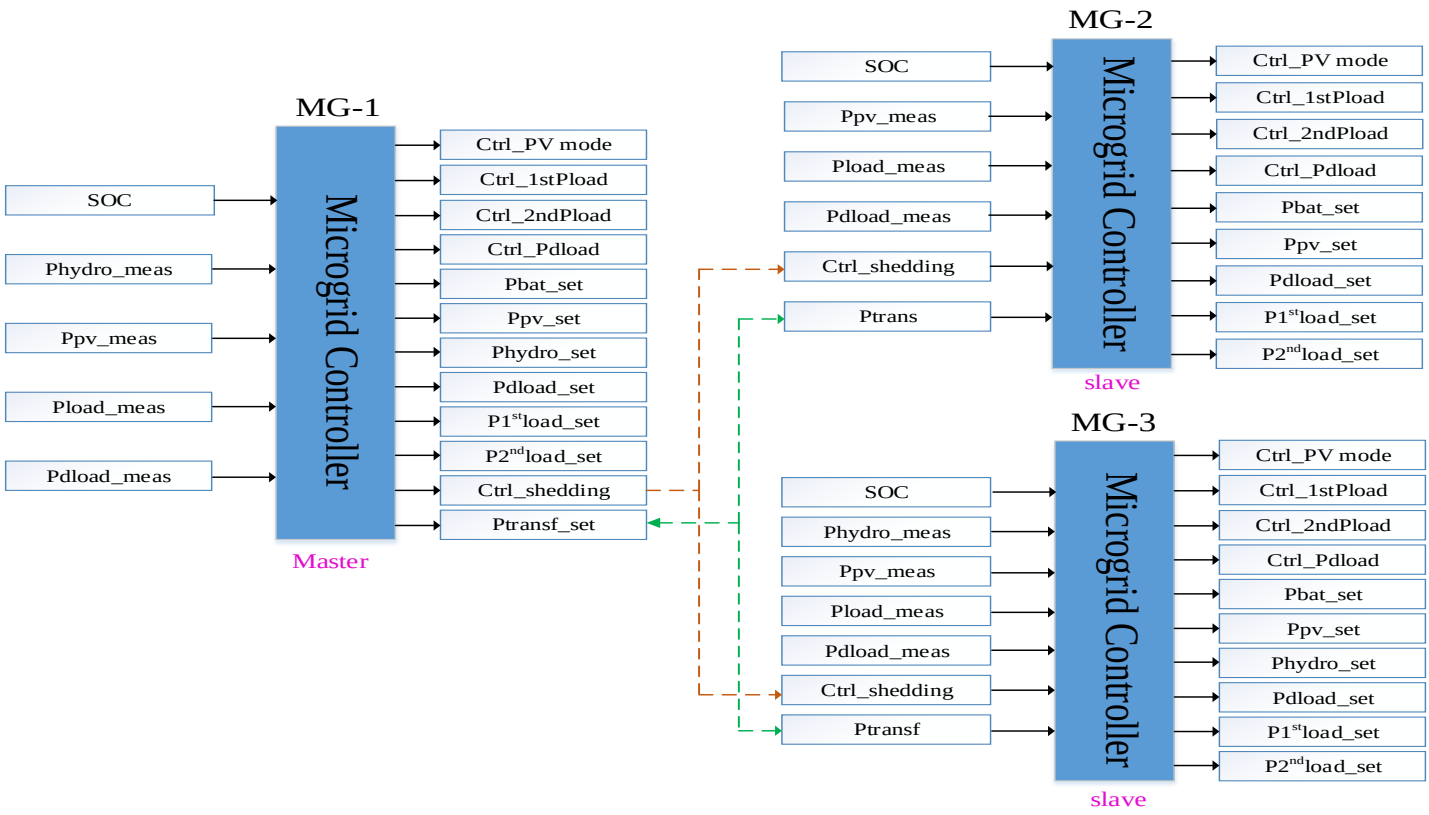


*Figure 3-18: Data exchange within MG cluster*

In master-slave control strategy each controller has its own responsibilities to perform in order to maintain the overall MG cluster operate stable. So the controlling strategy of master and slave controller are presented as follows.

### 3.8.4. Slave Control Strategy

In Figure 3-19, the flowchart illustrating the controlling strategy of the slave MG controller is shown and presented as follows: The controlling mechanism begins with initialization and specifying constraints of PV, micro-hydro, BESS, loads and transformer power exchange ($P_{transfer}$), defining battery behavior and load priority. Then, at each time step, the controller updates power measurement readings of PV, micro-hydro, load, transformer power exchange, calculates $P_{meas}$ and checks battery energy state. Depending on the state of $P_{meas}$, the controller follows either of the following two paths.

1. If $P_{meas} > 0$, then the battery could charge depending on whether $chargeE = 3, 2\ or 1$.

A. If $chargeE = 3$, i.e. $SOC \geq SOC_{max}$, then the deferrable load is switched on. If the deferrable power exceeds the maximum limit, then it will be set to $P_{defer} = P_{max}^{defer}$, and the extra power is sent to the master MG. Then, in the next time step, the controller starts again by updating measurement readings of MG components, and so on.

B. else $chargeE = 2$, i.e. $SOC_{min} \leq SOC \leq SOC_{max}$, in this state, the battery proceeds with charging. If $P_{bat} \geq P_{max}^{char}$, then the charging power is set to $P_{max}^{char}$, and the extra power supplies the deferrable load. If the deferrable power exceeds the maximum limit, then it will be set to $P_{defer} = P_{max}^{defer}$, and the remaining power is sent to the master MG. Then, in the next time step, the controller starts again by updating measurement readings of MG components, and so on.

C. else $chargeE = 1$, i.e. $SOC \leq SOC_{min}$, in this state, the battery charges. If $P_{bat} \geq P_{max}^{char}$, then the charging power is set to $P_{bat} = P_{max}^{char}$, and afterwards, the controlling strategy follows the same procedure as in part (B) above.

2. If $P_{meas} \leq 0$, then the battery could discharge depending on whether $chargeE = 3, 2\ or 1$.

a. If $chargeE = 3$, i.e. $SOC \geq SOC_{max}$, in this state, the battery discharges. If the discharging power exceeds the maximum limit, then the discharging power is set to $P_{bat} = P_{max}^{dischar}$, and the master controller sends available power, beyond its primary load demand, to this slave MG. However, if the available amount of transferred power is not enough to satisfy the primary load of the slave MG, then the master controller orders 1st priority load shedding for all MGs. If this is still insufficient, then 2nd priority load shedding will proceed. If even this is not enough, then extreme conditions, i.e. critical load shedding, will take place. However, with micro-hydro in two of the MGs, which can also supply power during night time, the probability of extreme conditions is very rare. Then, in the next time step, the procedure starts by updating measurement readings of MG components, and so on.

b. else $chargeE = 2$, i.e. $SOC_{min} \leq SOC \leq SOC_{max}$, the battery proceeds with discharging. If $P_{bat} \geq P_{max}^{dischar}$, then the battery discharging power is set to $P_{bat} = P_{max}^{dischar}$, and afterwards, the same control procedure as in (a) above is followed.

c. else $chargeE = 1$, i.e. $SOC \leq SOC_{min}$, the master controller sends available power, including discharging of the master MG battery if necessary, to the slave MG.

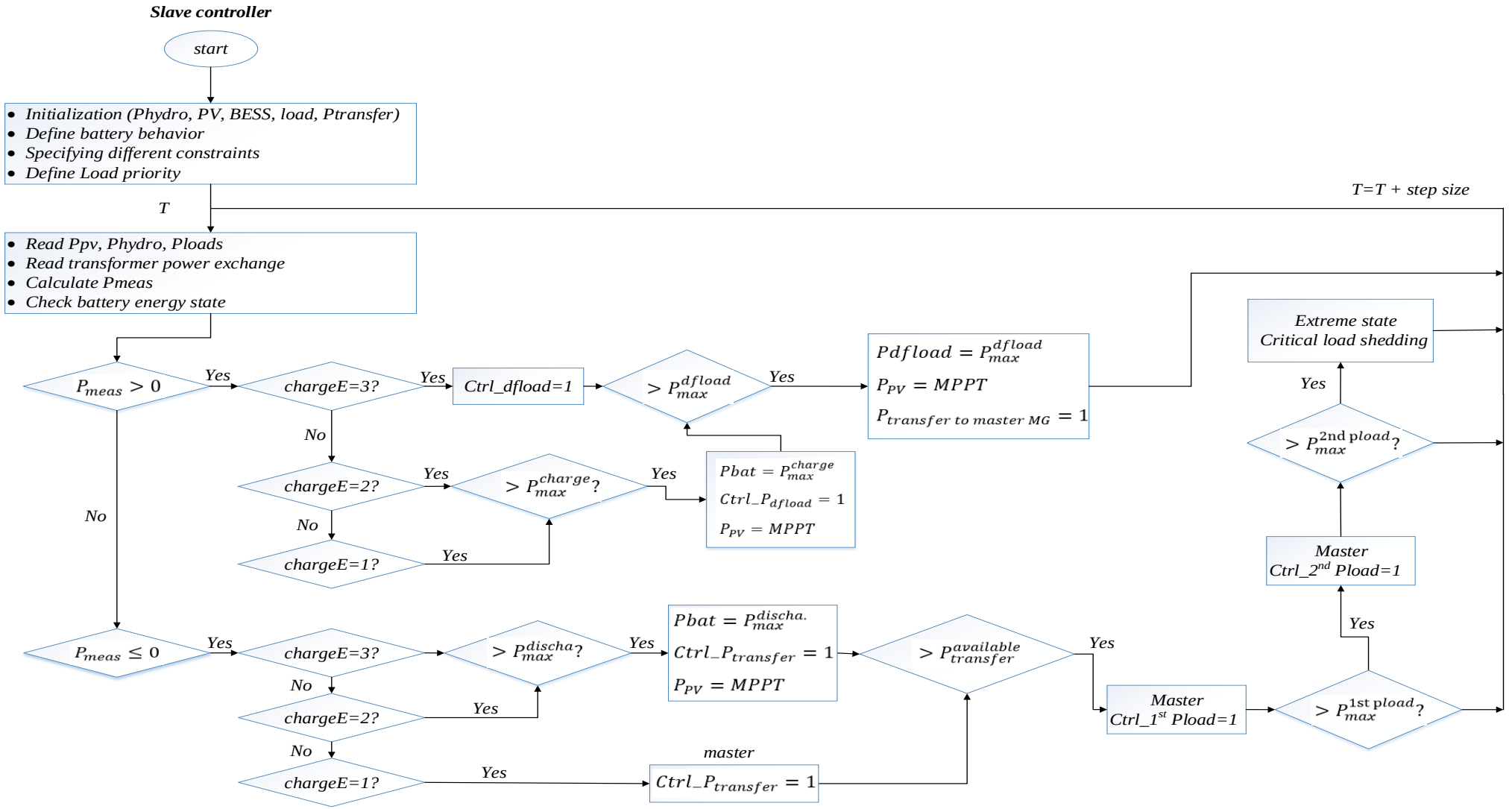


Figure 3-19: Flowchart of slave controller operation strategy.

if the available transfer power is not enough to balance the supply and demand of the slave MG, then the master controller sends a load shedding control signal for all MGs, and the next process proceeds in a similar way as explained in (a) above.

In slave MG, the PV operates only in MPPT mode, and there is no PV curtailment. Whenever extra power beyond $P_{defer} = P_{max}^{defer}$ , is available, it will be transferred to the master MG. Therefore, PV curtailment could be performed if necessary only in the master MG.

### 3.8.5. Master Control Strategy

Unlike slave controller, whose objective is to maintain the stable operation of that particular MG, the master controller oversees all MGs within the cluster and controls the stable operation of the MG cluster in addition to managing the local system. To achieve this objective, the master control strategy flowchart is shown in Figure 3-20 and presented as follows.

The controlling mechanism begins with initialization and specifying constraints of MG components, defining the battery behavior and load priority. After the initialization is completed, the algorithm proceeds to reading measurements such as PV power, micro-hydro power, loads, transformer power exchange, the energy state of all batteries within the MG cluster and $P_{meas}$. Having competed the initialization and assigned measured values, the overall controlling strategy then proceeds to one of two paths depending on the result of $P_{meas} + P_{transfer\ from\ slave\ MG}$. In the flowchart $P_{trans}$ indicate $P_{transfer\ from\ slave\ MG}$.

1. If $P_{meas} + P_{trans} > 0$ i.e. the battery of the master MG could charge, depending on whether $chargeE = 3, 2\ or\ 1$.

A. If $chargeE = 3$, i.e. $SOC \geq SOC_{max}$, in this state, the battery is fully charged. So, the controller checks if in anyone of the slave MGs $chargeP = 3$, i.e. battery discharging is taking place. If so, then the master MG, instead of starting its deferrable load, supports the slave MG. But if the slave MG is in the $chargeP = 1$ state, then the master MG starts its deferrable load instead of transferring power to the slave MG.

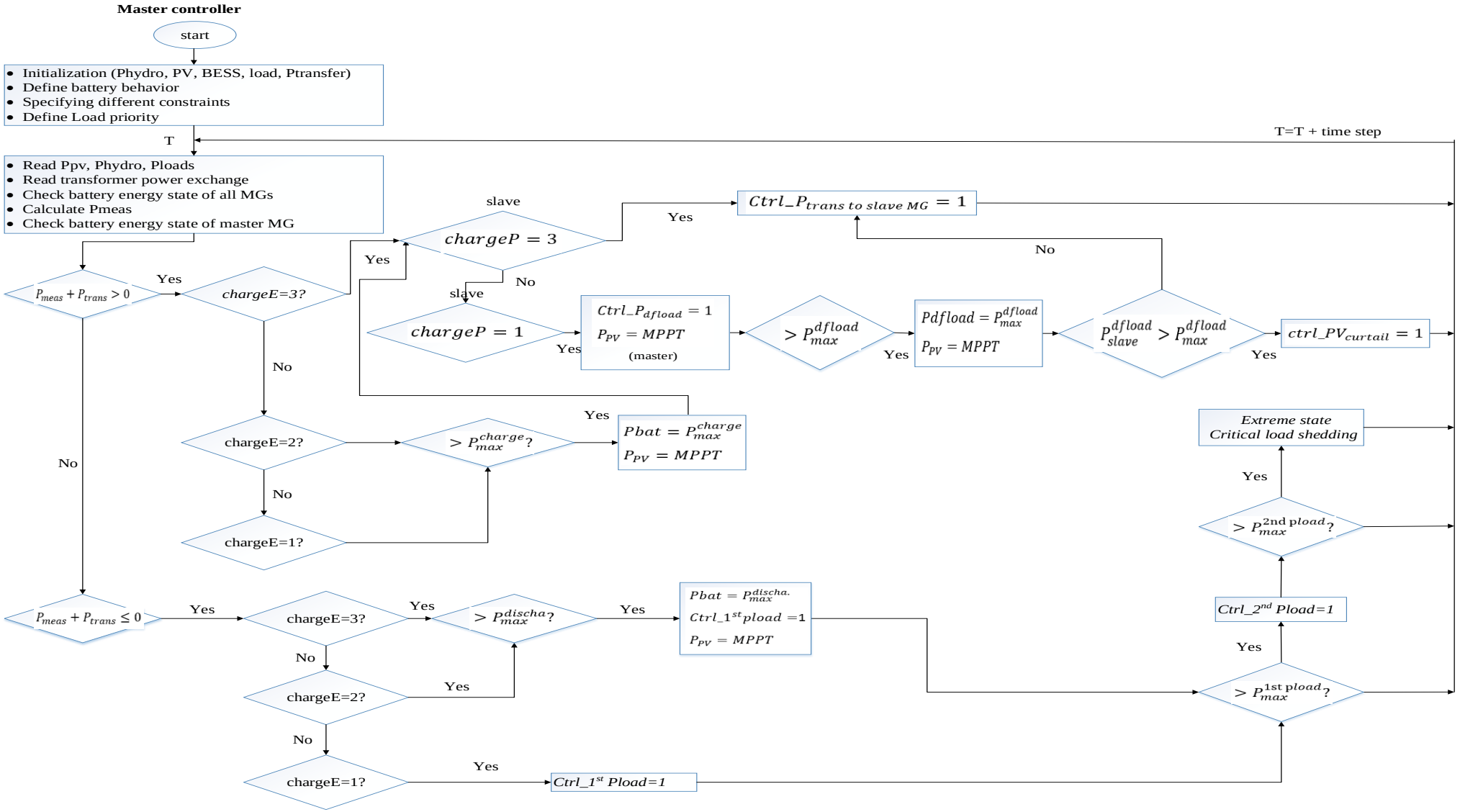


*Figure 3-20: Flowchart of master controller operation strategy.*

If in the master MG $P_{defer} \geq P_{max}^{defer}$, then the power is set to $P_{defer} = P_{max}^{defer}$ and the fate of the extra power beyond $P_{max}^{defer}$ depends on the deferrable load power state of the slave MGs. That is, if in the slave MG $P_{slave}^{defer} > P_{max}^{defer}$, then PV curtailment of the master MG takes place, whereas if $P_{slave}^{defer} < P_{max}^{defer}$, then the extra power in the master MG is transferred to the slave MG. In this strategy, the PV operates in MPPT except in the PV curtailment situation. Then, in the next time step, the procedure starts by updating measurement readings of MG components and so on.

B. else $chargeE = 2$, i.e. $SOC_{min} \leq SOC \leq SOC_{max}$, the battery proceeds to charge. if $P_{bat} \geq P_{max}^{char}$, then the charging power is set to $P_{max}^{char}$, and the fate of the extra power is decided considering the power state of the slave MG battery as explained in part (A) above. Then the procedure follows the same path.

C. else $chargeE = 1$, i.e. $SOC \leq SOC_{min}$, the battery charges. If $P_{bat} > P_{max}^{char}$, then the charging power is set to $P_{bat} = P_{max}^{char}$, and the fate of the extra power follows the same procedure as in part (A) above.

2. If $P_{meas} + P_{trans} \leq 0$, i.e. the battery of the master MG could discharge, depending on whether $chargeE = 3, 2, or\ 1$.

a. If $chargeE = 3$, i.e. $SOC \geq SOC_{max}$, the battery discharges. If the discharging power exceeds the maximum limit, then it is set to $P_{bat} = P_{max}^{dischar}$, and the extra power requirement is fulfilled by starting 1st priority load shedding in all MGs. If this is insufficient, then 2nd priority load shedding proceeds, and if still inadequate, extreme conditions requiring critical load shedding occur. However, due to the reasons explained in the previous section, the probability of extreme conditions is very rare. During this mode of operation, the PV operates in MPPT. Then, in the next time step, the procedure starts by updating measurement readings of MG components, and so on.

b. else $chargeE = 2$, i.e. $SOC_{min} \leq SOC \leq SOC_{max}$, the battery proceeds to discharge. If $P_{bat} \geq P_{max}^{dischar}$, then the battery discharging power is set to $P_{bat} = P_{max}^{dischar}$, and afterwards, the same control procedure as in part (a) above follows.

c. else $chargeE = 1$, i.e. $SOC \leq SOC_{min}$, the master sends 1st priority load shedding order to all MGs, and afterwards, the process proceeds in a similar way as explained in part (a) above.

# Chapter 4

# Results and Discussion

## 4.1. Optimal Sizing Result of Toba Microgrid

In the optimal sizing of the Toba microgrid, the main concern is to supply the predefined MTF based load demand with a minimum-cost solution. In the process of optimization, much effort is given to compromising between three quantities: cost, reliability, and affordability. For cost minimization analysis, NPC, COE, initial capital cost, operating cost, annual capacity shortage, and allowed minimum SOC are considered. The percentage of capacity shortage has an impact on the optimal sizing of MG components. In this study, a capacity shortage of 0 to 10 percent is studied, and since only clean energy is used, a renewable fraction of 100% is considered. A capacity shortage is a shortfall that occurs between the required operating capacity and the actual amount of operating capacity the system can provide. Figure 4-1 shows the optimal sizing of PV, battery, micro-hydro (assumed constant), and converter for different capacity shortages of the Toba microgrid.

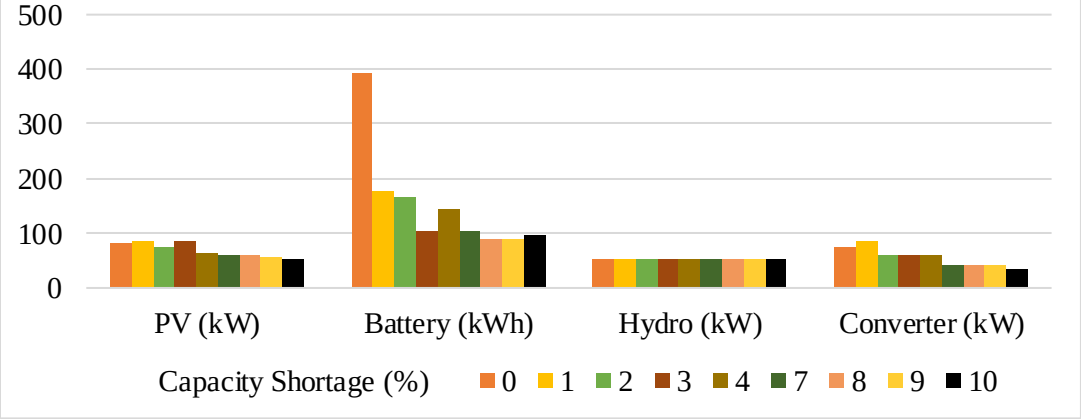


*Figure 4-1: Optimal sizing result of Toba MG with different capacity shortage.*

It is clearly shown that as the percentage of capacity shortage increases, the sizes of the MG components vary irregularly. For instance, the size of PV and battery for the capacity shortage of 3% are 85.81 kW and 104 kWh respectively, and moving one step ahead to a capacity shortage of 4%, their capacities become 62.35 kW and 144.0 kWh. This shows that as the capacity shortage increases from 3% to 4%, the size of PV is reduced whereas the battery capacity is increased. Since the size of micro-hydro power is assumed constant, the sizes of

PV, battery, and converter vary in order to satisfy the load of specified demand level with the least cost. So, such variation of component size for different capacity shortage levels is to satisfy the specified level of load with the minimum overall NPC or COE of the system.

How exactly does this variation of component size with capacity shortage affect the cost of the system? The answer is clearly presented in Figure 4-2 by indicating the NPCs, initial capital costs, capital costs of PV, battery, and converter, and COE of the Toba MG as the capacity shortage increases from 0 to 10 percent.

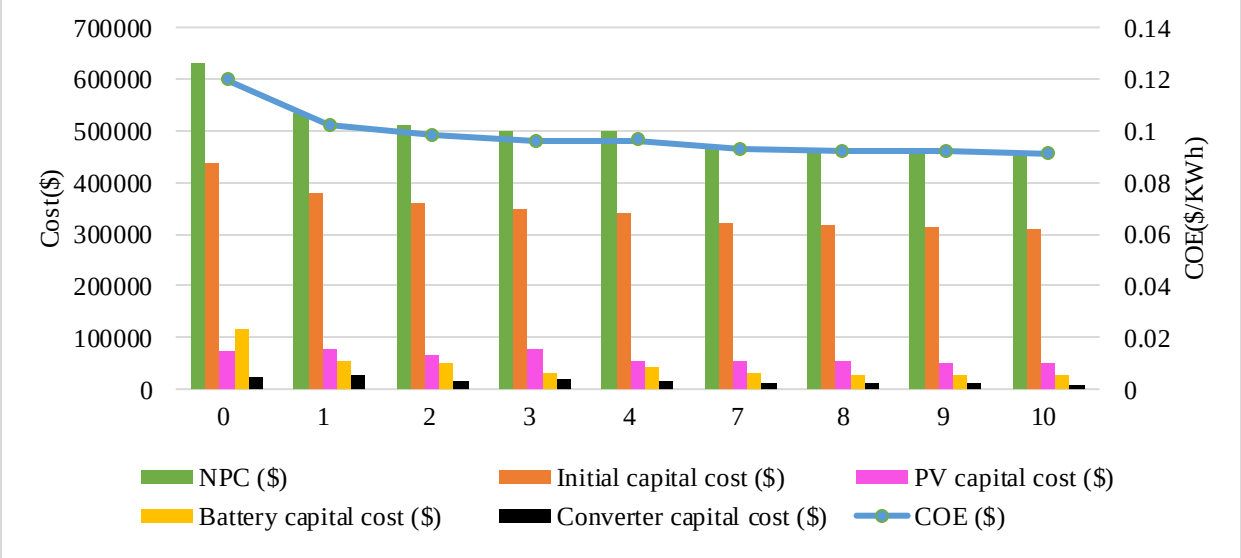


*Figure 4-2: Costs of Toba MG for different capacity shortages.*

In this MG, the NPC, initial capital cost, and combined capital costs of PV, battery and converter are reduced by 27.77%, 28.72%, and 58.83% respectively as the capacity shortage increases from 0 to 10 percent. Additionally, the COE, which is $0.1195/kWh for a capacity shortage of 0%, is reduced to $0.09104/kWh for 10% capacity shortage, i.e., a 23.82% reduction. Therefore, by increasing the percentage of capacity shortage, different system costs are reduced, which encourages the development of microgrids. But the question is, what about reliability?

In order to answer this, let's consider the impact of capacity shortage on reliability by expressing it in terms of unmet electrical load. The hourly power supply and demand for a capacity shortage of 10% in July, which has the minimum GHI, are shown in Figure 4-3a. In this month, there are 7 outages per week considering every outage and 4 outages per week

considering only major outages as shown in Figure 4-3b. So, for a 10% capacity shortage, there are 4 to 7 outages per week.

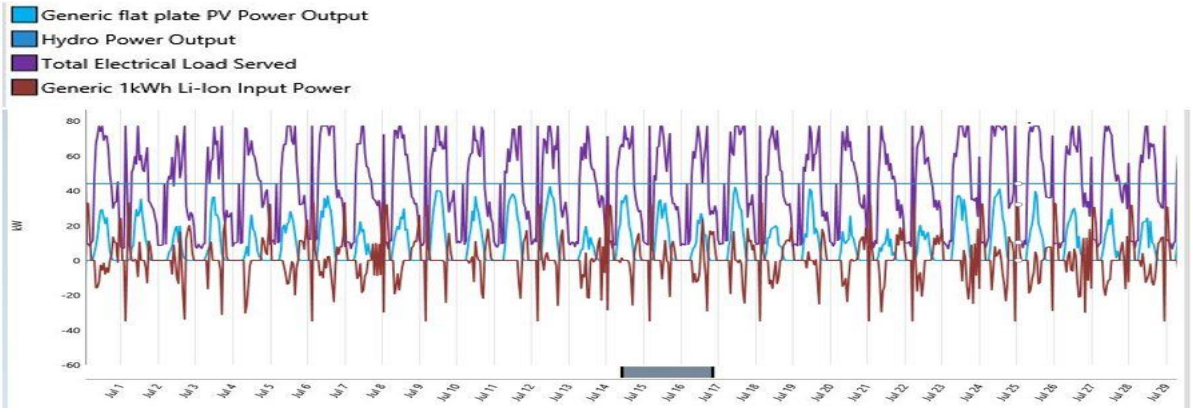


(a)

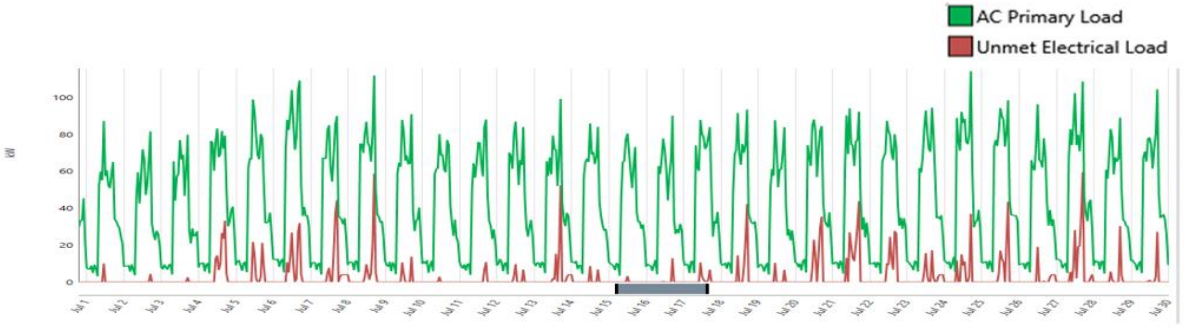


(b)

*Figure 4-3: For a capacity shortage of 10%, hourly power (a) supply & demand (b) Outages.*

In Figure 4-4, it is clearly shown that as the capacity shortage increases, the number of unmet electrical loads also increases. For instance, comparing a capacity shortage of 10% and 1%, the major power outages per month are 16 and 2, respectively.

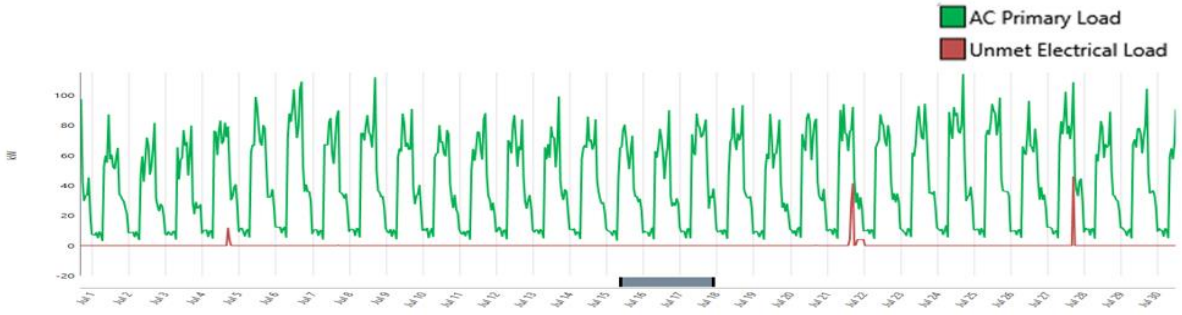


(a) 1% capacity shortage

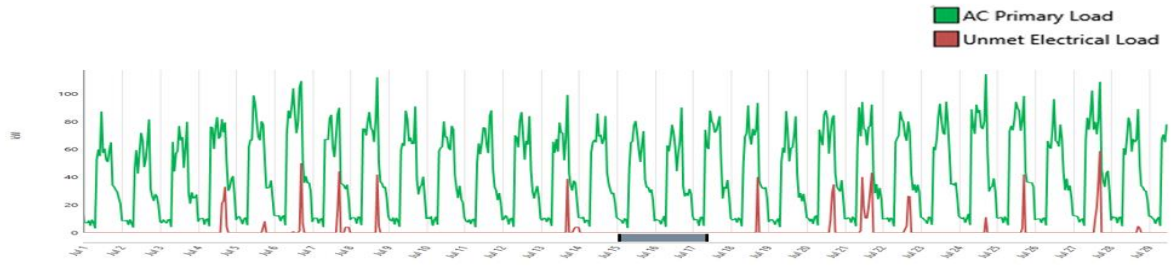


(b) 4% capacity shortage

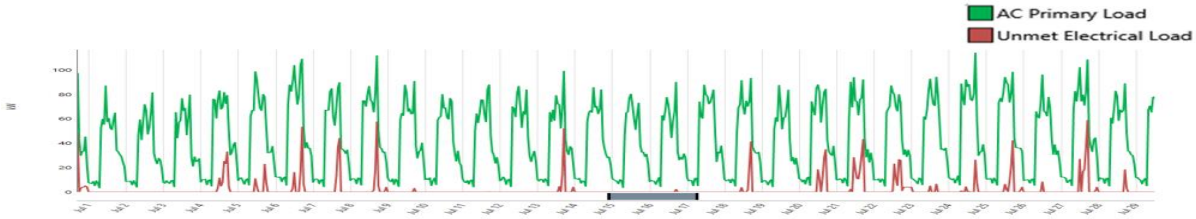


(c) 7% capacity shortage

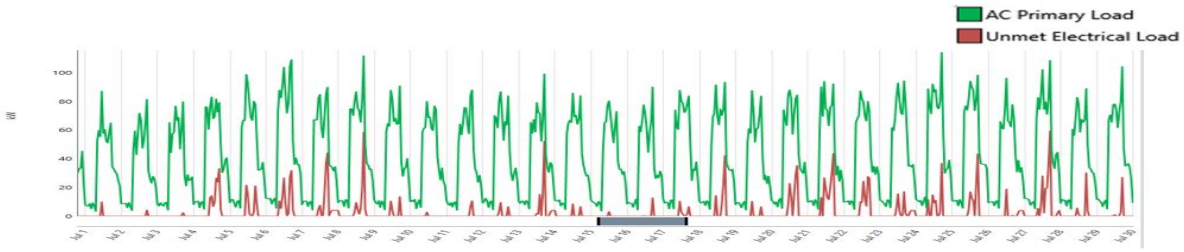


(d) 10% capacity shortage

*Figure 4-4: hourly unmet electrical load for a capacity shortage of a)1% b)4% c)7% &d)10%*

Therefore, as capacity shortage increases, the number of unmet electrical loads increases, i.e., reliability decreases. Now, before delving into the trade-off between reliability and capacity shortage, let's consider the existing reliability scenario.

According to NEP2.0, for 57.6% of grid-connected households, there are 4 to 14 outages per week, and the outage level for Tier 1 and Tier 2, which are the majorities in standalone MGs, is even higher than 14, though it is less than 14 times a week for Tier 3. Besides the number of outages for Tier 1 to Tier 3, the outage duration is not known for sure. So, considering the existing reliability, a capacity shortage of 10% could be a better choice for a reliability trade-off.

The COE for a capacity shortage of 1%, 4%, 7%, and 10% are $0.102/kWh, $0.0963/kWh, $0.0927/kWh, and $0.09104/kWh respectively, and it is clear that the cost reduces. But this cost reduction comes with the sacrifice of some unmet electrical loads. So, using a capacity shortage of 10% to make the MG more economical comes with a cost of reliability, but still not more than the outage standard of Tier 3. The capacity shortage and reliability of the system are compromised by taking a 10% capacity shortage, but does this guarantee affordability?

On average, the cost of electric power generation, transmission, and distribution is $0.09/kWh, but the current tariff in Ethiopia ranges between $0.04/kWh and $0.06/kWh, which is the lowest tariff in Africa. According to the EEU, the tariff should be at least between $0.08/kWh and $0.10/kWh for the EEU to be profitable [41].

As shown in Figure 4-2, for the capacity shortage of 0%, where there is no unmet electrical load, the COE is almost triple the current national grid tariff, indicating that attaining such a reliable system costs a lot and the MG faces affordability issues. This problem can be overcome by considering a 10% capacity shortage, which has a COE of $0.09104/kWh, within the EEU planned tariff range of $0.08/kWh to $0.10/kWh.

By increasing the capacity shortage of the MG system, costs are reduced and electricity becomes more affordable, but reliability decreases. Therefore, compromising cost, reliability, and affordability, in this study, a 10% capacity shortage is considered a good choice for rural electrification of the case study Toba, Koza, and Womba villages.

Now, optimal techno-economic results of Toba MG are explained in the following section, and for economic analysis, a project lifetime of 25 years is considered. Table 4-1 and 4-2 present the technical and economic results of Toba MG respectively, and Table 4-3 summarizes the detailed MG costs under 10% capacity shortage.

Table 4-1: Optimized Toba MG Technical Results.

| Component | Technical Results | | | |
|---|---|---|---|---|
| | Capacity | Power | Energy (KWh/yr.) | |
| PV | 54.5KW | Max. output | Total production | |
| | | 47.3KW | 88,262 | |
| Battery | 96.0KWh | Usable capacity | Energy in | Energy out |

| | | | | | |
|---|---|---|---|---|---|
| | | | 76.8KWh | 35,235 | 31,784 |
| Converter | | | Max. output | Energy in | Energy out |
| | inverter | 33.1KW | 33.1KW | 102,726 | 97,590 |
| | rectifier | 33.1KW | 33.1KW | 33,748 | 32,061 |

Table 4-2: Optimized Toba MG Economic Results.

| Component | Economic Results | | | | |
|---|---|---|---|---|---|
| | Capital($) | Replacement($) | O&M($) | Salvage($) | Total($) |
| PV | 49,053.32 | | 12,682.75 | | 61,736.07 |
| Battery | 28,800 | 28,399.95 | 7,446.25 | -632.81 | 64,013.39 |
| Micro-Hydro | 129,500 | | 34,826.73 | -5,816.76 | 158,509.97 |
| Converter | 9,922.06 | 4,209.67 | 2,565.35 | -792.3 | 15,904.78 |
| Distribution network | 94,000 | | 60,759.33 | | 154,759.33 |
| Total | 311,275.38 | 32,609.62 | 118,280.41 | -7,241.87 | 454,923.54 |

Table 4-3: Toba MG costs under 10% capacity shortage.

| System Parameter | Capacity Shortage | Initial Capital ($) | NPC ($) | Operating Cost ($/yr.) | COE ($/KWh) |
|---|---|---|---|---|---|
| Value | 10% | 311,275.38 | 454,923.54 | 11,111.81 | 0.09105 |

### 4.2. Sensitivity Analysis

To observe the impact of sensitivity variables on optimal sizing results, this section considers the effect of solar irradiation, battery price, PV price, and battery lifetime with respect to the allowed $SOC_{min}$, and conducts a sensitivity analysis study.

According to [42], in the long-term (48hrs. ~ 7days), GHI prediction varies from 20% to 63%. To account for this variability in Toba MG, a ±25% variation of GHI is considered. Figure 4-5 displays the sensitivity analysis results obtained by varying GHI, illustrating how different costs of the MG are affected as GHI is varied by ±25% from the value used to optimize the system.

As the GHI is reduced by 25%, the NPC, initial capital cost, PV + Battery capital cost, and COE increase by 4.96%, 4.89%, 16.34%, and 4.51% respectively. Similarly, these costs

decrease by 2.83%, 2.79%, 11.17%, and 2.97% as the GHI is increased by 25% from the base value. This demonstrates the necessity for accurate irradiation data and highlights the impact of the availability of good irradiation in obtaining more economic results.

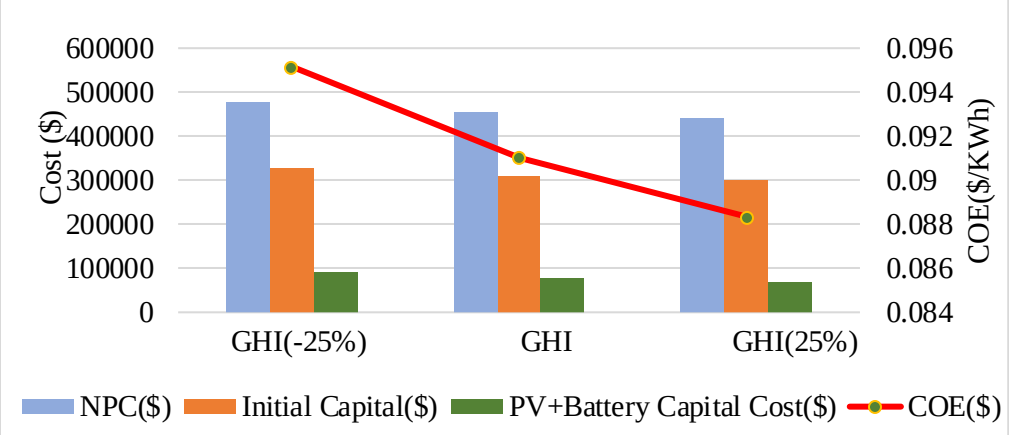


*Figure 4-5: Result of sensitivity analysis for variation of GHI by ±25%.*

The price of PV was decreasing each year toward 2020, almost by 20% as presented in [43]. However, at the end of 2020, the price increased by 15%, and it is expected to increase in the next few years due to increasing material and shipping costs [44]. So, in this study, to investigate the sensitivity, a ±15% and +20% variability of PV module price is considered. Figure 4-6 shows the impact of PV price on different costs of the system, with the price of PV varying by ±15% and 20% from the cost used for optimization of the system.

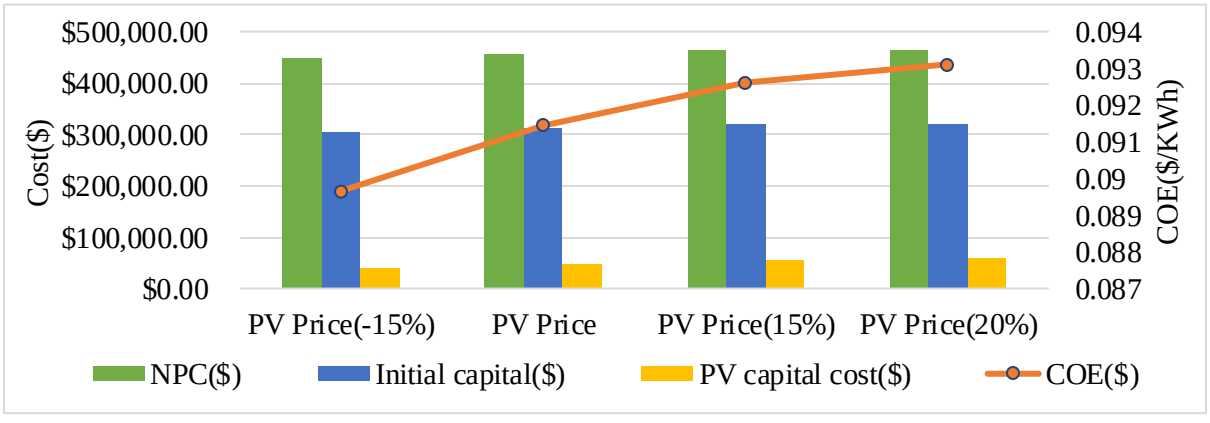


*Figure 4-6: Result of sensitivity analysis for variation of PV price.*

As the PV price reduced by 15%, the NPC, initial capital cost, and COE reduced by 1.62%, 2.37%, and 1.95% respectively. Conversely, as the PV price increased by 20%, the same costs

mentioned above increased by 2.16%, 3.16%, and 1.83% respectively. The result shows that varying costs of PV can have an impact on the overall system economy.

Now let us consider the sensitivity variables of the battery. The battery's currently available energy state, otherwise known as State of Charge (SOC), is the energy currently stored in the battery, as a percentage of the maximum capacity of the battery, and it varies from 0 to 100 percent. Batteries could degrade at different rates. Depth of discharge, temperature, and cycle of charging/discharging are quantities which highly affect battery degradation. 0% SOC means the battery energy can possibly be used fully, which gives an advantage of requiring fewer batteries, reduced COE, but it comes with the drawback of speeding up the degradation process and reducing lifetime, resulting in purchasing batteries before their expected period. Therefore, there should be a compromise between depth of discharge and economy. Figure 4-7 presents the cost of Li-ion LFP batteries over different capacities between 2020 and 2050 [45].

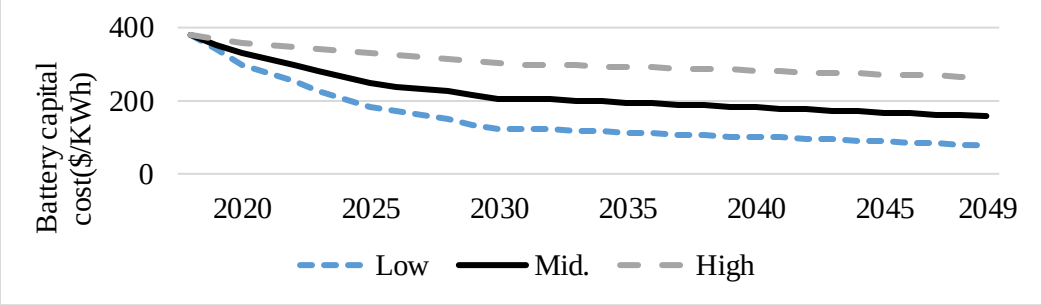


*Figure 4-7: The cost trend of Li-ion LFP battery from 2020 to 2050 [45].*

In Figure 4-8, different MG system cost reductions as the allowed usage level of the battery increases are presented. In the figure, moving from a 50% to 100% allowed battery usage level, NPC, initial capital cost, and PV + Battery capital cost reduced by 3.17%, 6.58%, and 22.8% respectively, and the COE reduces from $0.09361/kWh to $0.09054/kWh.

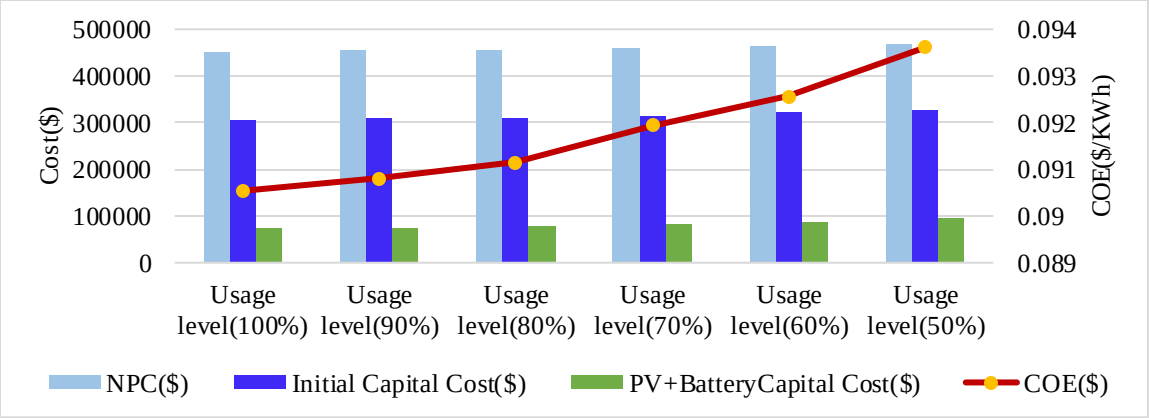


*Figure 4-8: Result of sensitivity analysis for varying usage level of battery.*

As indicated in Table 4-4, the reason for cost reduction as the allowed battery usage level increases is the reduction in the number of required battery strings. As we move from 100% to 50% of allowed battery usage level, the required number of battery strings increases. At 100% allowed battery usage level, the least number of battery strings is required. However, it should be noted that 100% usage level is not advisable since it reduces battery lifetime, so a compromise is required between cost and battery lifetime. In this study, an 80% allowed battery usage level is used.

Table 4-4: Number of battery requirement at different allowed battery usage.

| Allowed Battery Usage level | Required Battery Capacity (KWh) | No. of strings |
|---|---|---|
| 100% | 80 | 10 |
| 90% | 88 | 11 |
| 80% | 96 | 12 |
| 70% | 112 | 14 |
| 60% | 128 | 16 |
| 50% | 152 | 19 |

Now let's see the impact of battery price variation. As the battery price decreases, different costs of the MG also decrease, as clearly shown in Figure 4-9, considering a battery price decrease of 10% and 20%.

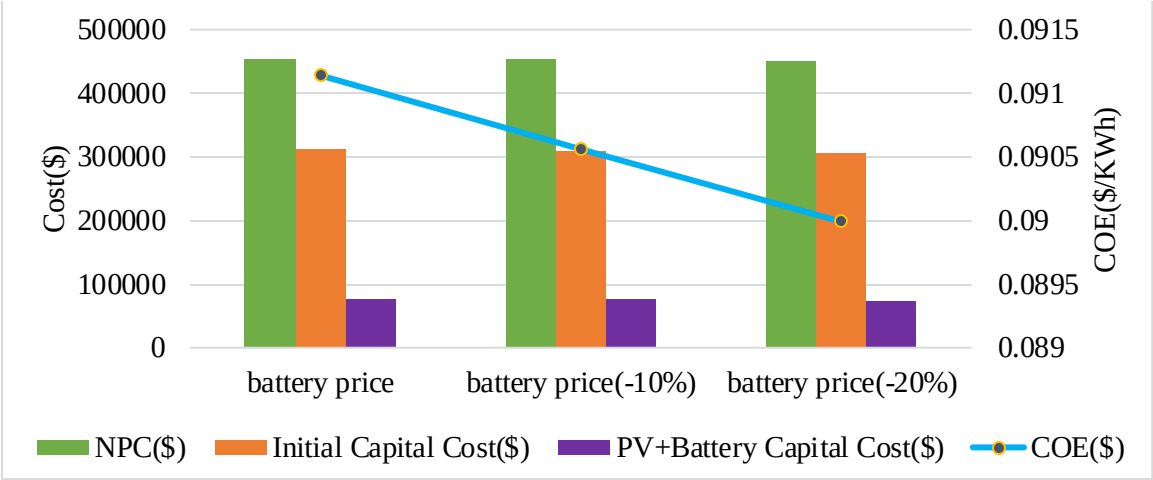


*Figure 4-9: Result of sensitivity analysis for varying battery price.*

For a price reduction of 20%, the battery capital cost is reduced by $5,760, and the COE decreases from $0.09104/kWh to $0.08999/kWh.

### 4.3. Optimal Sizing Result of Microgrid Cluster

In MG cluster analysis, in addition to each MG's distribution cost, the cost of interconnection between MGs is required, which causes the overall initial cost to be higher than if the MGs were operating independently. However, in order to determine whether this additional cost is justified, additional analysis from a different perspective is required.

For the individual development of Koza and Womba MGs, the same procedure used to develop the optimal Toba MG is reused. For MG cluster optimal analysis, a hypothetical MG is considered, comprising the loads (i.e., aggregate of all the residential, commercial, and deferrable loads) of the three villages, with the same hydro power potential as that of the combined Toba and Ergino micro-hydro, average GHI of the three villages, a combined distribution network cost of the three villages, and the cost of interconnection between MGs. For MG cluster analysis, a 10% capacity shortage is considered.

To gain a clear understanding and investigate the impact of clustering MGs, a comparison based on technical, economical, and reliability aspects is made between the MG cluster and three individually operating, non-interconnected MGs. In this study, they are denoted as '*Three Ind. MG* ' (three individual MGs).

Analyzing from an economical point of view, it's evident that developing a cluster requires interconnecting individual MGs, incurring additional costs to the system. As shown in Table 4-5, the initial capital cost increases by 10%, but MG clustering results in a significant reduction in the capital cost of PV, battery, and converter by 32.44%, 45.12%, and 35.17% respectively compared with *Three Ind. MGs*. Furthermore, there are reductions in NPC and operating costs. Additionally, the MG cluster's COE is lower than the average of the three individual MGs combined, which encourages clustering.

From a technical perspective, as depicted in Table 4-6a, the PV capacity, which was 300KW in *Three Ind. MGs*, is reduced to 203KW for the clustered MG, and the battery capacity also decreases from 656KWh to 360KWh. These capacity reductions are primarily due to Koza MG, which previously relied solely on PV and battery for load consumption in standalone operation. However, clustering allows Koza MG to access additional renewable sources from other MGs via interconnecting lines. This enables Koza MG to utilize transferred power, especially during nighttime, reducing its dependence on battery power alone. Table 4-6b shows that clustering MGs reduces unmet load by 6.85% and excess energy by 73.4%. In the MG cluster, excess power can be transferred to other connected MGs in need.

Analyzing from a reliability point of view, it's important to assess whether the economic advantages gained by clustering compromise the system's reliability beyond the required level or if it remains within the standard. Clustering reduces unmet load, which is a positive indicator of reliability.

Table 4-5: Costs of individual microgrids' and microgrid cluster

| | PV | | Micro Hydro | | Battery | | Converter | | System cost | | | |
|---|---|---|---|---|---|---|---|---|---|---|---|---|
| | Capital ($) | O&M ($) | Capital ($) | O&M ($) | Capital ($) | O&M ($) | Capital ($) | O&M ($) | Initial Capital ($) | NPC ($) | Operating ($/yr) | COE ($/KWh) |
| Toba | 49053 | 12683 | 129500 | 34827 | 28800 | 7446 | 9922 | 2565 | 311275 | 454924 | 11112 | 0.0911 |
| Koza | 169998 | 43953 | - | - | 156000 | 40334 | 25459 | 6582 | 478457 | 720883 | 18753 | 0.2381 |
| Womba | 51392 | 13287 | 58860 | 15823 | 12000 | 3103 | 10463 | 2705 | 214715 | 319908 | 8137 | 0.1276 |
| *Three Ind. MGs* | 270443 | 69923 | 188360 | 50650 | 196800 | 50883 | 45844 | 11853 | 1004447 | 1495715 | 38002 | |
| MG Cluster | 182719 | 47242 | 188360 | 50650 | 108000 | 27923 | 29720 | 7684 | 1105799.5 | 1488679 | 29617 | 0.1411 |
| Reduction (%) | 32.44 | | | | 45.12 | | 35.17 | | -10.1 | 0.47 | 22.1 | |

Table 4-6: Individual & clustered MG (a) Technical results (b) energy usage condition

(a)

| | PV | | Micro Hydro | | Battery | |
|---|---|---|---|---|---|---|
| | Capacity (KW) | Production (MWh/yr.) | Capacity (KW) | Production (MWh/yr.) | Capacity (KWh) | Annual Throughput (MWh/yr.) |
| Toba | 54.5 | 88.262 | 51.8 | 385.679 | 96 | 33.503 |
| Koza | 189 | 305.868 | | | 520 | 110.187 |
| Womba | 57.1 | 92.485 | 23.5 | 175.309 | 40 | 16.401 |
| *Three Ind. MGs* | 300.6 | 486.615 | 75.3 | 560.988 | 656 | 160.091 |
| MG cluster | 203 | 328.7701 | 75.3 | 560.988 | 360 | 85.334 |

(b)

| | Unmet Load | | Excess Energy | |
|---|---|---|---|---|
| | Unmet (%) | Unmet (MWh/yr.) | Excess (%) | Excess (MWh/yr.) |
| Toba | 5.19 | 21.136 | 16.3 | 77.157 |
| Koza | 7.69 | 19.507 | 15.7 | 48.123 |
| Womb | 6.83 | 14.211 | 25.5 | 68.329 |
| *Three Ind. MGs* | 6.57 | 54.854 | 19.167 | 193.609 |
| MG cluster | 6.12 | 53.266 | 5.1 | 45.334 |

### 4.4. Quasi Dynamic Simulation Result

#### 4.4.1. Quasi-Dynamic Simulation Result of Toba MG

In this section, the quasi-dynamic simulation results of Toba MG are presented. In this MG, due to the intermittency of PV, the considered 10% capacity shortage, time varying loads etc. there could be periods of the day with extra power to initiate deferrable load or power deficit that causes load shedding. Thus, to show the range of operating conditions and the respective controller management strategy, the result analysis of two cases is considered, such as:

Case-I: A day encompassing a load shedding period and

Case-II: A day encompassing a PV curtailment period.

Case-I: A day encompassing a load shedding period

Figure 4-10 illustrates the power supply and demand, deferrable load, and battery SOC for Toba MG. In the power supply and demand section, power (in MW) is plotted on the vertical axis, while time (in hours) is represented on the horizontal axis. This section depicts the PV output, which is zero during nighttime, the constant micro-hydro power (Prated), residential and commercial loads, and the charging/discharging power of the BESS, indicated by negative and positive power, respectively.

In the deferrable load section, it is shown that the deferrable load operates during the time periods from 2:41 to 8:00 and 22:00 to 1:00. During these periods, as depicted in the SOC section of the figure, the SOC $\geq SOC_{max}$, indicating that the battery stops charging and any surplus power is utilized to supply the deferrable load. At night, the micro-hydro power is sufficient to supply the residential and commercial loads, charge the battery, and, depending on the SOC, even support the deferrable load.

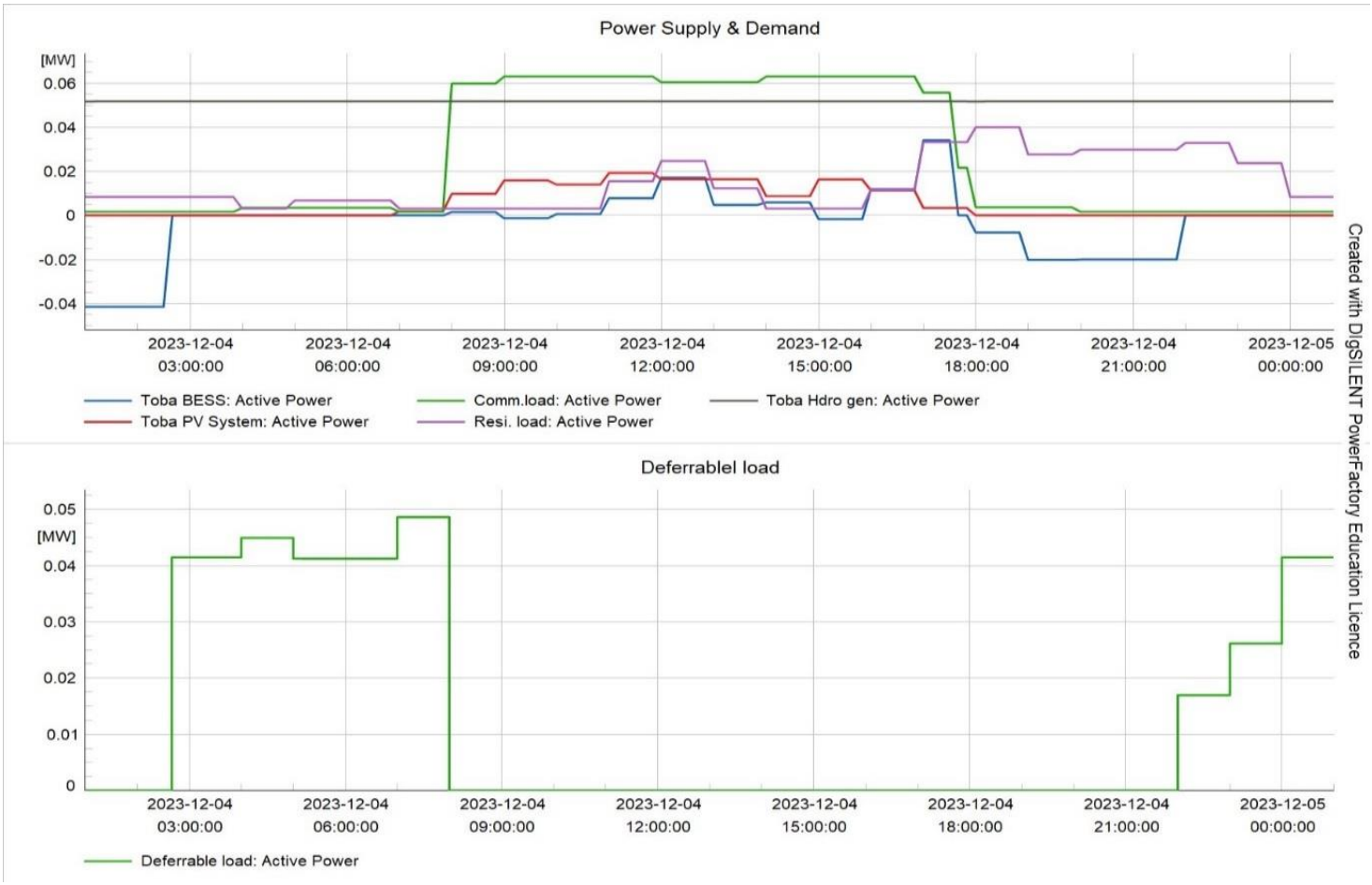

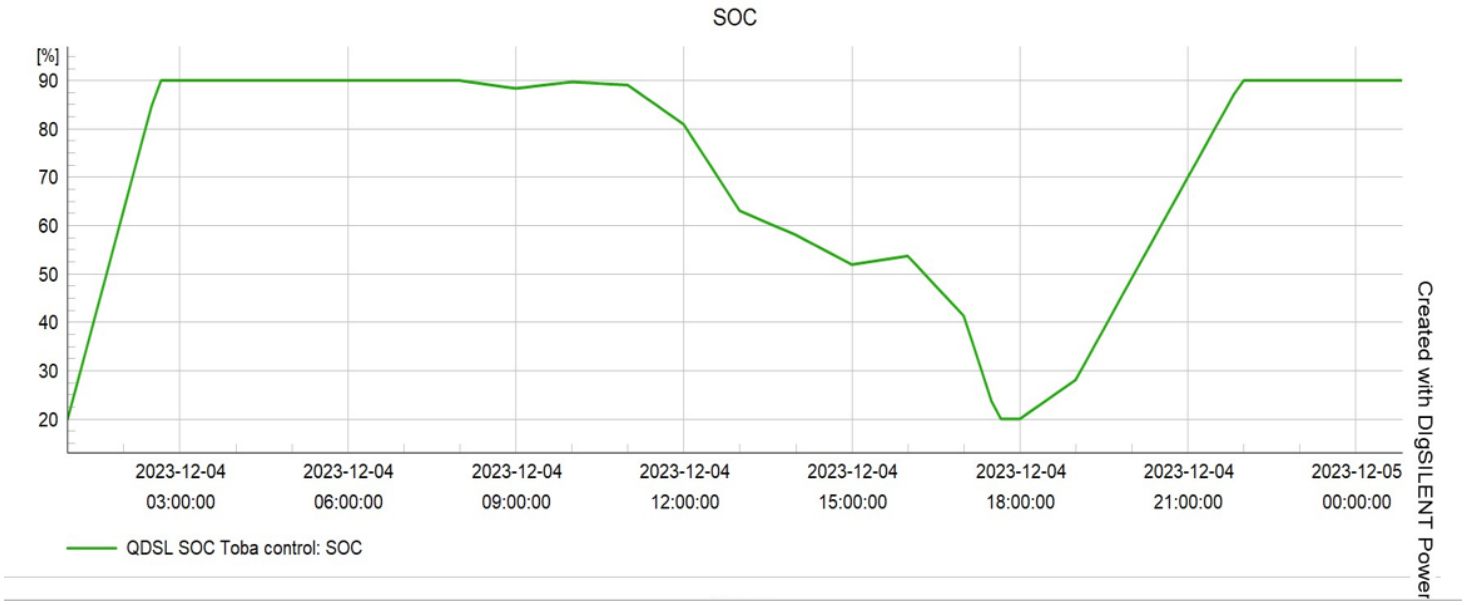


*Figure 4-10: power supply & demand, deferrable load and SOC of Toba MG*

In Figure 4-11, the relationship between $P_{meas}$ and SOC is depicted, where $P_{meas}$ represents the measured power, calculated as $P_{meas} = P_{PV} + P_{hydro} - P_{load}$. ($P_{load}$ indicating primary loads).

Until 8:00, $P_{meas}$ remains positive, signifying that the generated power is adequate to supply the primary load and charge the battery. As SOC reaches $SOC_{max}$ =90% at 2:41, the battery stops charging, and the deferrable load begins.

At 8:00, the commercial load commences, causing $P_{meas}$ to become negative, indicating insufficient generated power from PV and micro-hydro to cover the primary load, resulting in the initiation of battery discharge.

From 8:00 to 18:00, $P_{meas}$ is predominantly negative, necessitating the battery to supply the shortfall in power to maintain balance (i.e., ensuring $P_{PV} + P_{hydro} - P_{load} = 0$). Around 17:36, the day's worst-case scenario occurs, prompting load shedding. However, as the commercial load requirement decreases during this period, load shedding ceases swiftly.

By 18:00, $P_{meas}$ turns positive, enabling the battery to resume charging. At 22:00, with SOC reaching $SOC_{max}$ again, the deferrable load recommences.

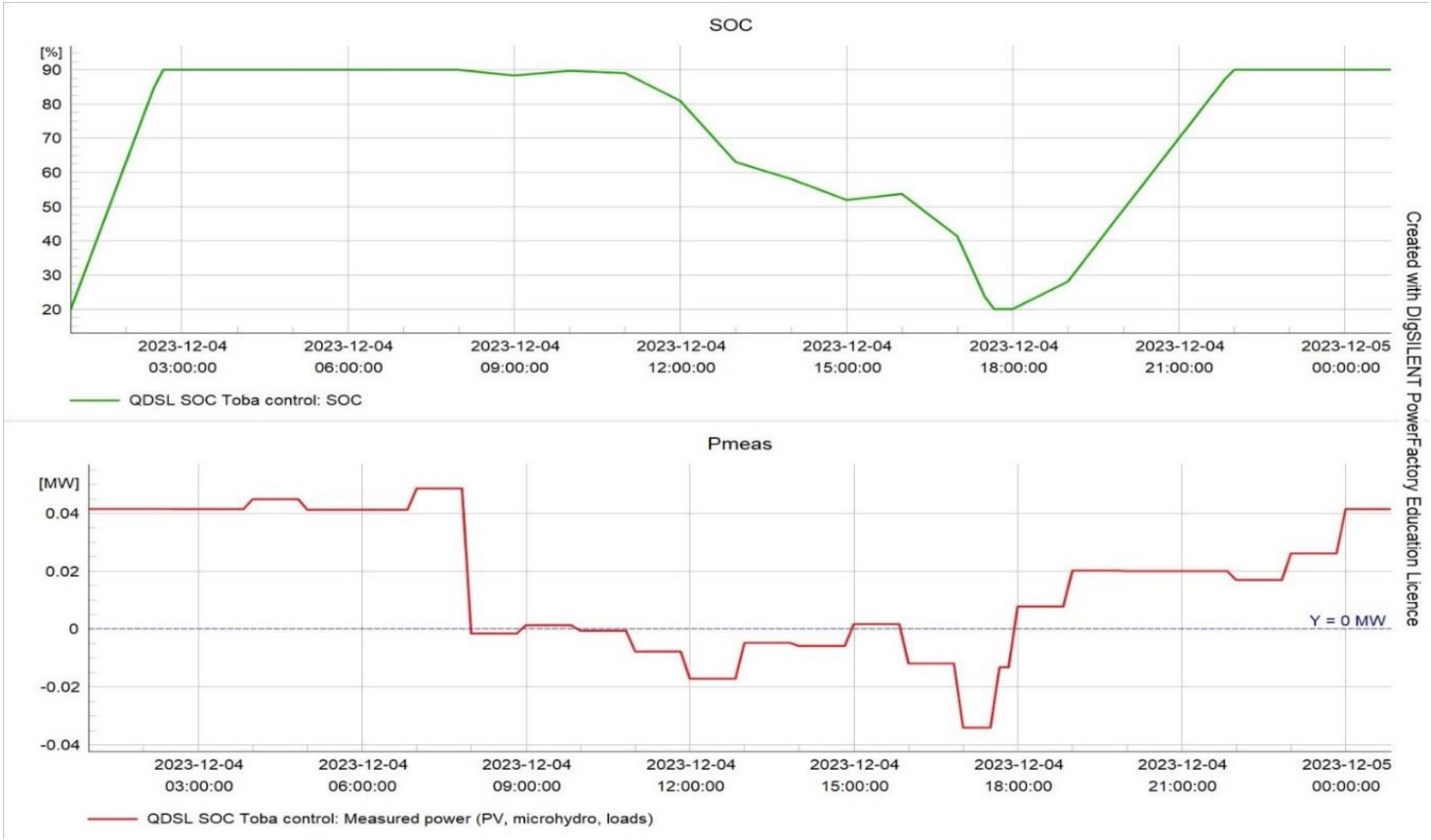


*Figure 4-11: SOC and $P_{meas}$ of Toba MG*

In Figure 4-12, the battery's charging/discharging mode is determined by considering both energy and power perspectives, as reflected in the $chargeE$ and $chargeP$ sections.

Initially, Toba MG's SOC is set at 20%, which also serves as $SOC_{min}$. Thus, at the outset, $chargeE$ is set to 1, indicating $SOC \leq SOC_{min}$,, as depicted in the $chargeE$ section of the figure. However, due to surplus power available for battery charging, SOC increases rapidly, advancing the state to $chargeE = 2$, corresponding to $SOC_{min} \leq SOC \leq SOC_{max}$. As $P_{meas}$ remains positive, the battery continues to charge, reaching $chargeE = 3$ at 2:41, where $SOC \geq SOC_{max}$, maintaining this state until 8:00.

Subsequently, $P_{meas}$ turns negative for the most part, attributed to the rise in commercial load demand, prompting the battery to discharge. Consequently, SOC decreases from $SOC_{max}$, and the state transitions to $chargeE = 2$ from 8:00 to 17:36. Around 17:36, the battery reaches a point where it cannot discharge further, indicated by $chargeE = 1$ ($SOC \leq SOC_{min}$). However, shortly after, $P_{meas}$ becomes positive again, initiating battery charging and

transitioning the state back to $chargeE = 2$. Eventually, the state progresses to $chargeE = 3$, as evidenced in the $chargeE$ section of Figure 4-12.

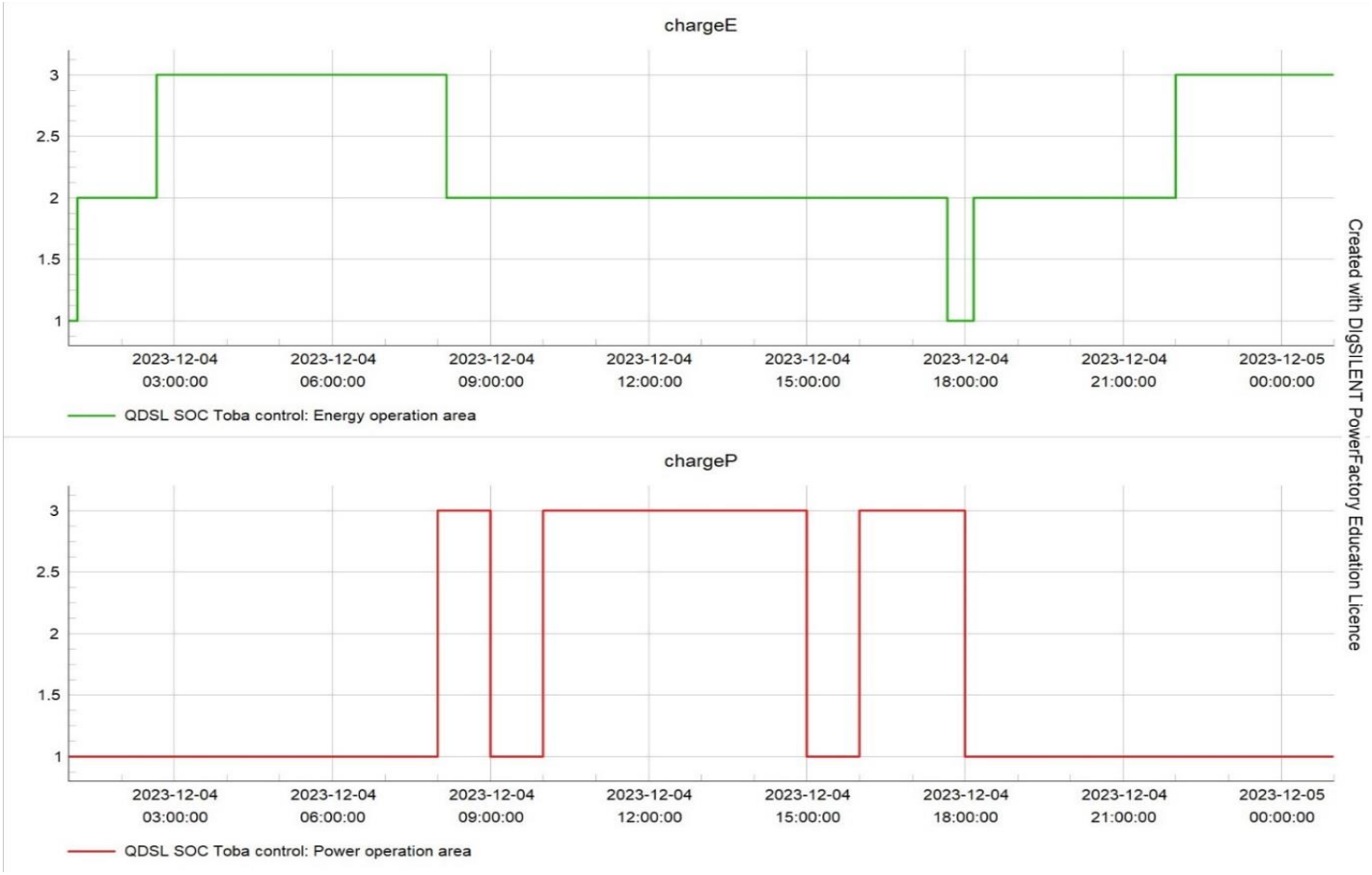


*Figure 4-12: $chargeE$ and $chargeP$ state of Toba MG battery*

In the $chargeP$ section of Figure 4-12, the power operation state from 1:00 to 8:00 starts at $chargeP = 1$, indicating the battery is in charging mode. In this study, only two states of $chargeP$ are considered: $chargeP$=1or3, as $P_{startstore}$ and $P_{startfeed}$ are both set to zero, rendering $chargeP = 2$ state unavailable.

At 8:00, coinciding with the change in $P_{meas}$ from positive to negative, the $chargeP$ state transitions from $chargeP = 1$ to $chargeP = 3$, signifying the switch to discharging mode.

Benefitting from the absence of $chargeP = 2$ state, the relationship between $chargeP$ and the sign of $P_{meas}$ is clearly depicted in Figure 4-13: if $P_{meas}$ is positive, $chargeP = 1$; otherwise, $chargeP = 3$.

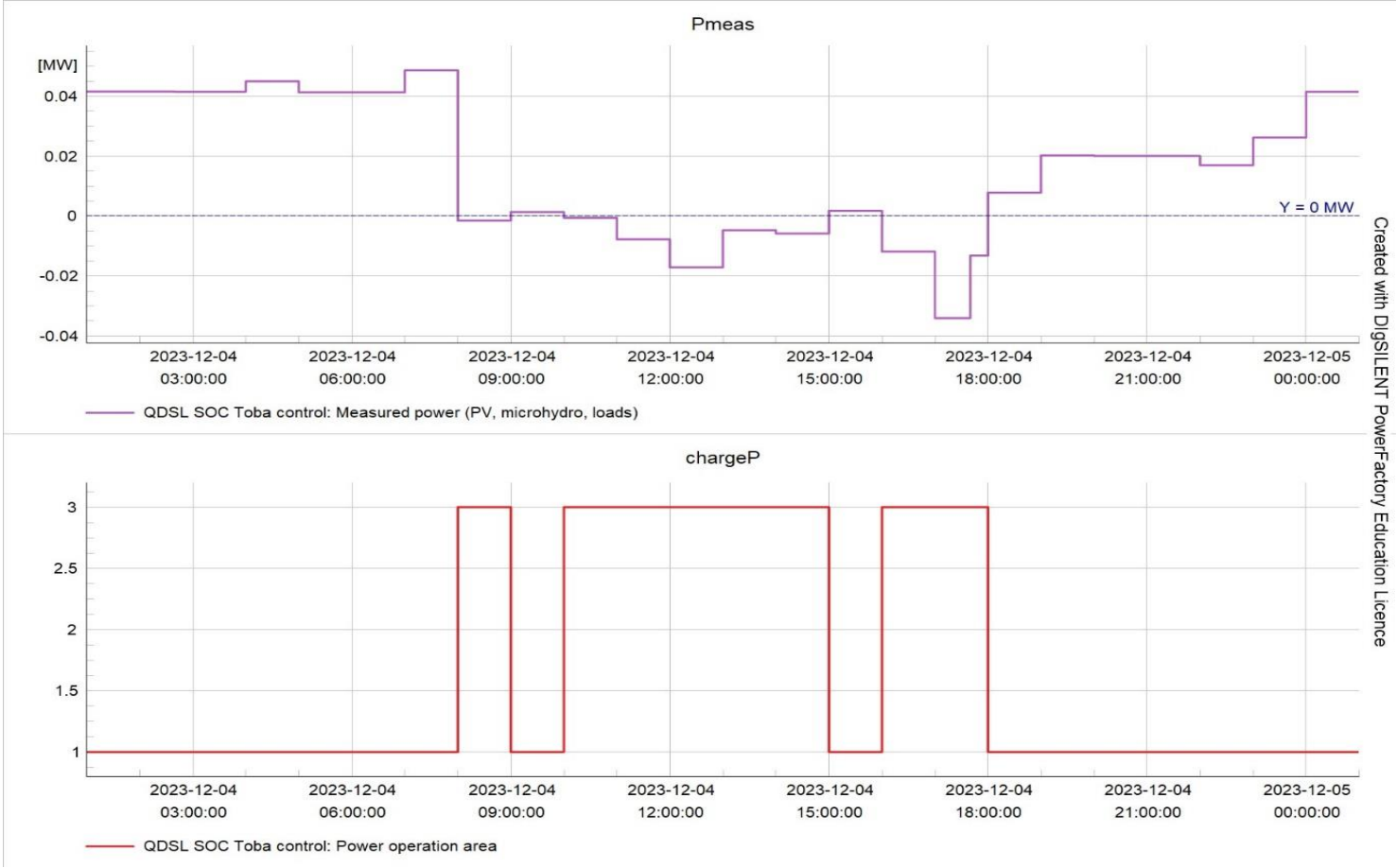


*Figure 4-13: Relation between $P_{meas}$ and chargeP of Toba MG*

In Figure 4-14, when the power generated by PV and micro-hydro is insufficient to meet the primary load, the battery begins discharging until $SOC \leq SOC_{min}$. However, beyond this point, the battery cannot provide further support. To maintain power balance, around 17:36, the system activates first priority load shedding. Remarkably, it takes less than half an hour for the system to restore its operation state without load shedding, as illustrated in Figure 4-14. During this period, only a certain percentage of first priority load shedding is necessary to maintain power balance.

In the load shedding section of Figure 4-14, the vertical axis represents the amount of first and second priority load supplied, expressed in Pu (per unit), denoted by the portion of commercial and residential loads, respectively. It is demonstrated that until the load shedding period, both loads were supplied 100%. However, during the load shedding period, first priority and second priority loads are supplied 38% and 100%, respectively, indicating that 62% of the first priority load undergoes load shedding.

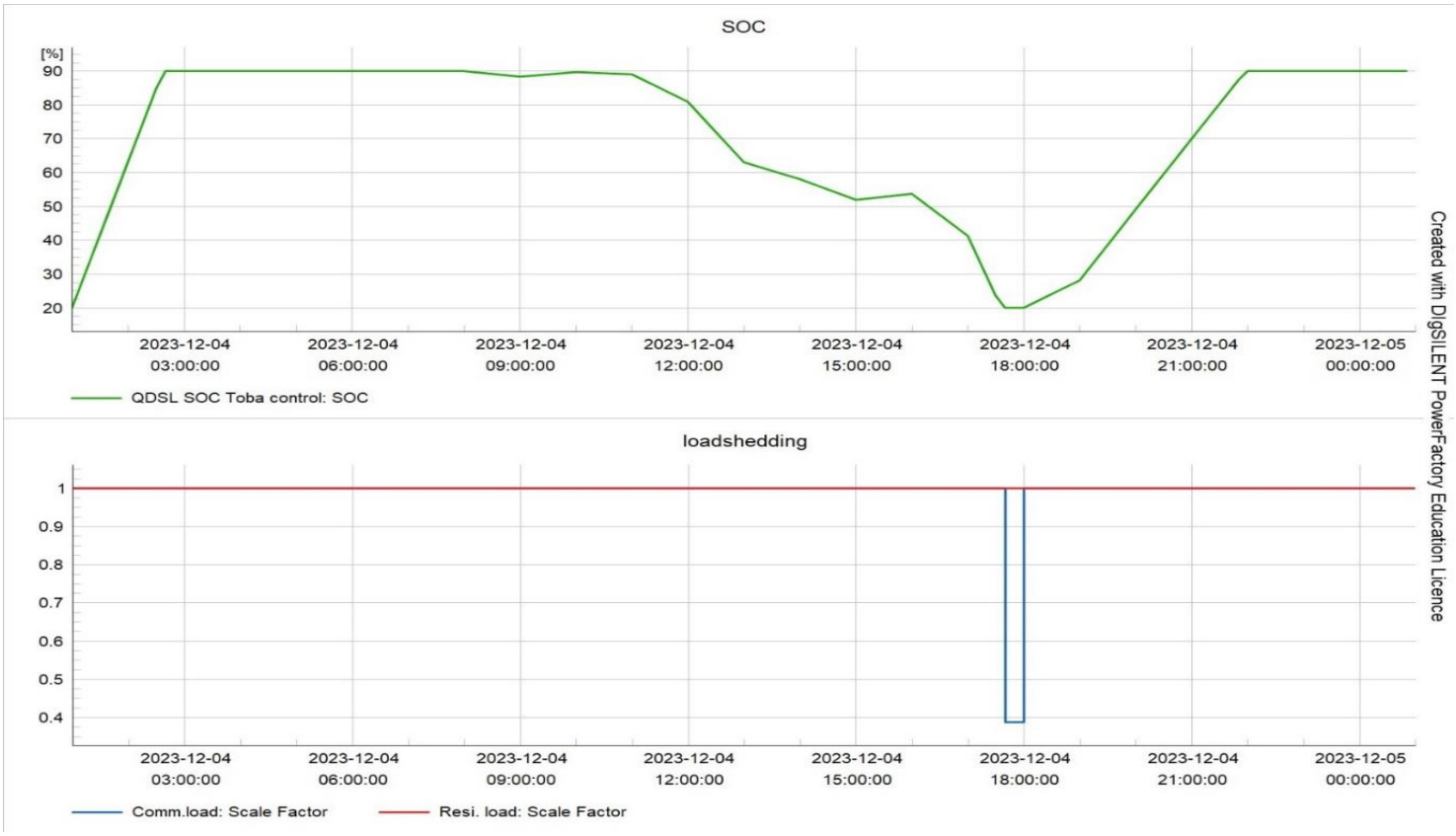


*Figure 4-14: SOC and load shedding in Toba MG*

In Figure 4-15, the bus voltage of Toba MG is depicted, with all buses maintaining a voltage magnitude within the range of 1 and 0.95 per unit throughout the day. The micro-hydro bus, connected to hydro power, and bus-1, linked to PV and BESS, exhibit nearly constant voltage magnitudes. Conversely, the voltage magnitude of load buses, such as bus-2 and bus-3, fluctuates within the range of 0.996 to 0.956 throughout the day.

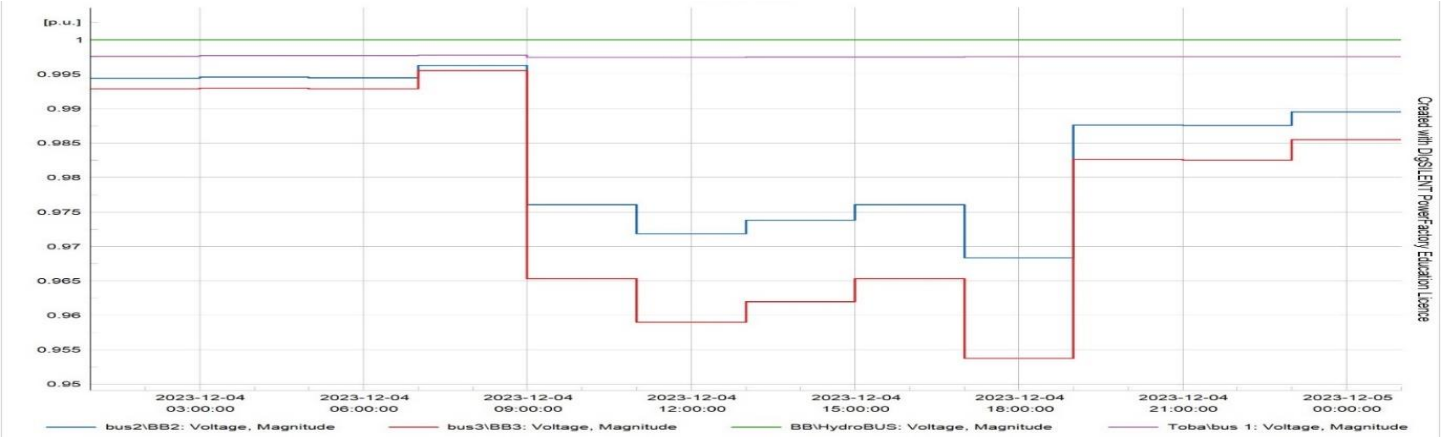


*Figure 4-15: bus voltage of Toba MG*

In Toba MG, for the considered day, there are four modes of operation as depicted in Figure 4-16.

Mode 8: In this mode, $P_{meas}$ is positive, and the battery energy state is within $SOC_{min} \leq SOC \leq SOC_{max}$, denoted as $chargeE = 2$, indicating that the battery is charging. Comparing $P_{meas}$ with $P_{max}^{char}$, it is observed that the battery is charging within the specified power limit, thus enabling the PV to operate in MPPT mode.

In this operational condition, neither the maximum charging power limit is exceeded nor $SOC_{max}$ is reached. Therefore, the deferrable load remains in the off state, and no load shedding action is required.

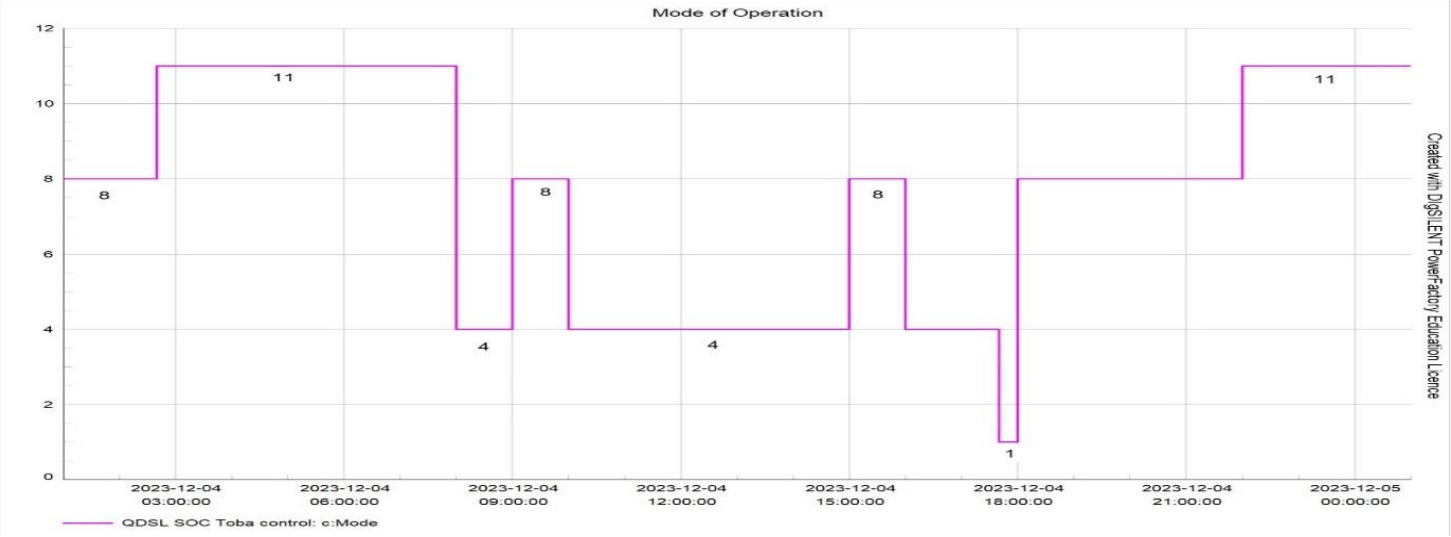


*Figure 4-16: Mode of operation in Toba MG*

Mode 11: In this mode, $SOC > SOC_{max}$, denoted as $chargeE = 3$, activating the deferrable load, although it has not reached its maximum limit. Consequently, the PV operates in MPPT mode, and no load shedding is required.

Mode 4: In this mode, $P_{meas}$ is negative, and the battery energy state is within $SOC_{min} \leq SOC \leq SOC_{max}$, i.e.,$chargeE = 2$, indicating that the battery is discharging. The PV operates with MPPT. Comparing $P_{meas}$ with $P_{max}^{discha}$, it is confirmed that the battery is discharging within the specified power limit, hence neither the deferrable load starts nor load shedding is activated.

Mode 1: In this mode, $SOC < SOC_{min,}$ i.e., $chargeE = 1$. To maintain power balance, first priority load shedding is activated, and the PV is set to operate with MPPT. In this scenario, the second priority load is supplied, and no deferrable load is activated.

Case-II: A day encompassing a PV curtailment period.

In this case, a PV curtailment condition is present, and for that, a day with mode 12 operation condition is considered, as shown in Figure 4-17. Mode 12 represents the scenario where the deferrable load is supplied to its maximum limit, yet there is surplus power available. To maintain power balance, the excess power beyond $P_{max}^{defer}$ is subjected to PV curtailment.


*Figure 4-17: Mode of operation and deferrable load of Toba MG*

In the considered day, $P_{meas}$ is positive for most hours of the day, and the battery SOC reaches $SOC_{max}$, as shown in Figure 4-18. Additionally, in the load shedding part of this figure, both 1st and 2nd priority loads are supplied 100% throughout the day.

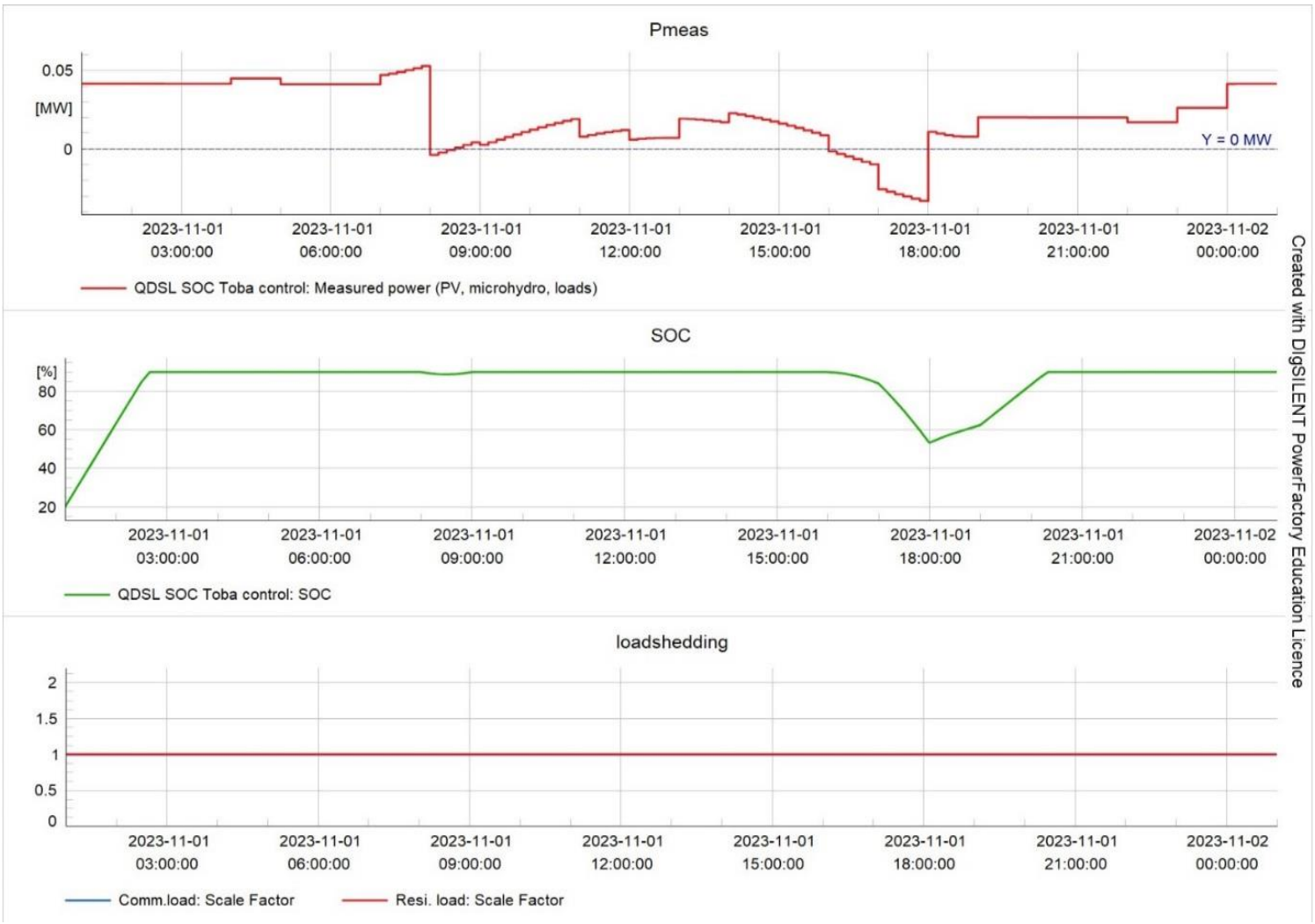


*Figure 4-18:$P_{meas}$, SOC & load shedding conditions of Toba MG*

### 4.4.1. Comparison b/n MG & MG Cluster using Quasi Dynamic Simulation Result

In this section, quasi-dynamic simulation results are utilized to compare individual MGs with MG cluster. Initially, the simulation results of MGs operating independently are analyzed. Subsequently, the simulation results of MGs operating within a cluster on the same day are examined and compared with the corresponding results of the MGs operating independently.

A. Quasi-Dynamic Simulation Result of MGs Operating Individually

The result analysis of Toba, Koza and Womba MGs operating individually is presented as follows.

### i. Result Analysis of Toba MG Operating Individually

The power supply and demand, $P_{meas}$, load shedding, SOC and deferrable load of Toba MG operating individually are shown in Figure 4-19. In this figure, the power supply and demand section displays all supply powers of the MG, BESS and primary loads. The power which could determine whether the battery charges or discharges is indicated as $P_{meas} = P_{PV} + P_{hydro} - P_{primary\ load}$ in the $P_{meas}$ part. The load shedding section indicates whether all primary loads are supplied or if part of it undergoes load shedding. The SOC of the battery illustrates the percentage of energy available in the battery at different hours of the day. Finally, the deferrable load section presents the load supplied if there is extra power available beyond charging the battery.

In the SOC part of the figure, until 1:50, the battery is charging, $SOC < SOC_{max}$ so the deferrable load is not activated. However, starting at 1:50, $SOC \geq SOC_{max}$ prompting the battery to cease charging. Since $P_{meas}$ remains positive, indicating surplus power, the deferrable load commences. Notably, on this day, the deferrable load doesn't reach its maximum limit, suggesting no PV curtailment.

Between 14:30 to 18:00, $P_{meas}$ turns negative due to high commercial load and significantly reduced PV output, even reaching zero after 16:00. Consequently, the battery starts discharging, and by 17:50, SOC drops below $SOC_{min}$, prompting the battery to halt discharging. During this period, to maintain power balance, the MG initiates load shedding based on required power and priority order. As illustrated in the load shedding section of Figure 4-19, 72% of the first priority load shedding is necessary to restore power balance.

At 18:00, the commercial load diminishes, and $P_{meas}$ becomes positive again, signaling the cessation of load shedding and the resumption of battery charging.

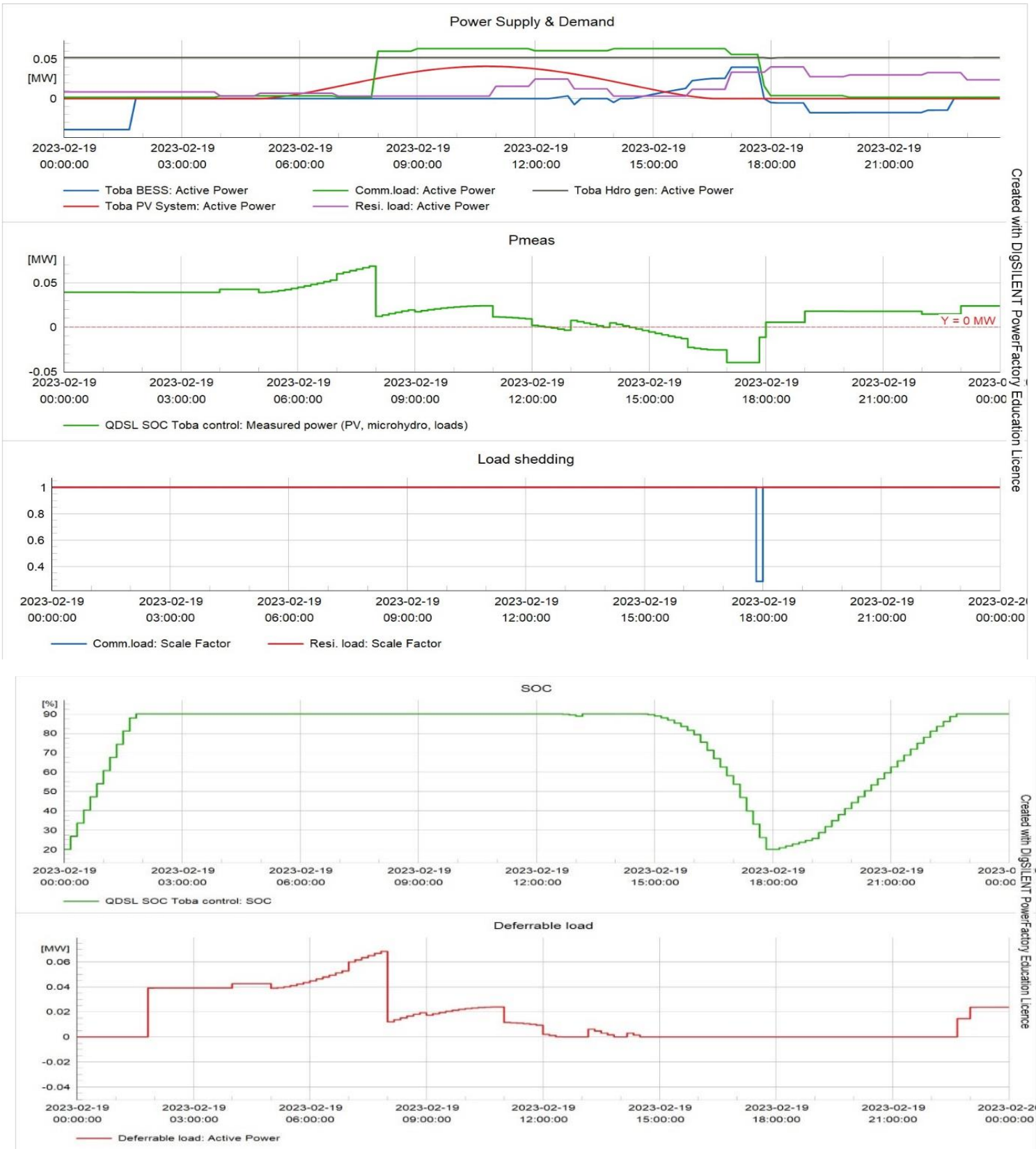


*Figure 4-19: quasi dynamic simulation result of Toba MG operating individually*

ii. Result Analysis of Koza MG Operating Individually

In Figure 4-20, the power supply and demand, $P_{meas}$, load shedding, SOC and deferrable load of Koza MG operating individually are depicted. Unlike the other two MGs, Koza MG lacks micro hydro power to supply loads during nighttime and its PV power drops to zero during this period. Consequently, the battery output aligns with the demand during nighttime.

Until 5:40 in Figure 4-20, $P_{meas}$ is negative, indicating battery discharge. From 5:40 to 15:40, $P_{meas}$ becomes positive. At 10:00, $SOC$ exceeds $SOC_{max}$, prompting the activation of the deferrable load. In this scenario, the deferrable load starts with $P_{defer} = P_{max}^{defer}$ and continues until 14:16. During this period, there is surplus power even beyond $P_{max}^{defer}$, leading to PV curtailment to maintain power balance, as indicated by Mode 12 in Figure 4-21. PV curtailment ceases at 14:16, but its output decreases and eventually reaches zero. Consequently, from 14:16 to 15:40, $P_{meas}$ and deferrable load power decrease until the deferrable load stops.

Starting from 15:40, $P_{meas}$ becomes negative again, and the battery resumes discharging. Throughout the day, load shedding is not required, as shown in the load shedding section of Figure 4-20.

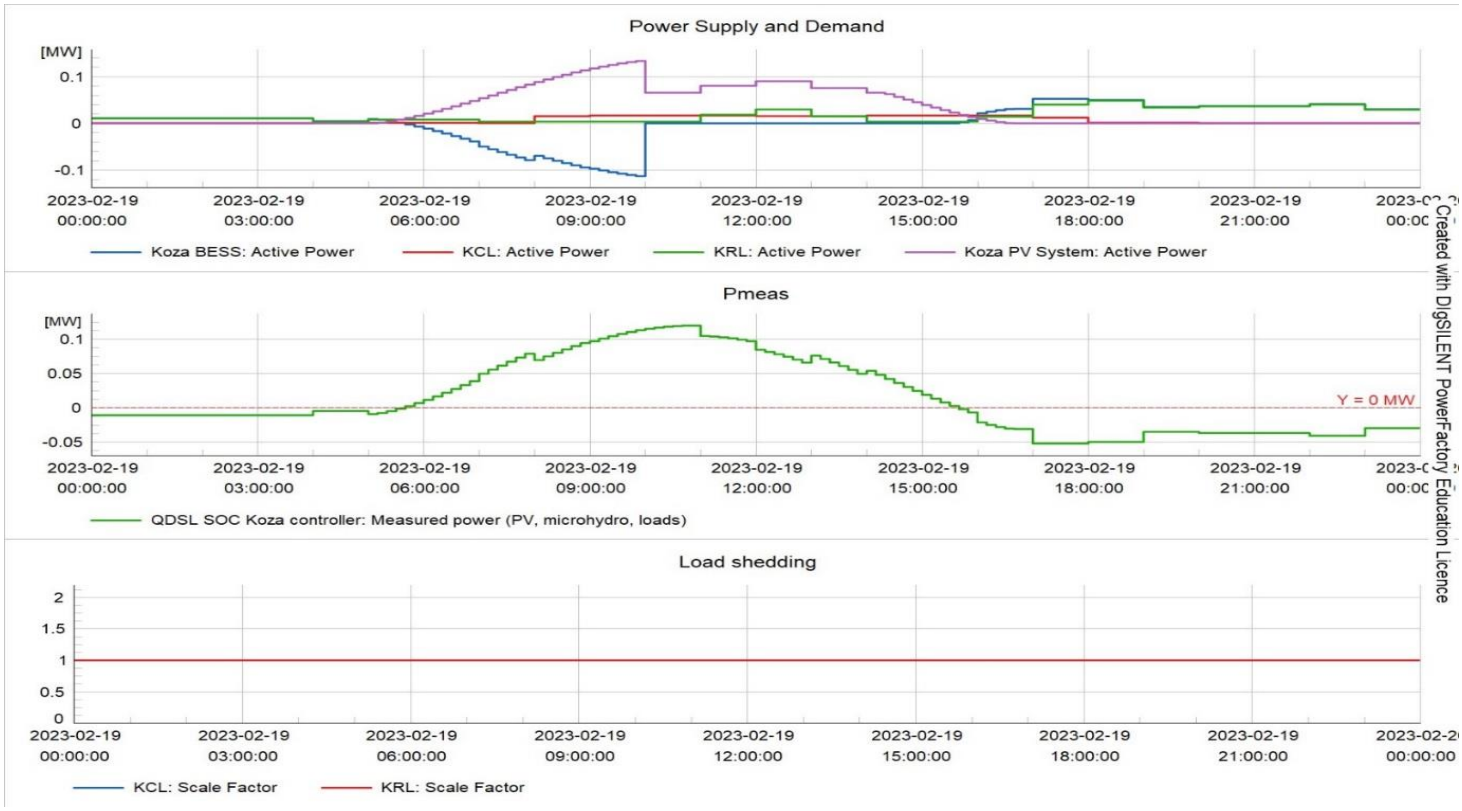

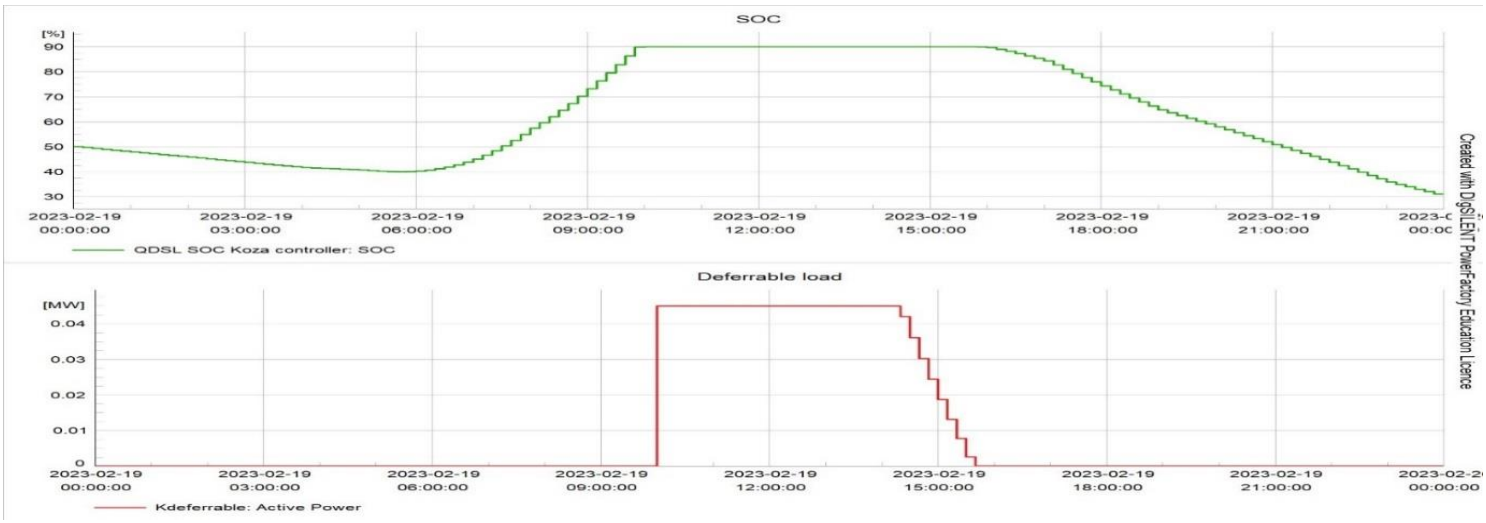


*Figure 4-20: quasi dynamic simulation result of Koza MG operating individually*

In Figure 4-21, different modes of operation and the PV output power curve of Koza MG are depicted. The section illustrating PV curtailment, running parallel with the mode 12 region, is clearly highlighted in this figure.

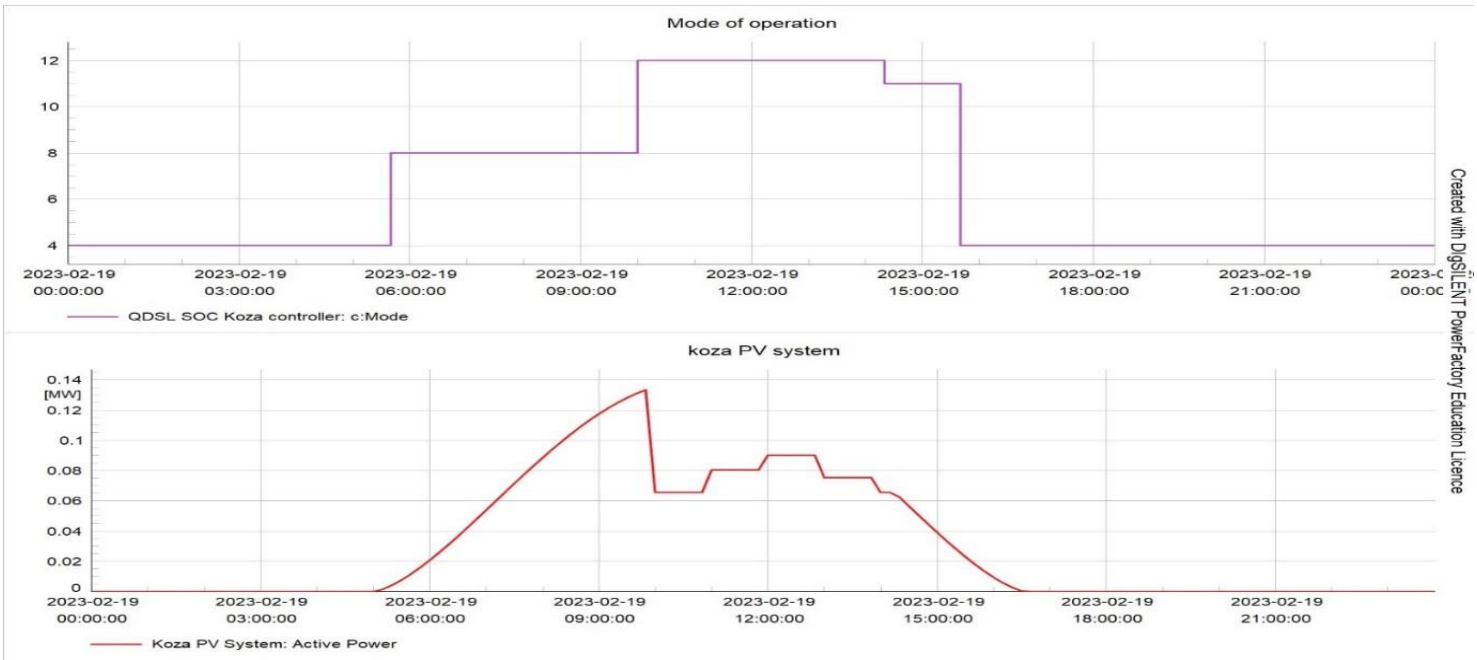


*Figure 4-21: Mode of operation & PV curtailment result of Koza MG operating individually*

iii. Result Analysis of Womba MG Operating Individually

In Figure 4-22, the power supply and demand, $P_{meas,}$ load shedding, SOC and deferrable load of Womba MG operating individually are illustrated. $P_{meas}$ remains positive until 16:20,

during which the battery charges initially until reaching $SOC \geq SOC_{max}$ at 1:50, at which point charging ceases, and the deferrable load is activated from 1:50 to 16:20.

From 16:20 to 23:00, $P_{meas}$ becomes negative, initiating battery discharge. However, at 18:59, $SOC \leq SOC_{min}$. and both the PV output power and micro-hydro supply fail to meet the primary load demand, indicating an insufficient power supply. Consequently, first priority load shedding commences at 18:59. Despite this, an hour later, additional load requirements necessitate the initiation of second priority load shedding.

Finally, at 23:00, the residential load demand decreases, causing $P_{meas}$ to become positive and load shedding ceases.

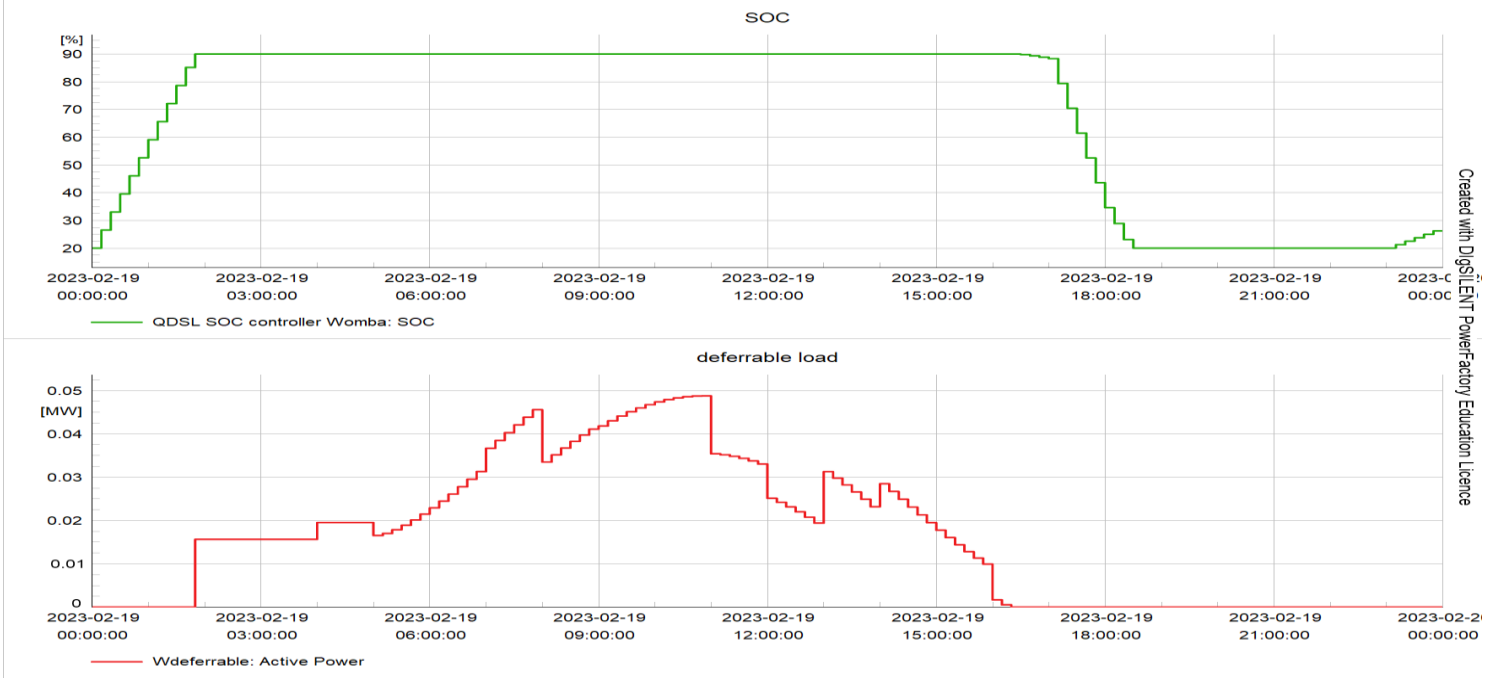


*Figure 4-22: Result of Wombs MG operating individually*

B. Quasi-Dynamic Simulation Result of MG Operating within MG Cluster

The following section presents the quasi dynamic simulation results of Toba, Koza and Womba MGs when operating within a cluster, along with their comparison to the corresponding results of each MG operating individually. When discussing the MGs within the cluster, it is important to reference the results discussed in the preceding section for each MG operating individually. It's essential to note that the comparison is made considering the same day for both individual and cluster operations.

When operating within the cluster, SOC, load shedding, and deferrable load of Toba MG are illustrated in Figure 4-23. The SOC exhibits minimal differences compared to Toba MG's individual operation. However, unlike the individual operation period, there is no load shedding throughout the day.

Moreover, in contrast to the individual operation, where the deferrable load power initially increases from 1:49 to 7:57 but subsequently decreases due to a rise in commercial load, resulting in a continuous reduction until it stops, during cluster operation, a similar pattern is observed initially until 9:43. However, thereafter, extra power is supplied from Koza MG, causing an increase in the deferrable load power, eventually reaching its maximum limit.

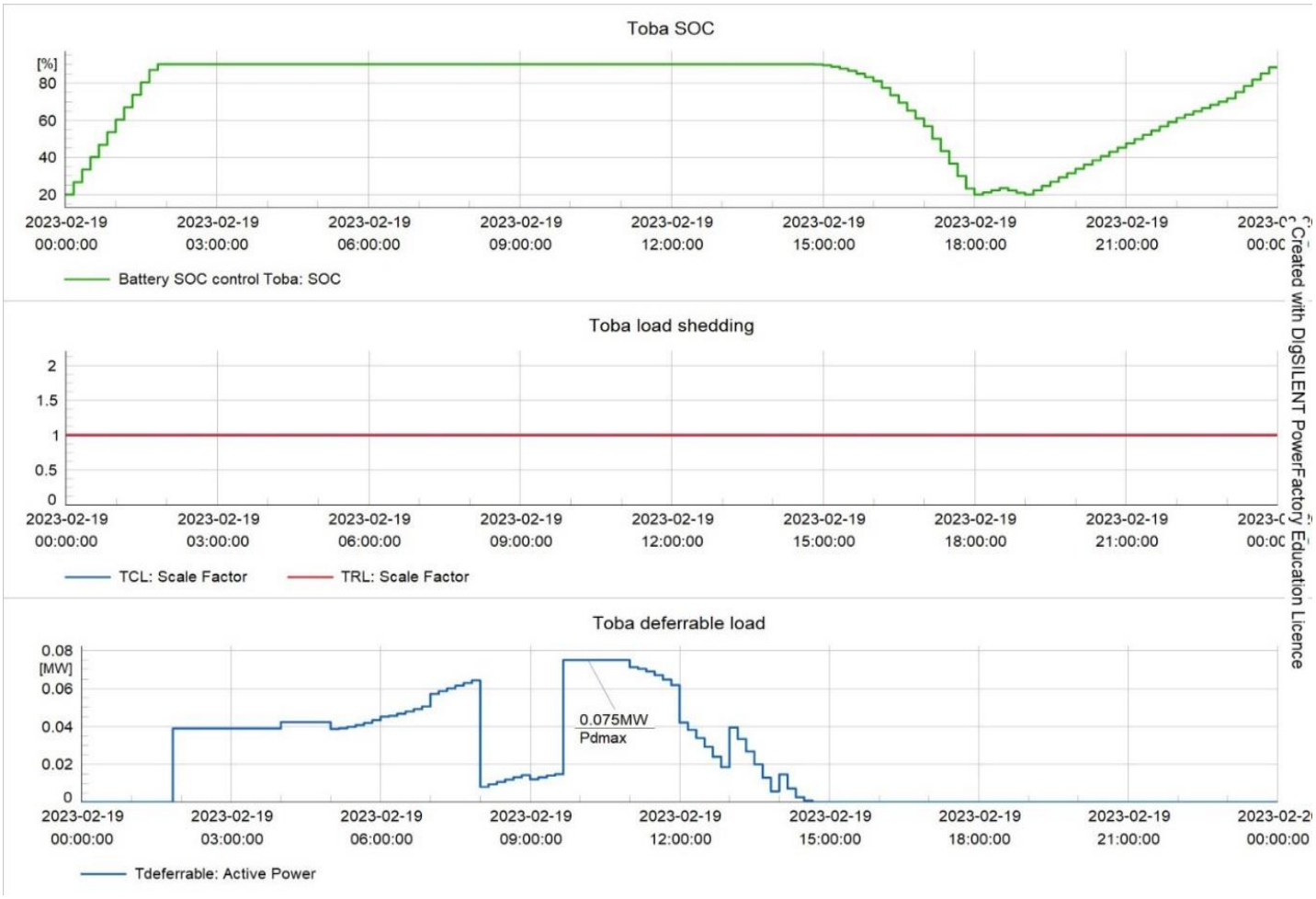


*Figure 4-23: Result of Toba MG operating in MG cluster*

When operating within the cluster, Koza MG exhibits no load shedding for the specified day, mirroring its operation when operated individually. Additionally, there is minimal difference observed in the SOC of the battery and deferrable load between individual and cluster operations.

However, a notable distinction arises in PV curtailment. During individual operation, Koza MG experiences PV curtailment, resulting in wasted power. Conversely, during cluster operation, there is no PV curtailment for Koza MG, as evidenced in the Koza PV system part of Figure 4-24. Instead, the excess power that would have been curtailed if Koza MG were operating individually is transferred to Toba MG. This surplus power is then utilized to increase the deferrable load power in Toba MG, reaching up to the extent of $P_{max}^{defer}$ around 9:43, as depicted in the Toba deferrable load part of Figure 4-23.


*Figure 4-24: Result of Koza MG operating in MG cluster*

When operating within the cluster, Womba MG demonstrates notable improvements compared to its individual operation. During individual operation, Womba MG's battery SOC reaches $SOC_{min} = 20\%$ at 18:59 and remains in that state for over four hours, as evident in the individual operation results. During this period, there is no PV power available, and the micro-hydro supply is insufficient to meet the primary load demand, resulting in the shedding of all first priority loads and an average of 19% of second priority load shedding.

In contrast, within the MG cluster, Womba MG's battery SOC only holds the $SOC_{min}$ state for half an hour. Importantly, there is no load shedding throughout the day, a significant advantage over individual operation. Remarkably, this advantage is achieved without affecting the deferrable load power that would have been supplied if Womba MG were operating individually, as depicted in Figure 4-25. The additional power preventing the occurrence of load shedding originates from Toba MG, starting from 18:30, as illustrated in Figure 4-26.

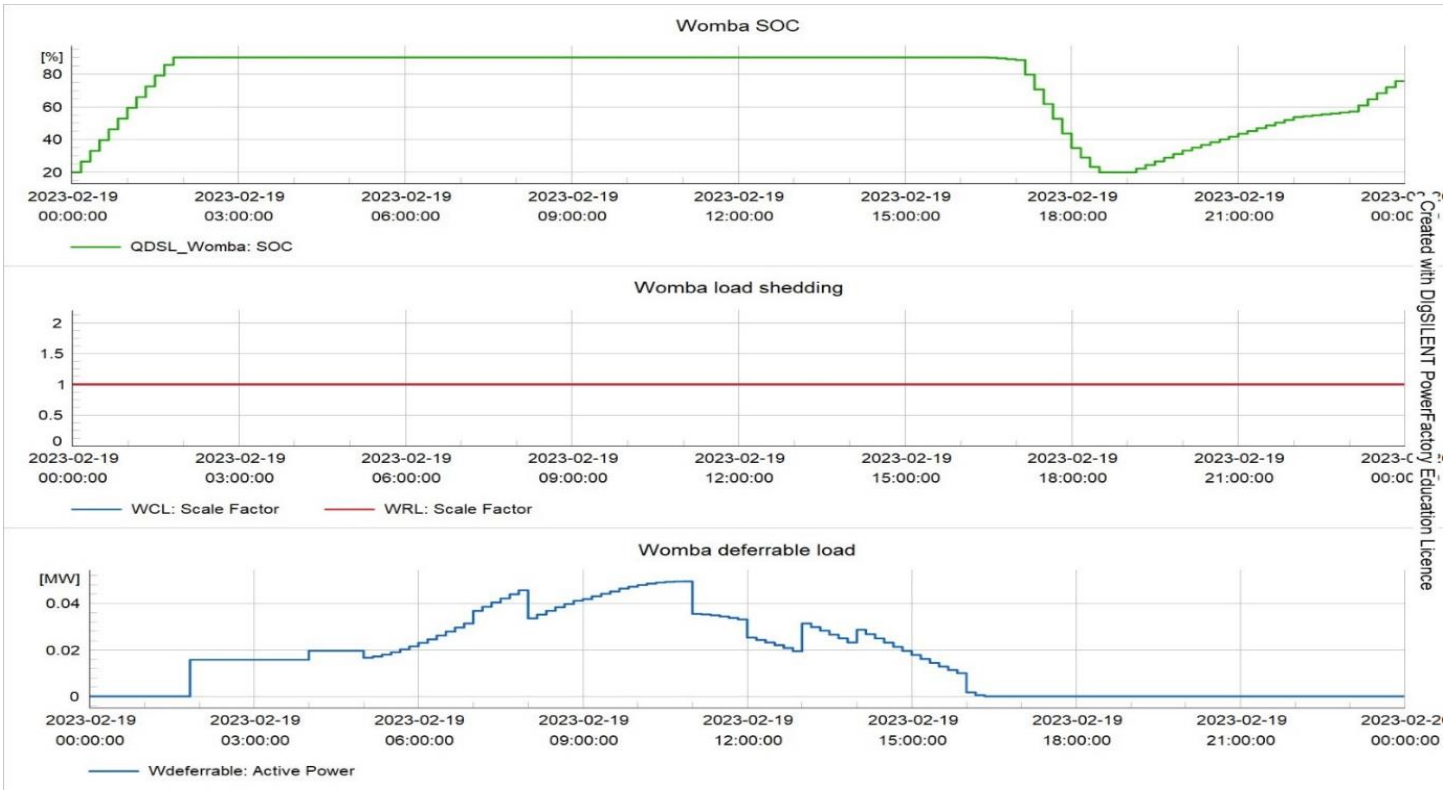


*Figure 4-25: Result of Womba MG operating in MG cluster*

During the development of the MG cluster, each individual MG becomes interconnected, facilitating power exchange through their respective transformers. As depicted in Figure 4-26, until 9:41, the power exchange through the transformers of Toba, Koza, and Womba MGs remains insignificant. In this figure, positive values indicate the amount of power transferred out of the MG, while negative values indicate the amount of power received by the MG.

At 9:41, in Koza MG, the available deferrable load power exceeds the maximal power limit. Thus, maintaining $P_{defer} = P_{max}^{defer}$, the extra power is transferred to Toba MG until 14:45. Subsequently, the available deferrable load power decreases from its maximum limit, and the power transfer ceases, although local deferrable load supply continues with $P_{defer} < P_{max}^{defer}$ . The deferrable load and power exchange scenario of Koza MG are illustrated in Figure 4-24 and Figure 4-26, respectively.

At 18:30, the SOC of Womba MG's battery reaches $SOC_{min}$, signaling a need for external power to prevent load shedding, as observed in its individual operation. However, this time, Toba MG provides the required power, alleviating Womba MG from load shedding. During this period,

Toba MG's $P_{meas}$ is positive. However, from 18:30 to 19:00 in Womba MG, there is a high power deficit, prompting the transfer of power from Toba MG to Womba MG beyond supplying its primary load. Despite this, the available power is still insufficient, leading Toba MG's battery to start discharging and transferring power to Womba MG to prevent load shedding.

Subsequently, the available power in Toba MG becomes adequate both to charge its battery and transfer to Womba MG. This prevents the load shedding that would otherwise occur. However, the time required for Toba MG's battery to reach $SOC_{max}$ is slightly delayed compared to its individual operation condition.

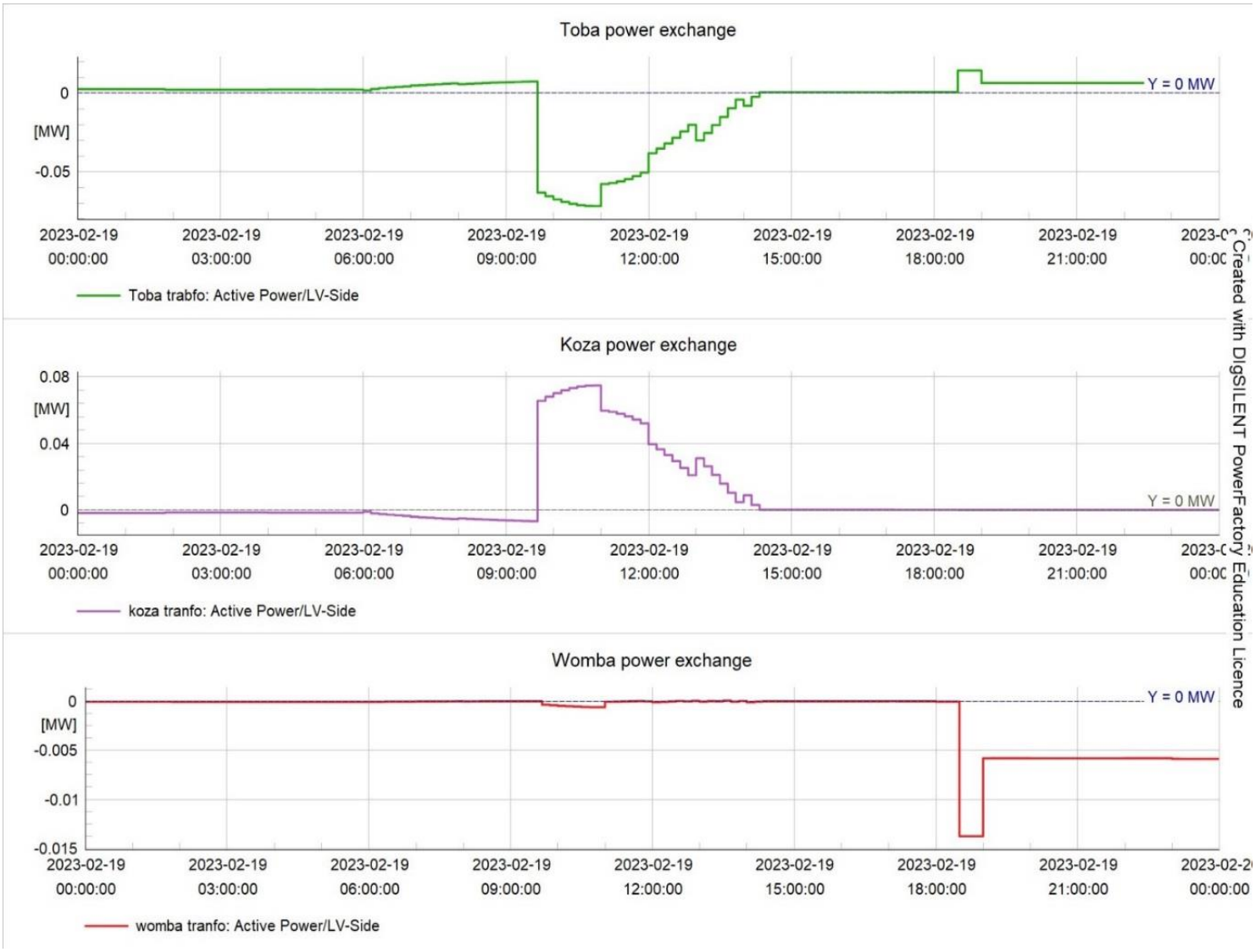


*Figure 4-26: Result of transformers power exchange within MG cluster*

### 4.5. Grid Extension

In this section, the feasibility of grid extension for Toba MG is examined. Grid extension, in this context, refers to the mechanism of connecting individually operating MGs with the national grid system. Toba village is situated 130 km away from the nearby Sawla substation. A grid capital cost of $12,417.22 per kilometer is considered, representing the initial capital cost of grid extension.

The concept of break-even grid extension distance is crucial in this analysis. It refers to the distance from the grid at which the NPC of extending the grid equals the NPC of the stand-alone system. Beyond this distance, the stand-alone system is optimal, whereas nearer to the grid, grid extension becomes optimal [28, p. 230].

Figure 4-27 illustrates that the breakeven grid extension distance is 15.02 kilometers. However, the distance of the MG from the Sawla substation far exceeds this threshold. Therefore, based on the current situation, grid extension is not a feasible alternative from an economic standpoint.

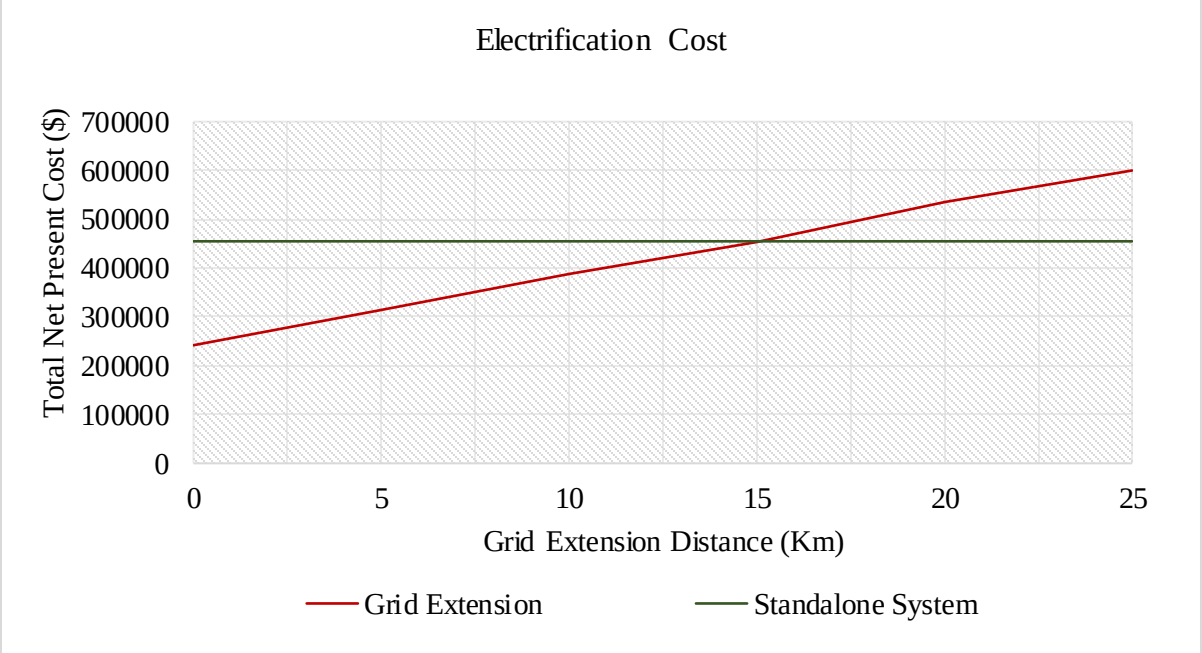


*Figure 4-27: Grid extension of Toba MG.*

# Chapter 5

# Conclusion

Based on the study presented in this work, several conclusions can be drawn:

Using an MTF-based strategy, the categorization of households' energy access varied based on income, appliances used, operation period, etc., which helps increase the accuracy of system optimization and yields more economical results than assuming average consumption for all households.

In this study, households are categorized into Tier 1 to Tier 3, with Tier 3 experiencing disruptions of less than 14 times a week, a frequency comparable to that of the majority of neighboring national grids, which range from 4 to 14 times a week. Therefore, without exceeding this disruption level, considering a 10% capacity shortage offers high economic benefits. For instance, comparing a capacity shortage of 0% to 10% in Toba MG, COE is reduced by 23.82%, providing economic benefits without compromising expected reliability levels. Thus, for optimal development of microgrids, a 10% capacity shortage is utilized to strike a balance between cost, reliability and affordability

The prediction of GHI is not always accurate, hence a margin of ±25% is considered. As the percentage of irradiance decreases, the costs of the system increase, while conversely, as irradiance percentage increases, system costs decrease. Therefore, accurate measurement values and careful consideration of site locations with higher irradiance for PV installation have a significant impact on the economy of the system.

The price of PV modules is subject to variation, with a downward trend observed leading up to 2020, followed by an increase starting from the end of 2020. These price fluctuations directly impact the economy of the system. For example, in the case of Toba MG, a 20% increment in PV price resulted in a 3.16% increment in the initial capital cost. Therefore, during the design stage, it is crucial to consider the timing of implementation to predict future module prices accurately, enabling more reliable economic estimations.

The price of the battery is decreasing, and this also has a direct impact on the economy of the system. In Toba MG, a 20% price reduction results in a $5,760 reduction in the battery's capital

cost. Therefore, during the design stage, it is also necessary to know the time of implementation for the battery in order to predict its price and ensure a more accurate economic estimation.

Deep usage of batteries reduces the quantity required and consequently lowers costs. However, this advantage comes with the trade-off of faster battery degradation, leading to the need for earlier replacement than expected. Therefore, a trade-off is necessary to determine the optimal usage level, balancing cost reduction with the lifespan of the battery.

While MG clustering requires additional costs for interconnection between individual MGs, the benefits it brings in terms of reduced unmet load, excess energy utilization, component size reduction, etc., outweigh the additional initial cost. Therefore, despite the added expense of interconnection, the advantages of clustering justify the investment.

The quasi-dynamic simulation results indicate that MG clustering can reduce both load shedding and the wastage of excess power observed in individually operating MGs.

In Toba MG, based on the calculated NPC and its distance from the nearby Sawla substation, grid extension is deemed economically infeasible.

# Future Work

Future work may explore the following points:

- Dynamic, contingency, power quality and reliability analysis of MG cluster.
- Comparison of master-slave control strategy with other controlling mechanisms for the developed MG cluster.
- System analysis without the assumption of constant micro-hydro power output.
- Incorporation of load forecasting in MG optimization process.
- Multi-Microgrid Cluster development and analysis.

# References


[1] "Access to electricity, rural (% of rural population) - Ethiopia | Data." [Online]. Available:https://data.worldbank.org/indicator/EG.ELC.ACCS.RU.ZS?end=2020&locations=ET&start=2000&view=chart. [Accessed Jan. 16, 2023]

[2] "Ministry of Water, Irrigation& energy 'Lighting to All : National Electrification Program 2.0: Integrated Planning for Universal Access,' Themat. Progr. Doc., no. October, p. 49, 2019, [Online]. Available: https://www.eastafricasummit.com/sites/default/fil," [Accessed Jan. 8, 2023].

[3] C. Guide, "Ethiopia - Energy." pp. 1–9, 2019. [Online]. Available: https://www.export.gov/article?id=Ethiopia-Energy. [Accessed Feb. 23, 2023].

[4] "Seboka, M.D. (2017) Ethiopian Energy Status, Challenges, and Opportunities. In: Presented at a Stakeholders Workshop on Alternative Pathways to Improve Electricity Access in Ethiopia, November 28, 2017, Addis Ababa, 5-12.".

[5] IEA, "Africa Energy Outlook Report," p. 20, 2019, [Online]. Available: www.iea.org/reports/africa-energy-outlook-2019. [Accessed Jan. 22, 2023].

[6] Y. He, X. Wu, K. Sun, X. Du, H. Wang, and J. Zhao, "Economic Optimization Scheduling Based on Load Demand in Microgrids Considering Source Network Load Storage," *Electronics*, vol. 12, no. 12, p. 2721, Jun. 2023, doi: 10.3390/electronics12122721.

[7] J. Das, "Optimal Component Sizing of an Isolated PV-Wind-Battery Microgrid in India using Multi Objective Optimisation," *2020 IEEE 17th India Counc. Int. Conf. INDICON 2020*, no. 1, 2020, doi: 10.1109/INDICON49873.2020.9342122.

[8] X. Li and G. Jones, "Optimal Sizing, Location, and Assignment of Photovoltaic Distributed Generators with an Energy Storage System for Islanded Microgrids," *Energies*, vol. 15, no. 18, Sep. 2022, doi: 10.3390/en15186630.

[9] M. Borghei and M. Ghassemi, "Optimal planning of microgrids for resilient distribution networks," *Int. J. Electr. Power Energy Syst.*, vol. 128, Jun. 2021, doi: 10.1016/j.ijepes.2020.106682.

[10] B. El Barkouki *et al.*, "An Economic Dispatch for a Shared Energy Storage System Using MILP Optimization: A Case Study of a Moroccan Microgrid," *Energies*, vol. 16, no. 12, p. 4601, Jun. 2023, doi: 10.3390/en16124601.

[11] S. Dinkhah, J. Salazar Cuellar, and M. Khanbaghi, "Optimal Power and Frequency Control of Microgrid Cluster with Mixed Loads," *IEEE Open Access J. Power Energy*, vol. 9, pp. 143–150, 2022, doi: 10.1109/OAJPE.2022.3148375.

[12] Y. Edisson Garcia Vera, R. Dufo-Lopez, and O. Daniel DIaz Castillo, "Optimization and feasibility of standalone hybrid diesel-pv-battery microgrid considering battery technologies," Oct. 2020, doi: 10.1109/ANDESCON50619.2020.9272144.

[13] W. Shen and M. Zeng, "Collaborative Planning Model of PV-Battery Storage System for Microgrid Considering Demand Response," *J. Phys. Conf. Ser.*, vol. 2433, no. 1, 2023, doi: 10.1088/1742-6596/2433/1/012008.

[14] T. M. Masaud and E. F. El-Saadany, "Correlating Optimal Size, Cycle Life Estimation, and Technology Selection of Batteries: A Two-Stage Approach for Microgrid Applications," *IEEE Trans. Sustain. Energy*, vol. 11, no. 3, pp. 1257–1267, 2020, doi: 10.1109/TSTE.2019.2921804.

[15] L. M. León, D. Romero-Quete, N. Merchán, and C. A. Cortés, "Optimal design of PV and hybrid storage based microgrids for healthcare and government facilities connected to highly intermittent utility grids," *Appl. Energy*, vol. 335, no. January, p. 120709, 2023, doi: 10.1016/j.apenergy.2023.120709.

[16] A. M. Jasim, B. H. Jasim, F. C. Baiceanu, and B. C. Neagu, "Optimized Sizing of Energy Management System for Off-Grid Hybrid Solar/Wind/Battery/Biogasifier/Diesel Microgrid System," *Mathematics*, vol. 11, no. 5, Mar. 2023, doi: 10.3390/math11051248.

[17] A. Ignat, E. Szilagyi, and D. Petreus, "Islanded Microgrid Simulation and Cost Optimisation," in *2020 IEEE 26th International Symposium for Design and Technology in Electronic Packaging, SIITME 2020 - Conference Proceedings*, Oct. 2020, pp. 426–429, doi: 10.1109/SIITME50350.2020.9292153.

[18] I. Tahirou Halidou, H. Or Rashid Howlader, M. M. Gamil, M. H. Elkholy, and T. Senjyu, "Optimal Power Scheduling and Techno-Economic Analysis of a Residential Microgrid for a Remotely Located Area: A Case Study for the Sahara Desert of Niger," *Energies*, vol. 16, no. 8, Apr. 2023, doi: 10.3390/en16083471.

[19] Y. Zhang, H. Zhou, L. Xiao, and G. Zhao, "Research on Economic Optimal Dispatching of Microgrid Cluster Based on Improved Butterfly Optimization Algorithm," *Int. Trans. Electr. Energy Syst.*, vol. 2022, pp. 1–16, 2022, doi: 10.1155/2022/7041778.

[20] V. V. V. S. N. Murty and A. Kumar, "Optimal energy management and techno-economic analysis in microgrid with hybrid renewable energy sources," *J. Mod. Power Syst. Clean Energy*, vol. 8, no. 5, pp. 929–940, 2020, doi: 10.35833/MPCE.2020.000273.

[21] C. Essayeh and T. Morstyn, "Optimal sizing for microgrids integrating distributed flexibility with the Perth West smart city as a case study," *Appl. Energy*, vol. 336, Apr. 2023, doi: 10.1016/j.apenergy.2023.120846.

[22] L. Bin *et al.*, "Scheduling and Sizing of Campus Microgrid Considering Demand Response and Economic Analysis," *Sensors*, vol. 22, no. 16, Aug. 2022, doi: 10.3390/s22166150.

[23] M. K. Kiptoo, O. B. Adewuyi, H. O. R. Howlader, A. Nakadomari, and T. Senjyu, "Optimal Capacity and Operational Planning for Renewable Energy-Based Microgrid Considering Different Demand-Side Management Strategies," *Energies*, vol. 16, no. 10,

May 2023, doi: 10.3390/en16104147.

[24] X. Wu, W. Zhao, X. Wang, and H. Li, "An MILP-Based Planning Model of a Photovoltaic/Diesel/Battery Stand-Alone Microgrid Considering the Reliability," *IEEE Trans. Smart Grid*, vol. 12, no. 5, pp. 3809–3818, Sep. 2021, doi: 10.1109/TSG.2021.3084935.

[25] W. Zhao, M. Xu, N. Ning, Y. Kang, and Z. Cai, "A Microgrid Capacity Optimization Method Considering Carbon Emission Cost," in *iSPEC 2020 - Proceedings: IEEE Sustainable Power and Energy Conference: Energy Transition and Energy Internet*, Nov. 2020, pp. 2219–2224, doi: 10.1109/iSPEC50848.2020.9351276.

[26] S. M. Ferdous, F. Shahnia, and G. M. Shafiullah, "Power Sharing and Control Strategy for Microgrid Clusters," Dec. 2019, doi: 10.1109/ICPES47639.2019.9105387.

[27] M. Bhatia and N. Angelou, "Beyond Connections: Energy Access Redefined,"ESMAP Tech. Rep., vol. 008/15, pp. 1–244, 2015, [Online]. Available: http://hdl.handle.net/10986/24368. [Accessed Jan. 9, 2023].

[28] "HOMER Energy LLC, 'HOMER Pro 3.1 User Manual,' HOMER Energy LLC, Boulder, CO, USA, 2014. [Online]. Available: https://www.homerenergy.com/products/pro/docs/HOMERPro_UserGuide_3.1.pdf." [Accessed: Jan. 17, 2023].

[29] Z. Girma, "Techno-Economic Feasibility of Small Scale Hydropower in Ethiopia : The Case of the Kulfo River , in Southern Ethiopia," vol. 2016, 2016.

[30] V. P. Sector, "Hydropower," vol. 1, no. 3, 2012.

[31] B. F. N. I. Loh PC, "Distributed operation of interlinked AC microgrids with dynamic active and reactive power tuning," *IEEE Trans Ind*, Sep. , doi: Appl 2013;49(5):2188–96.

[32] Y. H.-J. Nguyen T-T, Kim H-M, "Multi-frequency control in a standalone multi-microgrid system using a back-to-back converter.," *Energies 2017;10(6):1–18.*, Dec. .

[33] F. S. Shahnia F, Shafiullah G, "Power sharing and control strategy for microgrid clusters. In: 9th Int. conf. power and energy syst," *IEEE; 2019, p. 1–5.*

[34] L. C.-C. Wu X, Xu Y, Wu X, He J, Guerrero JM, "A two-layer distributed control method for islanded networked microgrid systems," *IEEE Trans Smart Grid 2019;11(2)942–57.*

[35] Y. G. Li Y, Dong P, Liu M, "A distributed coordination control based on finitetime consensus algorithm for a cluster of DC microgrids.," *IEEE Trans Power Syst 2018;34(3)2205–15.*

[36] Y. Chen, J. Li, Y. Wen, M. Sehnan, and W. Xu, "A Hybrid Master–Slave Control Strategy for Multiple Distributed Generators in Microgrid," *Energies*, vol. 16, no. 2, pp. 1–12, 2023, doi: 10.3390/en16020968.

[37] N. Cai and J. Mitra, "A multi-level control architecture for master-slave organized

microgrids with power electronic interfaces," *Electr. Power Syst. Res.*, vol. 109, pp. 8–19, 2014, doi: 10.1016/j.epsr.2013.11.027.

[38] T. Ding, Y. Lin, Z. Bie, and C. Chen, "A resilient microgrid formation strategy for load restoration considering master-slave distributed generators and topology reconfiguration," *Appl. Energy*, vol. 199, pp. 205–216, 2017, doi: 10.1016/j.apenergy.2017.05.012.

[39] Y. Shan, L. Ma, and X. Yu, "Hierarchical Control and Economic Optimization of Microgrids Considering the Randomness of Power Generation and Load Demand," *Energies*, vol. 16, no. 14, 2023, doi: 10.3390/en16145503.

[40] D. Saha, N. Bazmohammadi, J. C. Vasquez, and J. M. Guerrero, "Multiple Microgrids: A Review of Architectures and Operation and Control Strategies," *Energies*, vol. 16, no. 2, 2023, doi: 10.3390/en16020600.

[41] "Electricity tariffs must double to sustain profits: EEU - Capital Newspaper. [Online]. Available: https://www.capitalethiopia.com/2022/08/21/electricity-tariffs-must-double-tosustain-profits-eeu/." [Accessed Feb. 23, 2023]

[42] J. Ramirez-Vergara, L. B. Bosman, W. D. Leon-Salas, and E. Wollega, "Ambient temperature and solar irradiance forecasting prediction horizon sensitivity analysis," *Mach. Learn. with Appl.*, vol. 6, no. May, p. 100128, 2021, doi: 10.1016/j.mlwa.2021.100128.

[43] IRENA, "Renewable power generation costs in 2019 - Key findings," *Int. Renew. Energy Agency*, p. 160, 2020.

[44] M. Hall and Solar Magazine, "African solar installers feel the pinch of rising panel prices – pv magazine International." 2021.

[45] "'BESS costs could fall 47% by 2030, says NRE.' [Online]. Available: https://www.energy-storage.news/li-ion-bess-costs-could-fall-47-by-2030-nrel-says-in-long-term-forecast-update."[Accessed: Feb. 6, 2022].

# Appendix

Dynamic Programming Language (DPL) script for load flow equation of Toba MG

```
double Pgenerate, !battery active power
       Qgenerate, !battery reactive power
       Ppvgen, !PV generation power
       Phydrogene, !hydro generating power
       Pdfload, !deferrable load
       Pdfloadmax, !max. limit for deferrable load
       redFact, !reduction factor
       P1stfloadscale, !1st priority load shedding scale
       P2ndfloadscale, !2nd priority load shedding scale
       Prest; !residue power from battery support (net power of Pmeas & battery)
redFact = 1.0; !battery at ratted power
Ppvgen = Psolar;
Pdfload = 0;
Pdfloadmax = 0.075;
P1stfloadscale = 1; !1st priority load supplied 100%
P2ndfloadscale = 1; !2nd priority load supplied 100%
ActShed = 0; !No load shedding order
Pmeas = (Phydro + Ppvset- P1stfload*(1-P1stfloadscaleSet) -P2ndfload*(1-
P2ndfloadscaleSet)-Pessload);
if ({chargeP = 3}.and.{chargeE >= 2}) !battery could be discharging
if (Pmeas > -PFullFeed) {
   redFact = 1 - ((Pmeas + PFullFeed)/(-PStartFeed + PFullFeed));
   Pgenerate = Pfeed * redFact; ! !discharging with power less than Pfeed
   Qgenerate = Qfeed * redFact;
   Mode = 4;
  }
```

```
 else {
   Pgenerate = Pfeed * redFact;  !discharging with Pfeed, redfact=1
   Qgenerate = Qfeed * redFact;
   ActShed = 1; !load shedding is ordered
   Prest = Pmeas+Pgenerate;  !residue power from battery support
   if (Prest < P1stfload) {
        P1stfloadscale = 1-Prest/P1stfload;
        Mode = 5;
   }
   else{
        P1stfloadscale = 0; !all 1st priority load shedding
    if (Prest < P1stfload+P2ndfload){
        P2ndfloadscale = 1-(Prest-P1stfload)/P2ndfload;
        Mode = 6;
     }
      else {
        P2ndfloadscale = 0; !all 2nd priority load shedding
        Mode = 7; !rare case
        }
       }
   }
}
else if ({chargeP = 1}.and.{chargeE <=2}) { !battery could be charging
     if (Pmeas < PFullStore) {
        redFact = 1 - ((PFullStore - Pmeas)/(PFullStore - PStartStore));
        Pgenerate = -Pstore * redFact;  !charging with power less than Pstore
        Qgenerate = -Qstore * redFact;
        Mode = 8;
```

```
  }
  else {
        Pgenerate = -Pstore * redFact;  ! !charging with Pstore, redfact=1
        Qgenerate = -Qstore * redFact;
   if (Pmeas+Pgenerate > Pdfloadmax) {
       Pdfoad = Pdfloadmax;  !deferrable load set to max. limit
       Ppvgen = Psolar - (Pmeas+Pgenerate-Pdfloadmax);  !PV curtail
       Mode = 10;
   }
   else {
        Pdfload = Pmeas+Pgenerate;
        Mode = 9;
   }
  }
}
   else if ({chargeE = 3}.and.{chargeP = 1}){
       Pgenerate = 0; !battery stop charging, SOCmax
       Qgenerate = 0;
   if (Pmeas>Pdfloadmax) {
       Pdfload = Pdfloadmax;
       Ppvgen = Psolar - (Pmeas-Pdfloadmax);  !PV curtail
       Mode = 12;
   }
  else{
      Pdfload = Pmeas;
      Mode = 11;
   }
}
```

```
   else if ({chargeE = 1}.and.{chargeP = 3}){
        Pgenerate = 0;
        Qgenerate = 0;
        Prest = Pmeas;
        ActShed = 1;
    if (Prest < P1stfload) {
        P1stfloadscale = 1-Prest/P1stfload;
        Mode = 1;
   }
     else{
        P1stfloadscale = 0;
     if (Prest < P1stfload+P2ndfload){
        P2ndfloadscale = 1-(Prest-P1stfload)/P2ndfload;
        Mode = 2;
    }
else {
          P2ndfloadscale = 0;
          Mode = 3; !rare case
     }
   }
}
      printf('load flow calculation');
      SetEquation(0, Pset - Pgenerate);
      SetEquation(1, Qset - Qgenerate);
      SetEquation(2, Ppvset - Ppvgen);
      SetEquation(3, Pdfloadset - Pdfload);
      SetEquation(4, P1stfloadscaleSet - P1stfloadscale);
      SetEquation(5, P2ndfloadscaleSet - P2ndfloadscale);
```